Detecting the mechanisms of spatio-temporal changes in land use and endangered ecosystems induced by urban growth

Sharmin Shishir

A Dissertation submitted to

Graduate School of Environmental Science, Hokkaido University

for the Degree of

Doctor of Philosophy (Environmental Science)

September, 2018

Contents

Abstract

To understand the effects of urban growth on land use change and ecosystems, the following information is required: 1) detecting accurate land use changes at fine scale, 2) finding out the habitats for endangered species, and 3) investigating the structure and function of ecosystems. I conducted a series of field surveys in Purbachal, Bangladesh, for examining these issues. I hypothesized that fine scale data (less than 1 meter in the resolution) identify land use types precisely and detect land use types that are not detected by coarse resolution. These are confirmed by fine scale data from two satellites. There are various vegetation indices (VIs) proposed to classify land use types, suggesting that each VI has advantages and disadvantages on the classification of land use types. To solve this, a hierarchical land use classification was used with four popular VIs (Chapter 1). Based on this research, the present distribution of *S. robusta* forests is clarified. Secondly, I focused on the potential distribution of *S. robusta*, because this species is an umbrella species for ecosystem conservation (Chapter 2). The predictable distribution of *S. robusta* forest was examined by Maxent model, using two global warming scenarios, RCP4.5 (mean temperature increase 1.4 °C and 1.8°C) and RCP8.5 (mean temperature increase 2.0 °C and 3.7 °C) to the year of 2046-2065 and 2081-2100. The global warming scenarios supported the conservation and management strategies for protecting *S. robusta* forests by predicting the future potential localities of *S. robusta* forests and the impact of increased temperature and decreased precipitation on *S. robusta* forests ecosystem. To conserve the ecosystems and biodiversity in relation to land use change and endangered species, finally, ecosystem structures and functions are investigated by plant functional groups (PFGs) developed by the patterns of leaf reflectance spectra of 112 species. Then, I characterized the PFGs based on 48 species attributes (Chapter 3).

Detecting fine-scale spatiotemporal land use changes is a prerequisite for understanding and predicting the effects of urban growth and its related human impacts on the ecosystem. Land use changes are frequently examined using vegetation indices (VIs), although the validation of these indices has not been conducted at a high resolution. Therefore, a hierarchical classification was constructed to obtain accurate land use types at a fine scale (Chapter 1). The four VIs are the normalized difference VI (NDVI), green-red VI (GRVI), enhanced VI (EVI), and two-band EVI (EVI2). The reflectance data were obtained by the IKONOS (0.8-m resolution) and WorldView-2 sensor (0.5-m) in 2001 and 2015, respectively. The hierarchical classification of land use types was constructed using a decision tree (DT) utilizing all of the four examined VIs. The DT showed overall accuracies of 96.1% and 97.8% in 2001 and 2015, respectively, while single VI showed less than 91.2% of accuracy. These results indicate that each VI exhibits unique advantages. In addition, the DT was the best classifier of land use types, particularly for native ecosystems represented by *Shorea* forests and homestead vegetation, at the fine scale. Since the conservation of these native ecosystems is of prime importance, DTs based on hierarchical classifications should be used more widely.

Detecting the determinants of spatio-temporal distribution of species is prerequisite for ecological conservation and restoration. Maximum entropy (Maxent) modeling was applied to investigate the present and future potential distributions of an endangered canopy-tree, *S. robusta*, under urban growth in Purbachal, Bangladesh (Chapter 2). The model was constructed by 165 location records that cover the whole distributional range of *S. robusta*. Eight environmental variables in relation to climate, geography and soil were included in the models. Two scenarios proposed by IPCC (representative concentration pathways, RCP) were used for the prediction of distribution altered by global warming (from 2046 to 2065 and from 2081 to 2100). The accuracy of

predicted distributions was supported sufficiently by the binomial test of omission ($P \approx 0.00$) and area under the curve analysis (AUC > 0.97). The distributions were mostly determined by precipitation and soil nitrogen because *S. robusta* requires high precipitation and soil nitrogen. Maxent predicts that the suitable areas for *S. robusta* forest that will decline to 86.5% by 2100 in the RCP8.5 scenario.

Although plant functional group (PFG) is used broadly for analyzing ecological aspects, the relationships between PFGs and spectral reflectance, which is determined by photosynthesis and its related factors, have not been examined well. PFG and spectral reflectance were examined by using 48 traits of 112 plants in the central Bangladesh where plant species were diverse. Four PFGs were detected by Ward cluster analysis based on the spectral reflectance. Ten traits were statistically different between the four PFGs, those are: growth form (tree, herb and grass), wood, height, diameter at breast height (DBH), branching pattern (erect, spreading) and leaf hair. The four PFGs were represented by sub-canopy plant (Group A), hairy plant (B), slim-stemmed tree (C) and large tree (D). Group B showed the highest reflectance at visible and NIR spectra, while Group D did the lowest reflectance spectra at NIR. The overall reflectance was ordered as: groups D < C < A < B. These results suggested that the PFGs classified by reflectance spectra was associated with not only growth form but also branching pattern and leaf surface structure and characterized the ecosystems structure and function.

I concluded that urban growth (i.e. road construction, lake excavation etc.) was a trigger of *S. robusta* deforestation and changed the diverse landscapes and ecosystems. Although the *S. robusta* forest has been at risk of deterioration induced by global warming, the Maxent model suggested that the preservation of endangered forests is possible by finding out the potentially-suitable regions of *S. robusta* forests. The

substantial species and habitats can be preserved by identifying the PFGs and highlighting the environmental management.

General introduction

Land use change is an eminent feature in developing countries (Noss and Csuti 1994). Noticeable anthropogenic impacts on land use change are the reduction and fragmentation of habitats that isolate endangered populations and extinct native species (Zipperer 1993). Of anthropogenic activities, urban development causes the greatest loss of ecosystems and/or habitats (Marzluff 2001). When urbanization deteriorates various ecosystems, the species diversity and ecosystem function are also decreased through landscape fragmentation and climate change (Arnfield 2003; Wilby and Perry 2006; Barros et al. 2016; Booth et al. 2004). Due to urban growth in Purbachal, Bangladesh, forest and other land use types have been deteriorated (Hasnat and Hoque 2016).

Since urbanization deteriorates natural ecosystem for a short term, an up-to-date information on land use change is crucial to assess the impacts (Poh Sze Choo et al. 2005). One technique is remote sensing that detect land use change promptly when appropriate data are available (Boyle et al. 2014; Cotter et al. 2004). In addition, high-resolution sensors are desirable to detect fine-scaled land use changes (Ramankutty et al. 2006). Fine scale multispectral data extracts detailed spatial information to investigate land use types by reducing mixed-pixel problem and classification error (Lu and Weng 2009). Vegetation indices (VIs) are often used to classify land use types (Shivashankar and Hiremath 2011). In this research, I used normalized difference vegetation index (NDVI), enhanced vegetation index (EVI), two band enhanced vegetation index (EVI2) and green red vegetation index (GRVI) to detect the land use changes (Singh et al. 2016; Huete et al. 2002; Jiang et al. 2008; Motohka et al. 2010), because these VIs have the advantages to improve the classification accuracy and minimize the classification errors (Evrendilek and Gulbeyaz 2008). I made a hierarchical classification based on these four VIs to detect land use types, because single VI was not capable to separate all land use types. The hierarchical

classification used the combination of all the four VIs by selecting the suitable VI for each land use type according to the classification and accuracy.

Remote sensing technique is used widely in the conservation and management at species, ecosystem and landscape levels. Land use classification by fine scale data enhance and develop the decisions of the planners, ecologist and decision-maker involved in the management of environment for sustainable development (John and Chen 2003; Mustapha et al. 2010; Malinverni et al. 2010). Integration of GIS and remote sensing technology provides all-out information and analysis proficiencies regarding land use plan, conservation and management of ecosystems (Nellis et al. 1990).

The possible potential distributions and the vital environmental factors of an endangered tree species, *S. robusta*, were analyzed using Maxent modeling. Detecting distributions of endangered ecosystems is a key concern in conservation, management and restoration of biodiversity (Ferrier 1984; Purvis et al. 2000), including screening of biodiversity hotspots (Myers et al. 2000). Maxent is used for predicting species distribution based on the environmental predictors (Phillips et al. 2004; Elith and Leathwick 2006). The advantage of this model is that only the presence data is required with the environmental factors to predict the environmental conditions (Elith et al. 2011). Maxent modeling was applied and suitable in this study, because of the unavailability of the absence data. Therefore, I applied Maxent model to detect the potential distributions of *S. robusta* forests and to predict the existence of this forest under the global warming scenarios (RCP4.5 and RCP8.5). The impact of global warming on *Shorea robusta* forests was investigated, because global warming is responsible for the drastic changes in the distributions of species and ecosystems due to the projected temperature rise (Pacifici et al. 2015). *S. robusta* was used because this species is an umbrella species and least concern species recorded in the Red List (IUCN 2015). I focused on the essential environmental factors determining the *S. robusta* distributions followed by the impacts of RCP scenarios and urban growth on *S.*

robusta ecosystems. Because, not only climatic factors but also edaphic factors were essential to predict the possible distributions of the *S. robusta* forests. These results is likely to assist the *S. robusta* conservation by preserving existing habitats and restoring the suitable localities.

Finally, this research examined plant functional groups (PFGs) using 48 species traits of 112 species. Spectral reflectance of leaves was measured by a portable spectroradiometer. The reflectance patterns were related to PFGs that were basically developed by growth form. These results suggested that photosynthetic characteristics was related to the growth forms. Therefore, the PFGs characterized the ecosystems function and were related to the land use types. The essential ecosystems (e.g., *S. robusta*) can be conserve by the identification of this PFGs.

Study site

Field researches were conducted in Purbachal (23°49'45.53" - 23°52'30.72"N and 90°28'20.18" - 90°32'43.26"E), Bangladesh, because of urbanizing area (Figure S-1). Purbachal is located in the eastern-central part of Bangladesh. The study site is 2,489 ha and is drained by the two major rivers to the west and east (Zaman 2016). The site falls within the physiographic unit of Pleistocene terrace named as Madhupur tract and the Brahmaputra-Jamuna Floodplain (Brammer 2012) that form dendritic drainage systems (Rashid 1991). The terrace consists of low gentle-edged hills and ridges separated by shallow valleys and depression which floods extensively in the rainy season. The lithological landforms of Purbachal consists of Madhupur clay deposit of the Pleistocene age and alluvial deposit of recent age. The alluvial deposit was associated with valleys and depression characterized as silty clay, silt, fine sand, gray-light gray, and dark gray soil. The Madhupur clay deposit consisted of silty clay with fine sand, red, reddish-brown, and yellowish-brown soil found mostly in the hills. Oxidized soil with the accumulation of nodules was one of the soil characteristics at the Madhupur clay deposit (BBS 2013).

In the bottom of valleys and depression one-crop is cultivated in a year. The scattered homesteads (i.e., settlement and residential areas) and homestead vegetation (vegetation consisting of trees, shrubs and herbs on and around the settlement) observed in the hilly areas (Shapla et al. 2015). On the adjacent slopes, vegetables were cultivated in the winter season (Anonymous 2013).

This area is in a tropical monsoon climate (BBS 2013). The annual rainfall in the study site averages 2400 mm and the mean annual temperature is 28°C with the minimum monthly temperature 12.7°C in winter and maximum monthly temperature 36.3°C in summer. The summer is prolonged, with the intermittent monsoon and short winter. Period during March and November usually shows high temperature higher than 28°C (Shapla et

al. 2015). In addition air moisture is over 80% from March to June. Period from June to November is humid and rainy monsoon. Period from December to February is a cold and dry (Rafiuddin 2010).

The potentially-natural vegetation in Purbachal is *S. robusta* forest that now covers 7.8% of the forest areas (Hasan and Mamun 2015). The associated tree species are *Dipterocarpus turbinatus* Gaertn. f., *Albizzia lebbeck* (L.) Benth., *Dillenia indica* L., *Ficus benghalensis* L. , *Ficus religiosa L., Terminalia bellirica* (Gaertn.) Roxb., *Terminalia chebula* Retz., *Syzygium cumini* (L.), etc. Common shrub, herb and grass are *Flacourtia indica* (Burm. f.) Merr., *Lipocarpha squarrosa* (L.) Goetgh., *mimosa pudica* L., *Murdannia keisak* (Hassk.) Hand.-Maz, *Chrysopogon aciculatus* (Retz.) Trin., etc. The trees of fruits and crops are also grown, such as *Mangifera indica* L., *Artocarpus heterophyllus* Lam. and *Psidium guajava* L. Although the crop lands are developed, Purbachal is a sanctuary of natural ecosystems supporting ecologically important species and habitats (Mamun 2007). The rapid urban growth triggers massive ecosystem damages and forest reduction in the area. In particular, the *S. robusta* forest is rapidly disappearing (Roy 2012).

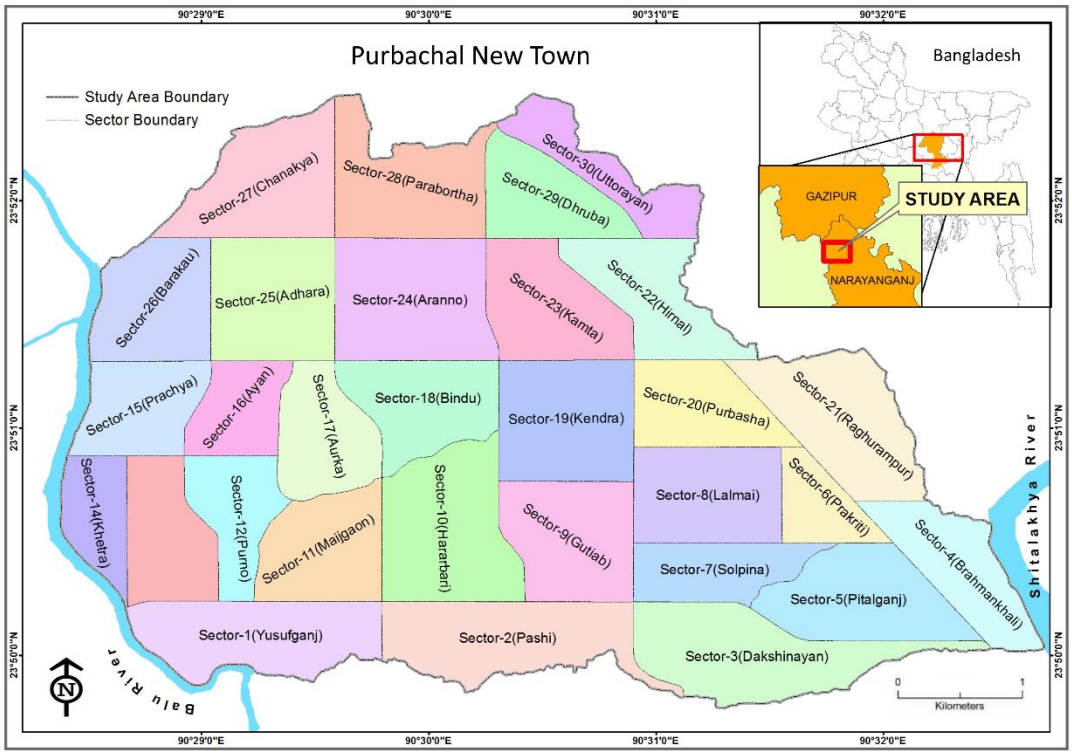

Figure S-1: A land use map of study site in 2015. The inset map shows the location of Purbachal in Bangladesh.

Chapter 1

Hierarchical classification of land use types using multiple vegetation indices to measure the effects of urban growth

1.1. Introduction

Since the construction of new towns within natural ecosystems can cause the rapid deterioration of endangered and threatened ecosystems and landscape diversities therein, it is necessary to predict the effects of land use changes to promote the conservation and restoration of ecosystems prior to urbanization. Fine-resolution data are desirable for detecting land use changes as a result of urbanization; accordingly, the resolution of land use maps should be sufficiently fine for detecting the effects of road networks and of related human impacts on adjacent areas (Nigam 2000; Erener et al. 2012; Akay and Sertel 2016). However, due to the lack of high-resolution data, such detailed analyses are scarce (Fonji and Taff 2014; Kalyani and Govindarajulu 2015). Two satellites, namely, IKONOS and WorldView-2 (WV2), recently provided high-resolution data with a resolution of less than 1 m (Aguilar et al. 2013). Such a resolution is likely to be suitable for analyzing land use changes caused by urbanization (Nouri et al. 2014), although the effectiveness of these datasets has not been examined. Therefore, the prime objective of the present study is to validate the applicability of these high-resolution satellite data to the detection of land use changes caused by urban growth.

The vegetation index (VI) was developed to detect the characteristics of vegetation and land use via the combination of two or more wavelength bands related to photosynthesis, i.e., the blue, green, red and near-infrared bands (Huete et al. 1999). A high VI indicates a high vegetation greenness related to the high activities and low

stresses of plants, and vice versa (Rocha and Shaver 2009). Therefore, VIs are often applied to analyses of land use and vegetation changes, e.g., to detect spatial variabilities (Matsushita et al. 2007), plant cover distributions and densities (Myneni et al. 1997; Saleska et al. 2007) and temporal changes (Lunetta et al. 2006). To evaluate the greenness of the ground surface, various VIs have been proposed (Joshi and Chandra 2011; Barzegar et al. 2015), and they are represented by the normalized difference vegetation index (NDVI), enhanced vegetation index (EVI), two-band enhanced vegetation index (EVI2) and green-red vegetation index (GRVI) (Jiang et al. 2007).

The NDVI is widely used to detect land use-land cover (LULC) changes (Sahebjalal and Dashtekian 2013; Singh et al. 2016). Additionally, measurements of the NDVI are employed to broadly assess the spatiotemporal characteristics of LULC, including the vegetation cover (Kinthada et al. 2014). The principle of the NDVI is derived from the reflectance characteristics of photosynthesis, i.e., through an examination of the vegetation greenness by using red band signals absorbed by plants and near-infrared band signals reflected by plants (Rouse et al. 1974). The weakness of this index lies in the fact that atmospheric and/or ground surface conditions, such as clouds and soils, often distort its accuracy (Kushida et al. 2015; Miura et al. 2001). Three indices, namely, the EVI, EVI2 and GRVI, were developed to reduce these obstacles, and they are popularly employed in addition to the NDVI (Phompila et al. 2015). The EVI enhances the greenness signal of the ground surface, which includes forest canopy structures, by using the blue band (Huete et al. 2002) and therefore reduces soil and atmospheric interference (Holben and Justice 1981). The EVI2 was modified from the EVI by removing the blue band to improve the auto-correlative defects of surface reflectance spectra between the red and blue wavelengths (Jiang et al.

2008), particularly when the background soil reflectance fluctuates (Kushida et al. 2015). The GRVI is often applied to evaluate forest degradation and canopy tree phenology, because this index is sensitive to changes in the leaf color at the canopy surface by using green wavelengths (Motohka et al. 2010).

The effectiveness of each of the abovementioned VIs has been compared well at coarse scales, e.g., at 30 m with Landsat TM5 data and at 250 m with both MOD13Q1 and NOAA-AVHRR imagery (Julien et al. 2011). However, only a few studies have been conducted to investigate LULC changes using VI time series (Markogianni et al. 2013). Land use classification schemes using VIs at a fine scale should be validated prior to examining land use changes, because the accuracies of these VIs at higher resolutions have not been examined thoroughly. A new planned township, namely, Purbachal New Town, is being prepared on the northeastern side of Dhaka, Bangladesh (Rahman et al. 2016a). High-resolution data are available for a land use comparison between the pre- and post-urbanization periods. Therefore, the effectiveness of each of the four popular vegetation indices, namely, the EVI2, EVI, GRVI and NDVI, were examined at a high resolution by comparing the two phases of urban growth (i.e., pre-urbanization and present-day) in the new township. Each VI has both strong and weak points with regard to the classification of land use types (Dibs et al. 2017). To solve this issue, a decision tree (DT) was also utilized in this study. The application of DTs has been increased for image classification purposes because of their accuracy and interpretation capabilities. DTs are effective for categorizing and selecting each class in a classification tree (Laliberte et al. 2007), and they have performed successfully with remotely sensed data for the analysis of land use changes at coarse resolutions (Brown de Colstoun et al. 2003; Sesnie et al. 2008), although their accuracy

was not examined for fine resolutions (high-resolution satellite imagery < 30 m and very high-resolution ≤ 5 m) (Fisher et al. 2017).

The first objective in this study was to examine the efficiencies of the VIs with regard to land use classification at a fine scale, because their efficiencies may differ between coarse and fine resolutions. The second objective was to characterize the VIs for each land type and to develop a hierarchical classification using a DT utilizing the characteristics of the examined VIs. Finally, the third objective was to characterize the land use changes induced by urban growth.

1.2. Materials and methods

1.2.1. Study area

Purbachal New Town, Bangladesh (23°49'45.53" - 23°52'30.72"N and 90°28'20.18" - 90°32'43.26"E) was selected as the study area (Figure 1-1). At a large scale, Purbachal New Town is located within eastern-central Bangladesh between large floodplains (i.e., the Old Brahmaputra Floodplains) and terraces and is sandwiched by two rivers, namely, the Balu and Sitalakkhya Rivers, on the west and east sides. The maximum mean monthly temperature is 26.3°C in August, and the minimum is 12.7°C in January (Shapla et al. 2015). The annual precipitation is 2,030 mm. The dry season generally ranges from December to February, and the rainy season lasts from June to September (Rahman et al. 2016b). The new town project was established to reduce the overpopulation in the capital city of Dhaka, the population density of which was 57,167/km² in 2011 (Khatun et al. 2015). The planned area of the new town is 2,489 ha (Zaman 2016). The construction started in 1995, and it did not cease until 2015. Prior to urbanization, the major land use types were forest (*Shorea robusta* Gaertner f., in the

Dipterocarpaceae family), homestead, homestead vegetation, cropland, and various others (Rahman et al. 2016a).

The expansion of urban areas in Bangladesh was inadequately planned and controlled due to truncated laws (Hossain 2013). Per the Environmental Conservation Act of 1995 and the Bangladesh Environmental Conservation Rules, 1997, the preservation of natural forests and privately owned commercial forests dominated by *S. robusta* should take priority during the land development planning of Purbachal New Town. The major forest products are edible fruits, timber and medicines. These preserved forests are expected to sustain endemic and/or invaluable flora and fauna, although land development activities often neglect these perspectives (Zaman 2016). Although the emphasis during the pre-planning stage was the *in situ* preservation of entire forests, the idea to maintain all of the patches of *Shorea* forest was later rejected because those isolated patches had already been exposed to human activities. To compensate for the loss of forested area, a green belt with a width of 15 m to be produced through afforestation was planned for the full perimeter of the township area (24.2 km^2) with a few exceptions. There were no interferences with the natural drainage systems that had maintained the pristine ecosystems in the region.

In total, the land use types of the study area were classified into eight categories (Table 1-4). Of those land use types, native forests with a maximum height of 36 m dominated by *S. robusta* have maintained the highest biodiversity, and they contain numerous endangered species (Gautam et al. 2006; Mandal et al. 2013). Therefore, the accurate detection of the distribution of *Shorea* forest was the priority for this land use analysis. The other land use types were homestead (i.e., settlement and residential areas), homestead vegetation (vegetation consisting of trees, shrubs and herbs on and around the settlement), cropland, grassland, agricultural low land, bare land and water bodies. In

general, therefore, homestead vegetation is larger than homestead. The homestead vegetation and agricultural low land types also support a high biodiversity (Hasnat and Hoque 2016). Currently, the forest ecosystems in the region are decreasing rapidly due to economical demands and human interferences, such as overexploitation, deforestation, excessive trash buildup and encroachment (Salam et al. 1999; Hassan 2004). Among the artificial land use types, cropland, the major products of which are rice, jute and vegetables (e.g., cultivars consisting of gourds, beans, cabbage, cauliflower and tomatoes), was distributed broadly prior to urbanization (Shapla et al. 2015).

1.2.2. IKONOS and WV2 data

The data were obtained from the satellite imagery of IKONOS at 04:35 (GMT) on May 1, 2001, and at 04:44 on February 16, 2002, prior to urbanization and from WV2 imagery at 04:41 on December 9, 2015 (Digital Globe - Apollo Mapping, Longmont, Colorado, USA) at present stage, since IKONOS terminated data acquisition after 2014 and WV started data collection in October 2009. The resolutions of the IKONOS and WV2 sensors are 0.8 m (true color) and 0.5 m (natural color), respectively. All of the images were devoid of clouds.

These remote sensing data were integrated via ArcGIS (version 10.2). Integrated analyses were conducted after checking the quality of the pre-processed data to remove noise and unify the georeferences. These images were re-projected onto the Bangladesh Transverse Mercator (BTM) projection to record the statistics of landscape changes, because of the projected coordinate system in Bangladesh (Dewan and Yamaguchi 2009).

1.2.3 Evaluation of the vegetation indices and hierarchical classification

The categories of land use types were matched with the land use map published by the Ministry of Housing and Public Works of Bangladesh (Anonymous 2013) with a few modifications adjusted to recently developed land use patterns. The modification was made by establishing three land use types, cropland, grassland and bare land, all of which were cultivable land in the original map (Anonymous 2013). Because the map was manufactured based on various datasets consisting of topographical, geographical and historical data at a fine scale, this map was utilized as a reference during the evaluation of land use classifications.

A total of eleven VIs was investigated to confirm the accuracy of land use change detection by using error matrix prior to the construction of DT. These eleven VIs were NDVI, EVI2, EVI, GRVI, atmospherically resistant vegetation index (ARVI), green difference vegetation index (GDVI), green normalized difference vegetation index (GNDVI), difference vegetation index (DVI), normalized green (NG), ratio vegetation index (RVI) and enhanced normalized difference vegetation index (ENDVI). The four examined VIs showed higher than 65% overall accuracy, while the other VIs showed less than 50%. Therefore, the four VIs, NDVI, EVI2, EVI, and GRVI were used for the further analysis.

The four examined vegetation indices were as follows:

$$NDVI = (NIR - red)/(NIR + red) \quad (1)$$

$$GRVI = (green - red)/(green + red) \quad (2)$$

$$EVI = G \times (NIR - red)/(NIR + C_1 \times red - C_2 \times blue + L) \quad (3)$$

$$EVI2 = 2.5 \times (NIR - red)/(NIR + 2.4 \times red + 1.0), \quad (4)$$

where near-infrared (NIR), red, green and blue represent (partially) atmospherically corrected surface reflectances, L denotes the canopy background adjustment used to address the nonlinear, differential transmittance of NIR and red wavelength radiances through a canopy, and C_1 and C_2 are the coefficients of the aerosol resistance term that uses the blue band to calibrate the aerosol influences in the red wavelength. The blue wavelength ranges from 445 nm to 516 nm on IKONOS and from 450 nm to 510 nm on WV2, the green wavelength ranges from 506 nm to 595 nm on IKONOS and from 510 nm to 580 nm on WV2, the red wavelength ranges from 632 nm to 698 nm on IKONOS and from 630 nm to 690 nm on WV2, and the NIR wavelength lies between 757 nm and 863 nm on IKONOS and between 765 nm and 901 nm on WV2. Therefore, the data collected by WV2 were comparable to the data acquired using the IKONOS sensor (Table 1-1).

Table 1-1. The four wavelength bands on IKONOS and WV2 images.

Band		Wavelength (nm)	
		IKONOS	WV2
Blue	Min	445	450
	Max	516	510
Green	Min	506	510
	Max	595	580
Red	Min	632	630
	Max	698	690
Near-infrared (NIR)	Min	757	765
	Max	863	901

The NDVI refers to two spectral bands of the photosynthetic output, i.e., the red and near-infrared bands (Huete et al. 1997). The NDVI ranges from -1 to +1 and increases with an increase in the vegetation greenness. However, the NDVI is skewed by background reflectances and atmospheric interference (Karnieli et al. 2013). In addition, the NDVI is saturated in regions with a high biomass (Miura et al. 2001). To reduce these

disadvantages of the NDVI, multiple VIs modified from the NDVI have been developed (Phompila et al. 2015).

The GRVI uses green and red bands to assess deforestation, forest degradation and canopy tree phenology (Motohka et al. 2010; Tucker 1979). The GRVI often focuses on seasonal fluctuations in the greenness by evaluating the colors of leaves at the canopy surface using the green band (Nagai et al. 2012).

The EVI was modified from the NDVI by adopting numerous coefficients within the EVI algorithm (Equation 3): L = 1, C_1 = 6, C_2 = 7.5, and gain factor (G) = 2.5 (Rouse et al. 1974; Huete et al. 1994). These parameters are used to improve the sensitivity to high biomass regions and the vegetation monitoring capability of the EVI by dissociating the canopy background signal and diminishing atmospheric influences (Huete et al. 1999).

Although the EVI2 measures the vegetation greenness without a blue band (Equation 4), it resembles the 3-band EVI when the data quality is high and atmospheric effects are insignificant (Jiang et al. 2008).

A DT classifier was applied to identify the land use types using the four examined VIs. The DT was implemented depending on multiple levels of decisions based on the properties of the input datasets (Mountrakis et al. 2011).

1.2.4. Accuracy assessment of the land use classification

Validating the land use classification is a prerequisite for confirming temporal land use changes (Foody 2002). Ground truth data of stratified land use classes at 182 locations marked with GPS were used for the validation (Figure 1-1). The ground truth points were selected by using a land use map (Anonymous 2013). These locations and their adjacent areas were recorded more than once to inspect the eight land use types. Based on the measurements, the land use types on the maps were repeatedly reclassified to minimize

classification errors. The accuracies of the land use classification schemes using the four VIs and of the hierarchical classification using the DT classifier were tested using an error matrix represented by an overall accuracy and a kappa *(κ)* coefficient at each ground truth point. The ESRI ArcMap (version 10.2) software was used for the data processing, including the statistical analysis.

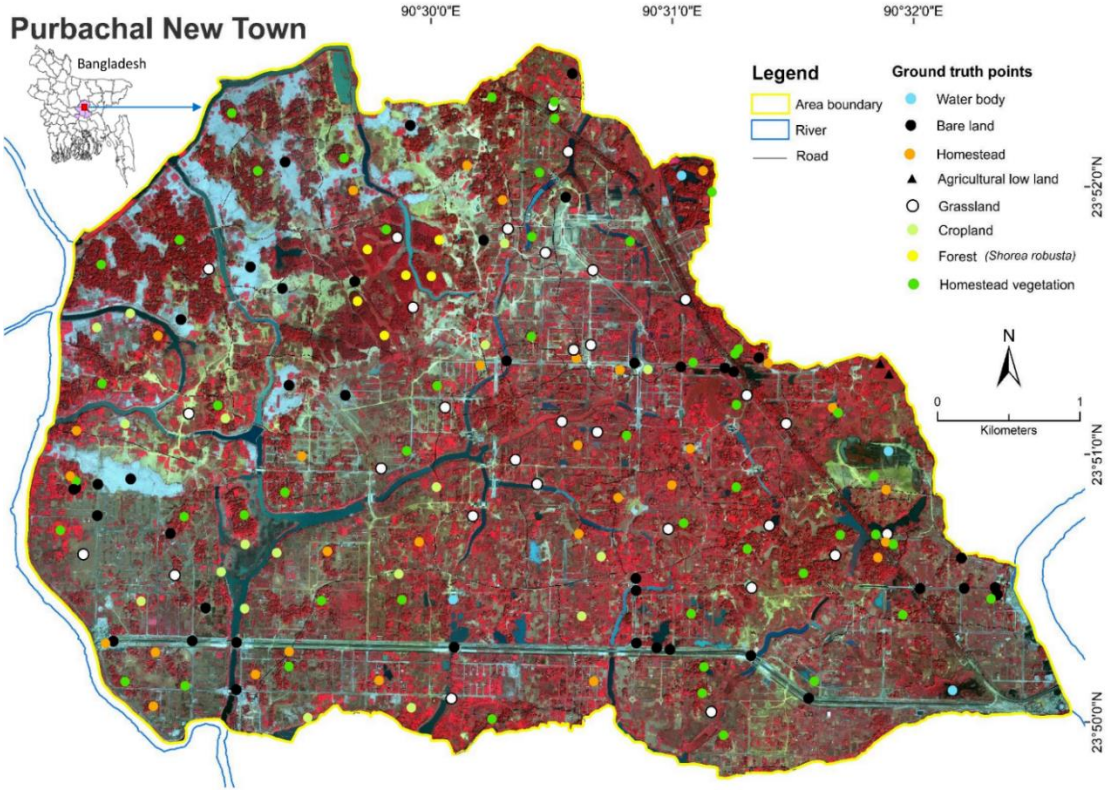

Figure 1-1. Image of Purbachal New Town in 2015 from the WV2 satellite. Two rivers, namely, the Balu and Sitalakhya Rivers, are distributed along the west and east sides of the township, respectively. The inset map at the top left shows Purbachal New Town in the country of Bangladesh. The 182 ground truth locations recorded via GPS in Purbachal New Town are shown on the WV2 natural color image using different colored circles for different land use types. The land use types were verified to assess the accuracy of the land use classification via satellite imagery and reference vegetation maps.

1.2.5. Relationships between land use types and VIs

One-way analysis of variance (ANOVA) was used to investigate the significant differences in the VI values among the land use types. When the ANOVA was significant, Tukey post hoc multiple comparison tests were applied to determine the significant differences in the VIs among the land use types confirmed using ground truth data (Zar 1999).

1.3. Results

1.3.1. Surface reflectances in the VIs

The spatial patterns of the surface greenness in 2001 and 2015 were different among the VIs (Figure 1-2). The GRVI effectively diagnosed the distributions of homestead vegetation and *Shorea* forest but often failed to discern cropland. The EVI detected the grassland distribution most correctly but could not clearly detect the *Shorea* forests. The NDVI differentiated water bodies and bare land but did not delineate the *Shorea* forest and homestead vegetation land use types, showing that the NDVI is not appropriate for classifying regions with dense green vegetation. The EVI2 distinguished vegetated land use types from non-vegetated land use types and clearly identified the homestead distribution.

The lowest NDVI value of -0.05 was obtained for water bodies due to the lack of vegetation (Figure 1-3). Homestead was detected within a few small patches with a low NDVI of 0.31 in 2001 and 0.21 in 2015, confirming that a fine-scale classification is required to detect these land use types. Homestead vegetation (i.e., vegetation enclosing homesteads) showed an NDVI of 0.91 in 2001 and 0.82 in 2015. Croplands had higher a NDVI than grassland of 0.67 in 2001 and 0.59 in 2015.

The lowest EVI values were shown for water bodies, while the second-lowest values were displayed over bare land (Table 1-2). The EVI did not separate these two

land use types clearly. The EVI of grassland was an average of 0.37, which is intermediate between the EVI values for bare land and forests. EVI values between 0.37 and 0.48 were associated with cropland and occasionally grassland, while EVI values ranging from 0.48 to 0.57 represented dense and/or deeply green vegetation.

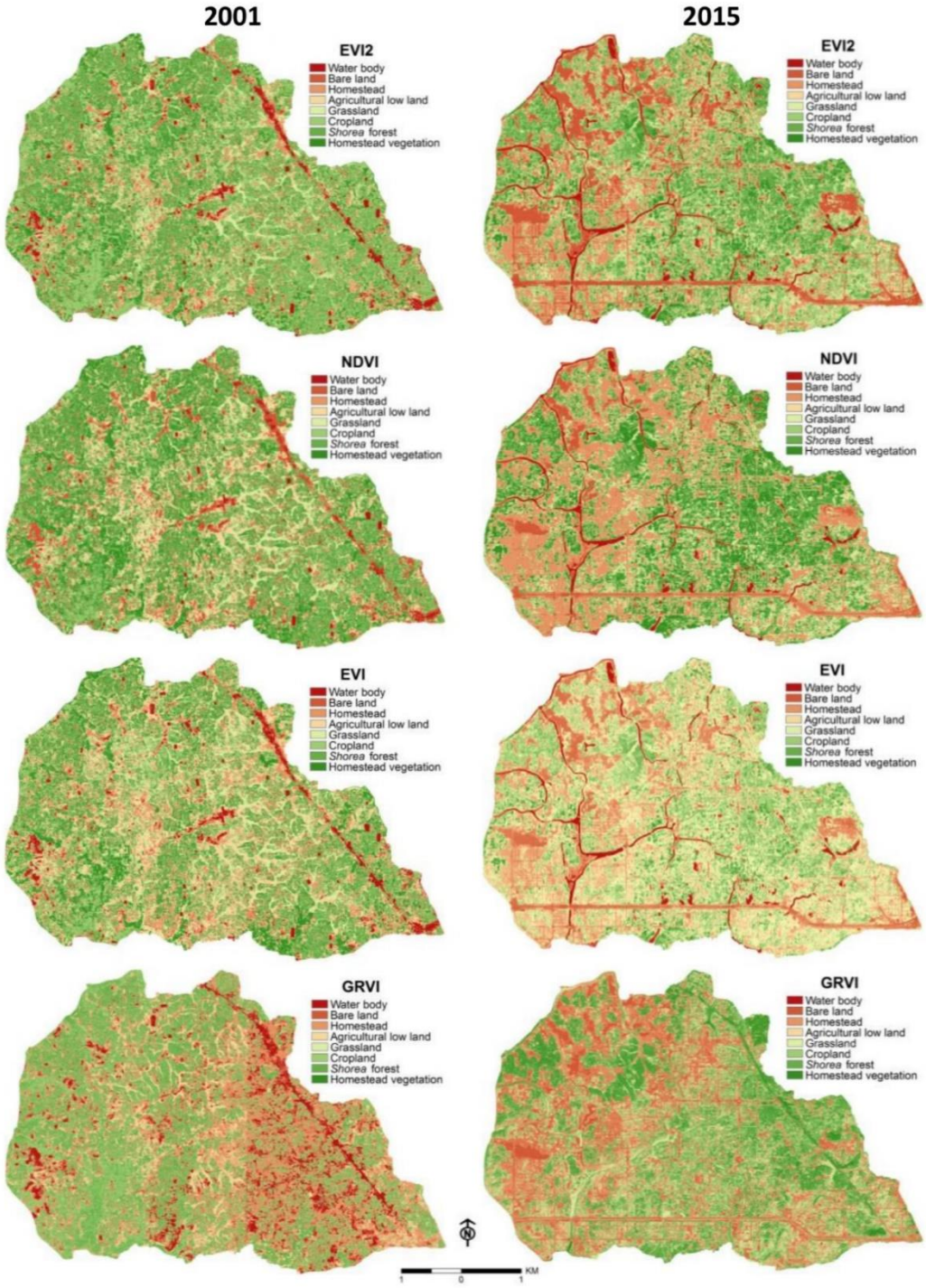

Figure 1-2. Surface greenness distributions evaluated using the four VIs based on multi-temporal information from the IKONOS and WV2 images in 2001 (left side) and 2015 (right side), respectively.

The highest EVI2 value, i.e., 1, represented dense vegetation, including homestead vegetation. The EVI2 value for *Shorea* forest was 0.97, which was the highest of the examined VIs (0.77 with the NDVI, 0.53 with the EVI and 0.25 with the GRVI). The EVI2 value for grassland ranged from 0.10 to 0.49, which is higher than those obtained with the EVI, NDVI and GRVI. The EVI2 sometimes misclassified cropland as grassland, probably because of double cropping. An EVI2 value lower than 0.10 indicated poorly vegetated land use types, such as bare land and sparse grassland. The GRVI demonstrated an appropriate detection of densely vegetated land use types, mostly due to the discrimination of *Shorea* forest and homestead vegetation. However, the GRVI did not effectively discriminate among water bodies, bare land and homestead (Figure 1-2). Non-vegetated land, i.e., water bodies and bare land, showed GRVI values of less than 0.18. Bare land and water bodies showed the lowest GRVI values of -0.04 and 0.01, respectively, while water bodies showed the lowest VI values overall. These results indicate that the GRVI performed better while distinguishing dense vegetation than other land use types characterized by sparse greenness.

In total, the NDVI had higher values than the EVI and GRVI, particularly when the reflectance was high (Figure 1-3). The GRVI occasionally showed negative values over bare land when it should have been higher than 0, which was probably due to soil interference. All of the VIs showed a clear gap between non-vegetated and vegetated land use types. However, in areas with a high vegetation, the VIs exhibited different responses to greenness.

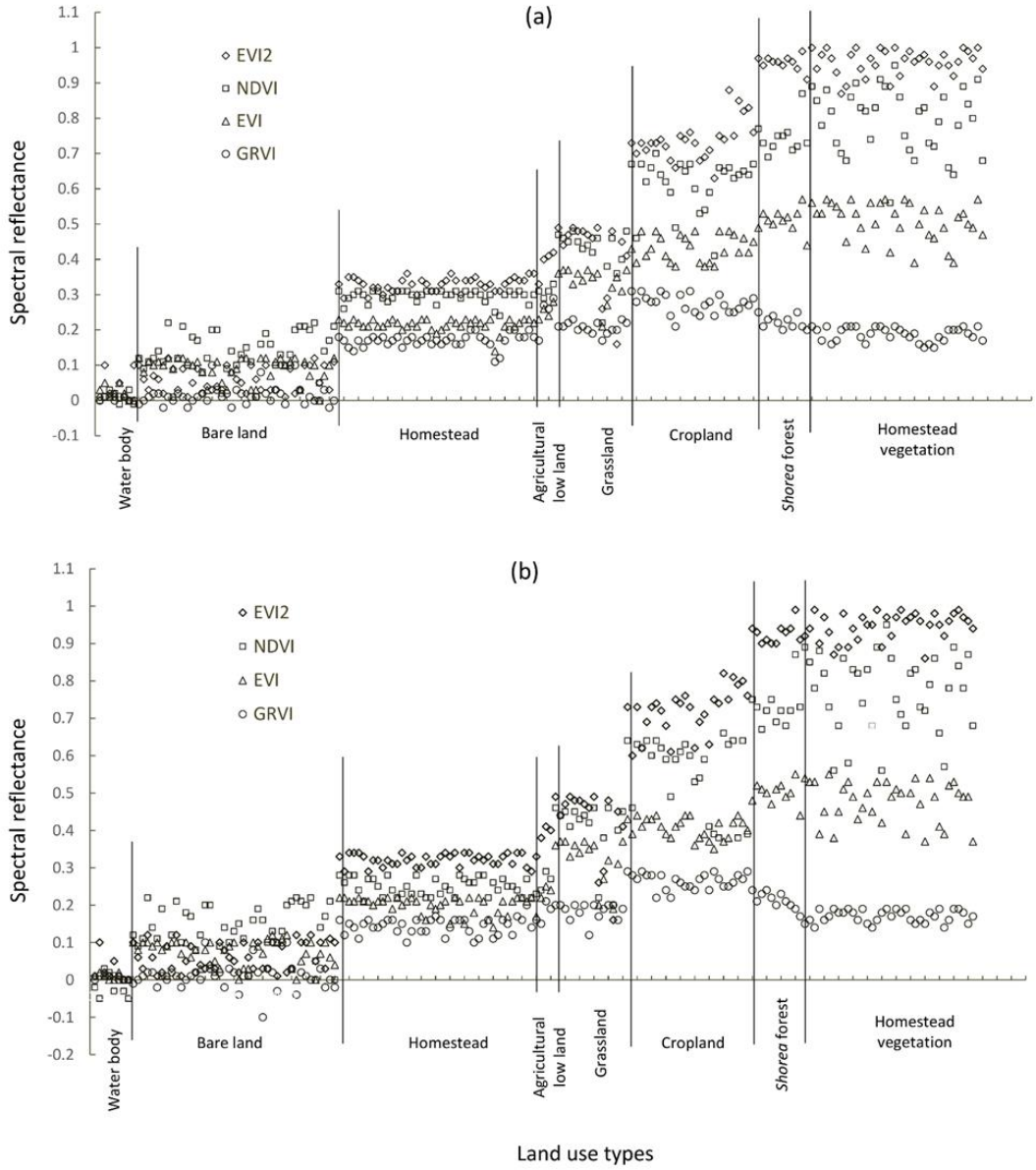

Figure 1-3. Spectral reflectance in the VIs extracted from 182 ground truth points for eight land use classes. The y-axis indicates the spectral reflectance among the four VIs, while the x-axis represents the eight land use types.

I.3.2. Validation of the VIs

The accuracies of the land type classification schemes were different among the VIs (Table 1-3). Each of the four VIs showed different values among the land use types (ANOVA, $p < 0.0001$) (Table 1-2). All of the VIs showed stable values over homesteads. The EVI2 and NDVI responses to grassland and cropland fluctuated, and the EVI

fluctuated largely over *Shorea* forest and homestead vegetation. Although the GRVI responses to *Shorea* forest and homestead vegetation were stable, the GRVI responses were lower than the responses of the other VIs.

The EVI2 exhibited different pairs of land use types except for grassland-agricultural low land, agricultural low land-homestead and bare land-water body (Tukey test, $p < 0.05$). The NDVI exhibited different pairs of land use types except for homestead vegetation-*Shorea* forest, agricultural low land-homestead and grassland-agricultural low land. The homestead vegetation-*Shorea* forest and agricultural low land-homestead pairs were not significantly different in the EVI, although the rest of the pairs were different. The GRVI was capable of distinguishing between homestead vegetation and *Shorea* forest, but the other three VIs could not differentiate these two land use types. The GRVI did not reveal significant differences in the comparisons between the other land use types ($p < 0.05$). The GRVI was most effective at differentiating the *Shorea* forest-homestead vegetation pair; meanwhile, the EVI2 and NDVI effectively detected homestead, bare land and water bodies, and the EVI effectively detected the distributions of agricultural low land, grassland and cropland.

Table 1-2. Mean and standard error (SE) of each VI for the eight land use types. All of the VIs obtained in 2001 and 2015 among the land use types are significantly different (one-way ANOVA, $p < 0.0001$). Identical letters indicate that the VIs are not significantly different between those land use types (Tukey test, $p < 0.05$).

		Water body	Bare land	Homestead	Agricultural low land	Grassland	Cropland	Forest (*Shorea robusta*)	Homestead vegetation
2001	EVI2	0.04 ±0.02 a	0.06 ±0.01 a	0.32 ±0.00 b	0.42 ±0.01 c	0.42 ±0.03 c	0.74 ±0.01 d	0.96 ±0.00 e	0.96 ±0.01 e
	NDVI	0.01 ±0.01 a	0.14 ±0.01 b	0.30 ±0.00 c	0.31 ±0.01 cd	0.42 ±0.02 d	0.62 ±0.01 e	0.73 ±0.01 f	0.79 ±0.02 f
	EVI	0.02 ±0.01 a	0.09 ±0.01 b	0.22 ±0.00 c	0.26 ±0.01 c	0.34 ±0.01 d	0.43 ±0.01 e	0.51 ±0.01 f	0.51 ±0.01 f
	GRVI	0.01 ±0.00 a	0.01 ±0.01 a	0.17 ±0.00 b	0.27 ±0.01 cef	0.21 ±0.00 dfg	0.27 ±0.01 e	0.23 ±0.01 f	0.19 ±0.00 g
2015	EVI2	0.03 ±0.01 a	0.06 ±0.01 a	0.32 ±0.00 b	0.40 ±0.01 bc	0.42 ±0.03 c	0.72 ±0.01 d	0.92 ±0.01 e	0.95 ±0.01 e
	NDVI	-0.02 ±0.01 a	0.14 ±0.01 b	0.25 ±0.00 c	0.27 ±0.02 cd	0.41 ±0.02 d	0.56 ±0.02 e	0.71 ±0.01 f	0.77 ±0.02 f
	EVI	0.01 ±0.00 a	0.08 ±0.01 b	0.2 ±0.00 c	0.24 ±0.01 c	0.33 ±0.02 d	0.41 ±0.01 e	0.50 ±0.01 f	0.48 ±0.01 f
	GRVI	0.01 ±0.00 a	0.01 ±0.01 a	0.14 ±0.00 b	0.18 ±0.02 bcdf	0.18 ±0.01 ce	0.26 ±0.00 f	0.22 ±0.01 d	0.17 ±0.00 e

1.3.3. Hierarchical classification of land use types

A hierarchical land use classification was developed using a DT classifier with the four VIs (Figure 1-4).

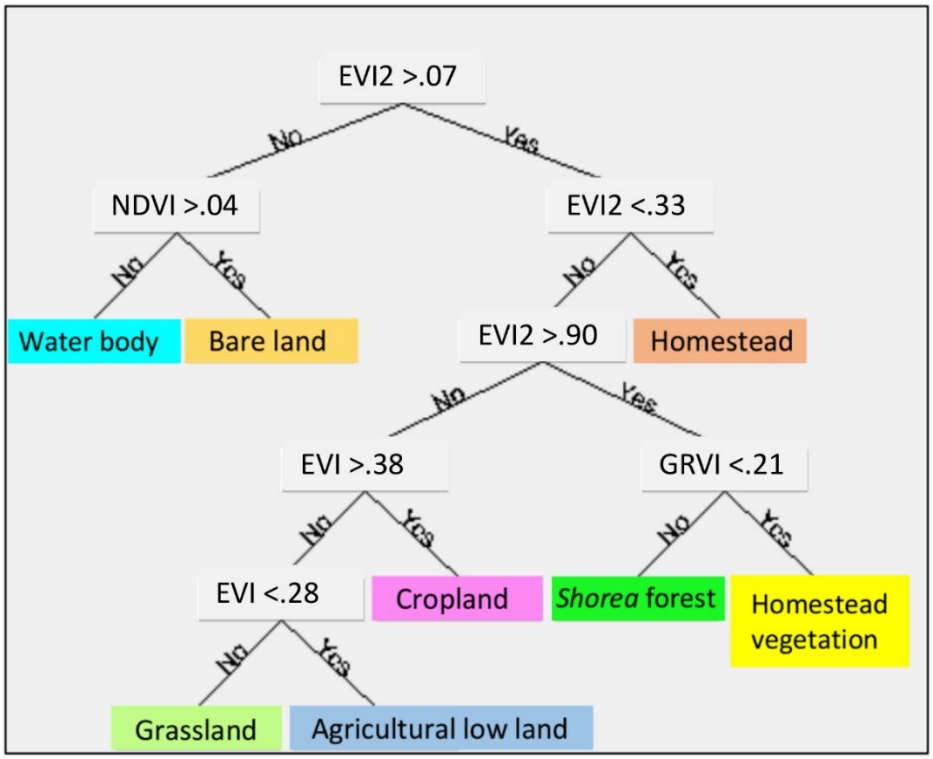

Figure 1-4. A DT constructed using the hierarchical classification of land use types. Numerals with inequality signs indicate the VI values that represent the thresholds of the classifiers.

The DT begins with the EVI2, which then separates the land use types into vegetated and non-vegetated land use types. The NDVI then separates the non-vegetated land uses into water bodies and bare land. Meanwhile, among the vegetated land use types, the EVI2 extracts the homestead distribution and the EVI detects agricultural low land, grassland and cropland. Among the four VIs, homestead vegetation and *Shorea* forest were separated only through the GRVI.

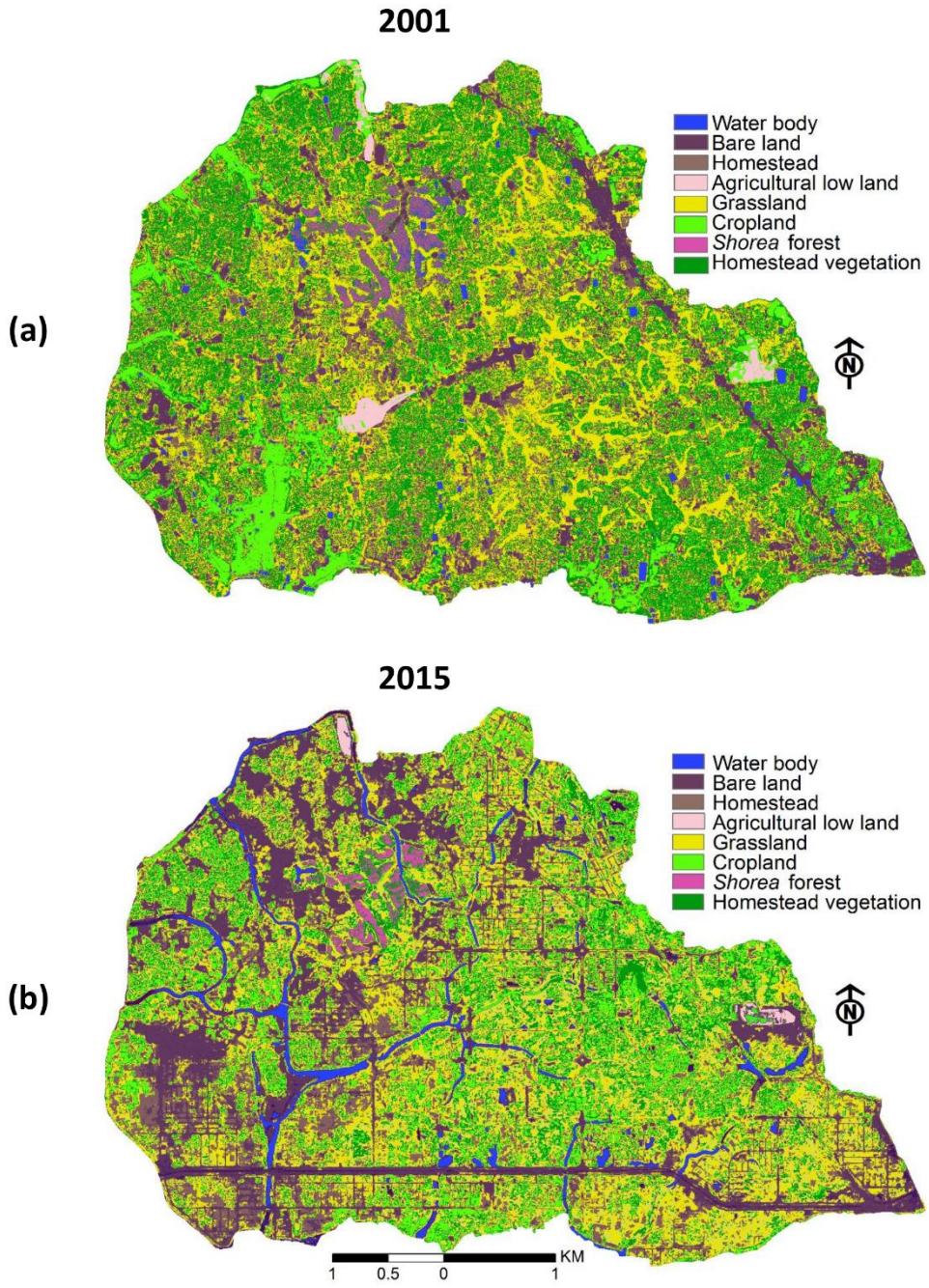

Figure 1-5. Land use maps produced through a hierarchical classification using the DT approach. These maps show the temporal changes in the land use-land cover throughout Purbachal New Town from 2001 to 2015. a) Land use patterns detected using the IKONOS sensor in 2001. The land use patterns were verified using a pre-project land use map (Anonymous 2013). b) Land use patterns in 2015 were detected using WV2 multi-spectral imagery. The land use types are represented by their respective colors.

Table 1-3. Classification accuracies examined using an error matrix of κ coefficients.

	2001		2015	
Classification	Overall accuracy (%)	κ coefficient	Overall accuracy (%)	κ coefficient
EVI2	90.1	0.88	91.2	0.89
NDVI	88.5	0.86	89. 6	0.87
EVI	66.5	0.60	67.6	0.61
GRVI	74.2	0.69	77.5	0.73
DT	96.1	0.95	97.8	0.97

The DT approach showed the highest accuracy (with an accuracy greater than 95% and a κ of greater than 0.95, see Table 1-3) during the land use classification, indicating that the DT constructed using the four VIs was the most effective at predicting the land use types (Figure 1-5). The second-highest accuracy and κ values (91.2% and 0.89, respectively) were exhibited by the EVI2 measurements from 2015, indicating that the DT effectively improved the land use classification scheme.

1.3.4. LULC changes

Based on the land use changes from 2001 to 2015 (Figure 1-5), the characteristics of the land use changes were examined (Table 1-4). Road networks and their adjacent areas were clearly observed. Homestead vegetation, grassland, cropland and homestead were the dominant land use types prior to urbanization, but more than three-quarters of the area of each land use type was lost thereafter. Approximately one-half of the area of *Shorea* forest was lost subsequent to urban growth. Since the distribution of bare land increased greatly, the reduction in the area of each land use type can be derived according to an increase in bare land originating from road construction and other related construction projects, and

the water body area was also increased due to the excavation of artificial lakes and canals. Grasses colonized in the filed up agricultural low land and consequently, the grassland increased. Since most of the water bodies were small and/or narrow, those changes were detectable only at a high resolution.

Table 1-4. Changes in the eight land use types from 2001 to 2015 based on satellite imagery.

Land use types	2001		2015	
	Area (km^2)	(%)	Area (km^2)	(%)
Water body	0.59	2.37	2.12	8.52
Bare land	0.14	0.56	16.97	68.17
Homestead	3.02	12.13	0.86	3.46
Agricultural low land	0.67	2.69	0.04	0.16
Grassland	1.03	4.14	1.06	4.26
Cropland	6.26	25.15	0.59	2.37
Forest (*Shorea robusta*)	0.77	3.09	0.42	1.69
Homestead vegetation	12.41	49.86	2.83	11.37

1.4. Discussion

1.4.1. Effectiveness of the VIs and the DT approach

A comparison among the DT and VIs indicates that all four of the examined VIs showed specific advantages and disadvantages with regard to the land use classification at a fine resolution. The reflectances of the blue and green wavelengths can characterize the spatiotemporal fluctuation patterns of VIs (Huete 1988). The EVI2 differentiated between vegetated and non-vegetated land use types without using the blue band. Only the GRVI classified dense vegetation, i.e., homestead vegetation and *Shorea* forests, probably because the GRVI is sensitive to the canopy surfaces of forests (Nagai et al. 2012). Therefore, the GRVI constituted a prerequisite for the classification of deeply green areas, i.e., forests, although the overall accuracy of the associated classification was low.

The EVI2 showed the highest accuracy among the examined VIs at a fine resolution (Kushida et al. 2015). However, the EVI2 did not effectively differentiate between homestead vegetation and *Shorea* forest. The EVI2 maintains a high sensitivity and linearity to high phytomass densities (Rocha and Shaver 2009). However, there are many difficulties when using the EVI2 to conduct a land use classification in tropical/sub-tropical regions such as Bangladesh, because persistent evergreen forests show high reflectances both in and out of season (Cristiano et al. 2014). The accuracy of the NDVI land classification was slightly lower than that of the EVI2 results. The NDVI is skewed by the background reflectance, including those of bright soils and non-photosynthetic plant organs (i.e., trash and tree trunks) (Van Leeuwen and Huete 1996). Because the examined data did not contain a substantial amount of clouds, the EVI2 and NDVI seemed to synchronize their fluctuations.

The EVI effectively classified the grassland, cropland and agricultural low land types, but it did not distinguish the other land use types, suggesting that the blue band used only by the EVI influenced the resulting land use classification. However, the EVI is distorted by the soil adjustment factor L in Equation (3), making it more sensitive to topographic conditions (Wardlow et al. 2007). Therefore, the EVI did not seem to function well.

The DT using the four VIs largely improved the accuracy of the land use classification. The accuracy of the DT was slightly different between the two surveyed years (96.1% in 2001 and 97.8% in 2015, see Table I-3). One cause of this difference was probably derived from differences in the quality of the data, i.e., with regard to the resolution, photographing conditions and sensors, from IKONOS in 2001 and from WV2 in 2015.

1.4.2. Temporal land use changes caused by urban growth

This research used highly resolved, multi-temporal satellite data to develop a methodology for assessing land use changes. The results of the VIs vary between fine and coarse resolution. The fine-scale land use classification scheme clearly detected fine-scale land use patches generated by the development of road networks subsequent to urban growth that cannot be detected during coarse-scale analysis. Accordingly, land use classification schemes are often dependent upon the resolution (O'Connell et al. 2013). Since roadways are a few tens of meters wide, high-resolution data are required for the classification of urban landscapes. Fine-scale data can delineate land cover classes more accurately, because such data can identify small and/or linear patches while retaining their shapes (Boyle et al. 2014). Ongoing urbanization has been followed by drastic changes in the land use types, biodiversity and fragile ecosystems of urbanized areas (Merlotto et al. 2012; Zhou and Zhao 2013; Pigeon et al. 2006). The urban growth of Purbachal New Town was characterized by a substantial loss of homestead vegetation and cultivable land. Furthermore, approximately one-half of native *Shorea* forests were lost, even though the master plan of urbanization considered their conservation (Hasnat and Hoque 2016). Land use changes associated with deforestation have not been detected well. The endangered *Shorea* forests are likely to be restored and conserved through the identification of small and isolated patches using the fine-scale analysis. The species distribution modeling should be executed for the restoration of the threatened ecosystems using the identified distinct small patches. Also, land transformation model would be implemented using fine-scale data to show the process of land use changes (Pijanowski et al. 2002). These approaches are the pronounced concern for the planners to protect and preserve the endangered ecosystems from being extinction.

Imagery acquired by two or more satellites is often used to examine temporal land use changes depending on the data availability. This study used two sets of satellite imagery, namely, from the IKONOS and WV2 sensors. Using multiple sensors can often cause errors in the land use classification due to heterogeneities in the spatial resolution of the data (Joshi et al. 2016; Xie et al. 2008). However, integrating the IKONOS and WV2 data resulted in a smaller error and higher accuracy; this was probably because of the finer resolutions and greater overlap of the wavelength bands. Fine-resolution data may partly resolve such errors by reducing the mismatches in the overlays of wavelength bands.

1.5. Conclusion

A DT constructed using a hierarchical classification greatly improved the classification of land use types at a fine resolution. The DT was developed using all of the four examined VIs because each VI demonstrated unique strengths and limitations. For example, the GRVI showed the lowest overall accuracy, but it was retained in the DT because the GRVI can effectively classify areas with a high greenness. The land use classification scheme using the DT clarified that the changes in Purbachal New Town are characterized by the effects of road networks on deeply green ecosystems, which are unlikely to be detected clearly at coarse resolutions. Therefore, this research showed a significant monitoring source to investigate the continuous changes in land use types and assist the planners and decision makers to develop land use management plans.

Chapter 2

Potential distribution and conservation of threatened *Shorea robusta* forest examined by Maxent modeling

2.1. Introduction

Anthropogenic activities, particularly alteration, reduction and fragmentation of habitats decline forest ecosystems and the biodiversity (Popradit et al. 2015; Tittensor et al. 2014). Urbanization postures one of the threats to global biodiversity alters the distribution of endemic species and forests (Seto et al. 2012; McDonald et al. 2008). *Shorea robusta* C. F. Gaertn. (Dipterocarpaceae) is a deciduous tall tree, naturally distributed on the Pleistocene tracts (Madhupur tracts) in Bangladesh (Rashid et al. 2006). The *S. robusta* developing the largest forest patches in this region acts a vital role in maintaining the balance of the ecosystems (Rahman et al. 2007). Nowadays, the total area of *S. robusta* forest is 0.12 million hectares of land in Bangladesh. The area explains 0.8% of the country area and 7.8% of the forest area (Hasan and Mamun 2015). The *S. robusta* forests have been declined owing to the utilization for economic and medicinal use by the agrarian rural people (Deb et al. 2014), although *S. robusta* is recorded as a "least concern" species in the Red List (IUCN 2015). This species is a keystone species to support various endangered species (Hasnat and Hoque 2016). The genus *Shorea* includes 192 species in the world, in particular, in tropical regions (Tsumura et al. 2011). Of these *Shorea* species, 34 species are endangered (IUCN 2015). Most of all *Shorea* species develop large forests and thus they can be umbrella species (Gautam et al. 2014). This also means that the

conservation of *S. robusta* forests leads the protection of endangered species on the forest floors. The *S. robusta* forests, developing more than 30 m tall, have kept the highest biodiversity and contain numerous endangered species in the region (Gautam et al. 2006; Mandal et al. 2013). Therefore, *S. robusta* was used for the representative species to examine the characteristics of the distribution of endangered and umbrella species that can be applied to decide the conservation plans.

I used maximum entropy (Maxent) model to analyze the present and future geographic distributions, because of the high precision of distribution prediction derived by the combination of locations of species and the environments (Phillips et al. 2004; Peterson and Shaw 2003). Therefore, Maxent was applied to find out the potential distributions of *S. robusta* forests, some of which had been already lost and will be altered more by global warming (Elith et al. 2006). Maxent is developed by the deterministic algorithms that are guaranteed to converge to the optimal (maximum entropy) probability distribution (Phillips et al. 2006). Maxent uses only presence data of species distribution, while the other popular distribution models, such as the genetic algorithm for rule set production (GARP) and generalized linear model (GLM), need the absence data (Elith et al. 2011; Marcer et al. 2013; Stockwell and Peters 1999). In all the models includes Maxent, the species distribution is predicted by the environmental determinants. These are climatic variables (temperature and precipitation), geology, soil property, soil type, vegetation type, etc. Since the absence data of *S. robusta* is not available, models requiring the absence data cannot be applied.

Global warming alters the distributions of species and ecosystems, owing to drastic changes in the appropriate habitats and regions (Pacifici et al. 2015; Pearson et al. 2014). The present climate in Purbachal is that the annual mean temperature is 28^{o}C and the annual precipitation is 2400 mm (Shapla et al. 2015). The urbanization in Purbachal

will increase the temperature up to 39.6ºC in maximum and decrease the precipitation < 2000 mm (EIA 2013). Two RCP scenarios of RCP4.5 and RCP8.5 were used to predict the potential distribution of *S. robusta*. RCP4.5 that means radiative forcing increase 4.5 W/m^2, which assumes that greenhouse gas emissions soothe through mid-century and decrease abruptly afterward. RCP8.5 corresponds to persistent increases in greenhouse gas emissions up to the end of the 21st century (Fisher et al. 2007; IPCC 2008). The projected temperature of RCP4.5 for 2046-2065 and 2081-2100 was 0.9 to 2.0 °C and 1.1 to 2.6 °C, while RCP8.5 was 1.4 to 2.6°C and 2.6 to 4.8 °C respectively (IPCC AR5 WG1 2013). The predicted temperature rise in Purbachal induced by urbanization matches with the IPCC scenarios of RCP4.5 and RCP8.5. Therefore, these two scenarios were applied to predict the changes in *S. robusta* forest in this century.

The major objectives of this study were: 1) assessing the distribution and vulnerability of *S. robusta* forests in Purbachal and the environmental determinants by Maxent model, 2) predicting the potential future distribution of *S. robusta* forest under RCP4.5 and RCP8.5 at local scale, and 3) discussing the conservation and management strategies for protecting the *S. robusta* forests.

2.2. Materials and methods

2.2.1. Study area and species

S. robusta is distributed in Purbachal (23°49'45" - 23°52'30"N and 90°28'20" - 90°32'43"E) and its neighboring areas, Bangladesh (Figure 2-1). Purbachal covers an area of 2489 ha which includes a large terrace area of Madhupur tracts developed in the Pleistocene Era in the central part of Bangladesh (Zaman 2016). The monthly average temperature varies from 10 ºC to 34ºC and annual precipitation is from 2000 mm to 2700

mm with acidic, red-brown terrace soil and low organic matter content (BBS 2013). The expansion of urban areas in Bangladesh leads the reduction of natural ecosystems, represented by *S. robusta* forests. Therefore, the prediction of the future distributions of *S. robusta* forests was the priority for saving the biodiversity.

S. robusta exists as a large continuous belt and supports diverse biological resources (Alam et al. 2008). There are 24 climbers, 27 grasses, 3 palms, 105 herbs, 19 shrubs and 43 trees in *S. robusta* forests of Madhupur tracts in Bangladesh (Green 1981). *S. robusta* often grows on deep, moist, acidic (5.1 - 6.0), fine-textured (sandy to silty loam) and productive soils in south-ecntral Asia, including Bangladesh, with high temperature and rainfall (Dhar and Mridha 2006). *S. robusta* facilitates the diversity of forest floors in the regions (Kabir and Ahmed 2005). When the forest canopy is dominated by *S. robusta*, the forest allows the establishment of numeral associated species with various growth forms, trees, shrubs, herbs and climbers (Banglapedia 2008).

For silvicultural management, *S. robusta* forests has been maintained as coppice forest (Rahman et al. 2010). Nowadays, the agroforestry, as well as coppice forestry, is applied in a few regions (Alam et al. 2008).

2.2.3. Data sampling

The localities of *S. robusta* in the Purbachal were collected in 2016 and 2017 by field investigations. I recorded 165 localities that included all inhabitants and isolated patches of *S. robusta* forests using GPS (Garmin 64, Garmin Corporation, Taipei, Taiwan). The localities of *S. robusta* before the urbanization were extracted from the satellite imagery of IKONOS at 04:35 (GMT) on May 1, 2001 and 4:44 on February 16, 2002 and WorldView-2 (WV2) at 04:41 on December 9, 2015 (Digital Globe - Apollo Mapping, Longmont, Colorado, USA). These GPS data and remote sensing data were integrated via

ESRI Arc-map (version 10.2) for data processing. The analyses were conducted after checking the quality of pre-processing data to remove the noise and unify the geo-references (Dewan and Yamaguchi 2009).

Pearson's correlation coefficients, *r*, were used to detect the multi-collinearity concerning 11 environmental variables. When *r* was higher than 0.81 the two variables considered to be autocorrelated. Based on the importance of variables on *S. robusta* regeneration, the weaker variables were excluded (Sarma and Das 2009). These variables were: soil organic matter, phosphorus (P) and potassium (K).

Finally, I selected 8 environmental variables, including two climatic, two physicals and four soil variables to investigate species-environmental relationships. The climatic data, i.e., precipitation and temperature, were provided by BMD (2017). The data of elevation and geomorphology were obtained from RAJUK (2016). Geomorphology was defined as (RAJUK 2016): the physical features of landscape considered as the graphical inventories of landforms and surface (i.e., road, canal, marshland, homestead, homestead vegetation, water bodies, agriculture low land, and *Shorea* forest etc.). Therefore, the unit of geomorphology is meter. The data of pH, organic matter, phosphorus (P) and potassium (K) in soil were obtained from SRDI (2015). Organic carbon (OC), calcium (Ca) and nitrogen (N) in soil were derived from BCA (2006). All of these data were converted into the format of ASCII raster grids with the same geographic boundary of which cell size was 9.99×9.99 m^2 followed by WGS 1984 Longitude-Latitude projection.

2.2.4. Analyses of species distribution

Green-red vegetation index (GRVI) was used to evaluate the density of *S. robusta* (Xue and Su 2017) because GRVI detected the large canopy density and coverage more precisely. The equation of GRVI is:

$$GRVI = (green - red)/(green + red), \text{ range: } -1 \text{ to } 1 \quad (1),$$

where green and red means the reflectance of green and red bands, respectively. GRVI ranging from 0.22 to 0.23 showed the most plausible distribution of *S. robusta* forests. The presence of *S. robusta* forests in the previous (2001) and current (2015) stages was examined by GRVI under ArcGIS to investigate the accuracy of distributions predicted by Maxent. The sensors of two satellites, IKONOS and WV2, were used. The data in 2001 and 2015 were obtained from IKONOS and WV2, respectively, depending on the data availability. The green bands range from 506 nm to 595 nm on IKONOS and from 510 nm to 580 nm on WV2. The red bands range from 632 nm to 698 nm on IKONOS and from 630 nm to 690 nm on WV2. The resolution is 0.8 m on IKONOS and 0.5 m on WV2. Therefore, the quality and quantity of data were not different largely between the data obtained from the two satellites.

2.2.5. Maxent modeling

Maxent (version 3.4.1) was used to predict the species distribution (Phillips et al. 2018), because it performs well even with small sample sizes (Kumar and Stohlgren 2009). In this model, 75% of data are selected for the occurrence localities as training data and 25% are reserved for testing the model (Phillips 2008). The algorithms run on the 10 selected localities, taking advantage of these available data to provide the best estimates of the

species potential distributions. I used the threshold-independent options on the model including the regressions of linear, quadratic, product and hinge features (Merow et al. 2013) to estimate the effects of environmental variables on *S. robusta*. The logistic threshold with 10 percentile training presence was selected to explain the least possibility of suitable habitat because the data were combined from various sources with some probable errors. The suitable habitat was predicted by this threshold using 90% of the data to develop the model (Phillips et al. 2006). Jackknife analyses were executed to determine variables that reduce the reliability of the model while omitted. Receiving Operator Curve (ROC) was used to evaluate the confidence of model results (Qin et al. 2017). When Area Under the Curve (AUC), ranging from 0 to 1, is over 0.50, it specifies that the distribution is not random. The value of 1 specifies the complete discrimination (Fielding and Bell 1997). The optimal distribution areas were predicted from 0.62 to 1.00 as the most suitable regions (Yang et al. 2013).The results were imported into ArcGIS for the further analysis.

2.3. Results

2.3.1. Previous and present occurrences of S. robusta

GRVI indicated that the forests were distributed mostly in the northern part of Purbachal (Figure 2-1). The distribution of *S. robusta* forests in 2001 was larger than the distribution in 2015. The area of *S. robusta* was 0.77 km^2 in 2001 before the urbanization and was 0.42 km^2 in 2015 at recent stage. These indicated that about a half of forests were lost by the urban growth. The major patches of *S. robusta* were distributed including a few dissected small patches in 2001. One of the patches including all the dissected minor patches has been removed by the urban growth.

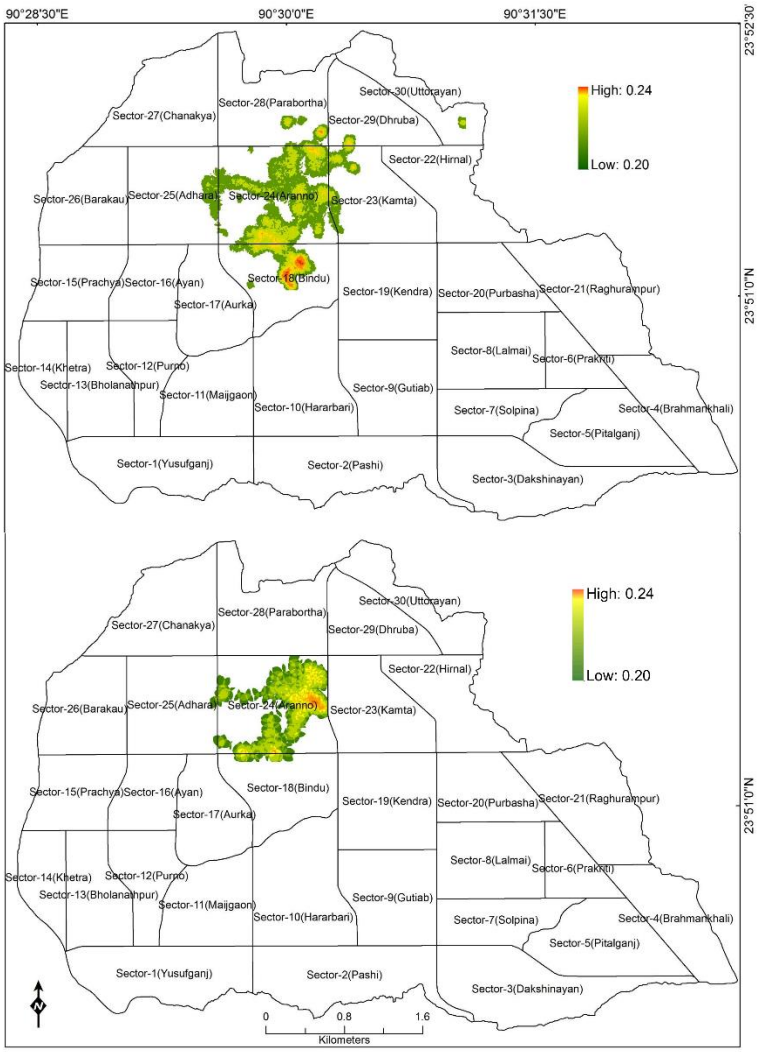

Figure 2-1. Densities of *Shorea robusta* in Purbachal, estimated by GRVI; a) density of *S. robusta* in 2001 at 0.8 m resolution, b) density of *S. robusta* in 2015 at 0.5 m resolution.

2.3.2. Models and evaluation

The algorithm in Maxent converged at 400 iterations. At the time, threshold-independent ROC analysis indicated that the distribution of forest was not random before and at the recent stage. The training AUC was 0.97 ± 0.01 (mean with standard deviation) and testing AUC was 0.96 ± 0.01. Therefore, the distributions obtained by Maxent were accurate and were used to the further analyses without the conjecture forests.

2.3.3. Potential distribution in current stage

Maxent indicated that the suitable regions for *S. robusta* were distributed in the central northwestern part, associated with the current distribution (Figure 2-2). *S. robusta* potentially developed the forests in the north-western, central-northern and central-south-eastern parts. The models showed 1.02 km^2 of distributional areas but the present area was 0.42 km^2. The most suitable regions were predicted > 0.62.

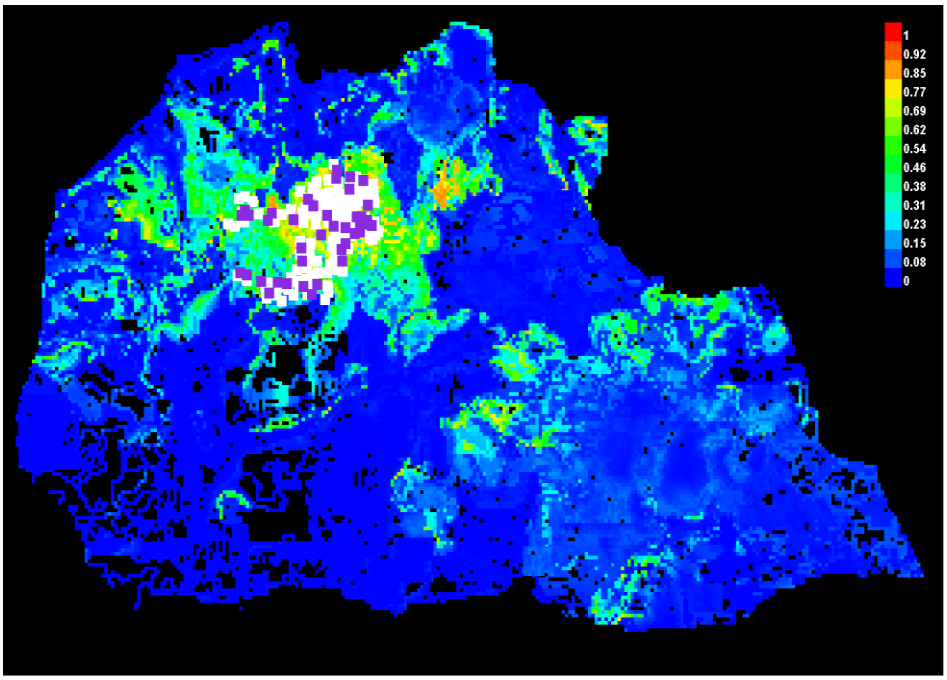

Figure 2-2. Predicted potential geographic distributions of *S. robusta* determined by 165 location records and eight examined environmental variables in Purbachal, Bangladesh. Warmer colors show the prediction of presence is more accurate. White squares show the presence locations used for training and violet squares show test locations.

2.3.4. Analysis of variable contributions

I checked the relative significance of these variables for *S. robusta* by a Jackknife test (Figure 2-3). These results showed that soil pH achieved the least gain while N explained the distribution well. The precipitation was the most important environmental variable. Of

the eight examined environmental variables, annual precipitation and N showed the highest contribution percentages, > 30% (Table 2-1). The cumulative contribution of annual precipitation and N were 67.9%. These indicated that the distribution of *S. robusta* was predicted mostly by these two variables. Ca and OC in the soil showed approximately 10% of contribution.

Table 2-1. The contribution percentages of the eight environmental variables used to predict the distribution of *S. robusta* in Purbachal.

Environmental variables	Contribution (%)
Annual mean temperature (ºC)	6.2
Annual precipitation (mm)	37.8
Geomorphology (m)	5.2
Elevation (m)	0.3
Soil calcium (meq/100g)	11.1
Soil organic carbon (kg/Acre)	9.1
Soil nitrogen (kg/Acre)	30.1
Soil pH	0.2

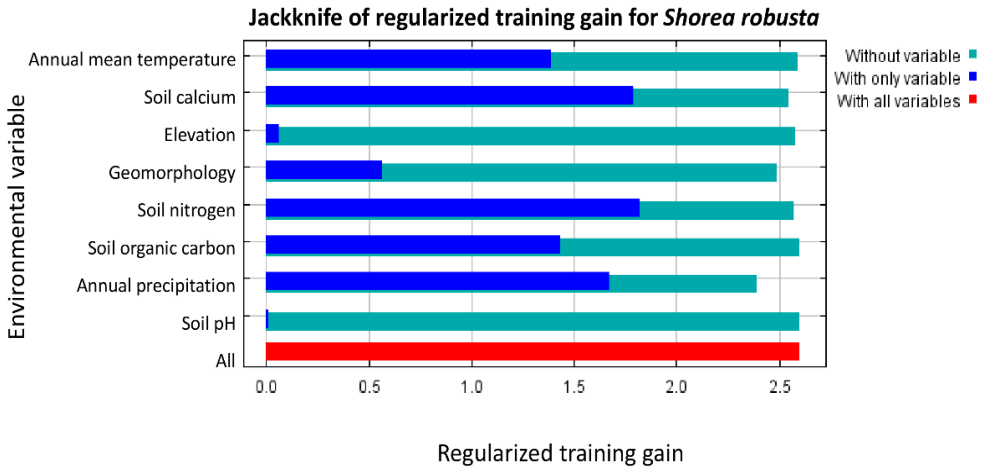

Figure 2-3. The relative importance of environmental variables for *Shorea robusta* in Purbachal evaluated by Jackknife test.

The response curves of the environmental variables on the prediction of *S. robusta* distribution showed that the precipitation, the prime determinant on the distribution of *S. robusta* (Table 2-1), was optimal in 2700 mm (Figure 2-4). In addition, the distribution

was limited in the areas with high precipitation. The optimum mean annual temperature was 28°C, although the contribution was low probably because of the narrow range between 25°C and 28°C. The ground levels in Purbachal varied with the dominating average land level at +6.0m which occurs above the normal flood level. Geomorphology showed the concentration of *S. robusta* forests in the ground level from a minimum of < 2m to a maximum of > 9m. Of the soil variables, N determined the tree distribution well. The forest tended to develop with high N. Although Ca and OC in the soils had lower contributions than N, the forests favored the high concentrations. The forests established in areas with moderate elevation, ranging from 400 m to 900 m and showed that the forests were not developed at low and high elevation.

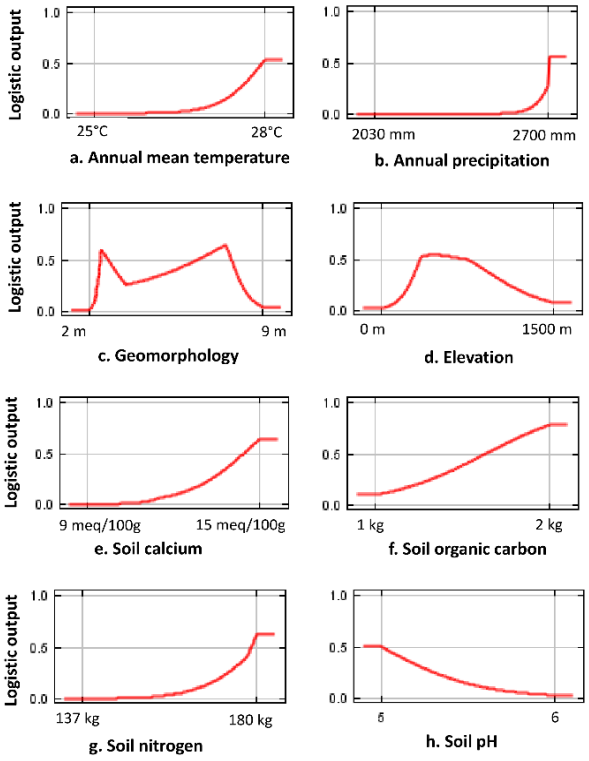

Figure 2-4. Response curves of the eight environmental variables for predicting the future distributions of *S. robusta* forests.

2.3.5. Predicted potential distribution

The area of *S. robusta* forest was 0.42 km^2 in 2015. The two RCP scenarios predicted the two types of future distribution of *S. robusta*, e.g. RCP4.5 in 2046-2065 > RCP4.5 in 2081-2100 > RCP8.5 in 2046-2065 > Current > RCP8.5 in 2081-2100. The forest areas predicted by RCP4.5 increased 0.09 km² in 2046-2065 and 0.06 km² in 2081-2100 (Figure 2-5).

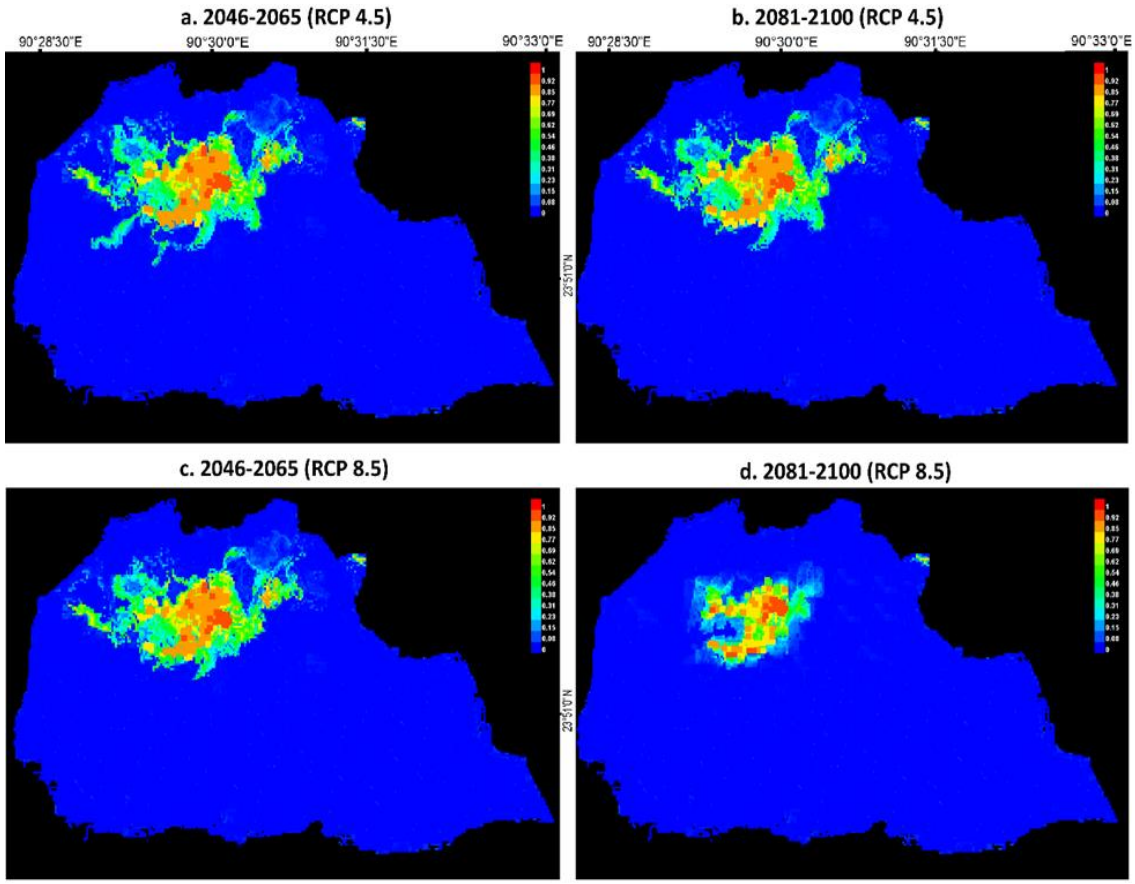

Figure 2-5. Distributions of *S. robusta* predicted based on two RCP scenarios. a. RCP4.5 (2046-2065), b. RCP4.5 (2081-2100), c. RCP8.5 (2046-2065), and d. RCP8.5 (2081-2100).

The scenario of RCP8.5 predicted 0.04 km² increase in *S. robusta* forests in 2046-2065 and 0.05 km^2 decrease in 2081-2100. However, the *S. robusta* forests present in the southern parts will be decreased even if the RCP4.5 scenario is applied. These indicated that the effects of climate change on the distribution of *S. robusta* were different regionally

even at a large scale within 24.9 km^2. Maxent results showed that climatically-suitable habitats for *S. robusta* decline by 86.5% by 2100 under RCP8.5.

2.4. Discussion

2.4.1. Distribution of S. robusta *forests and its environmental factors*

Since the potential distribution of *S. robusta* forests enclosed the current distribution, the current distribution was restricted or reduced by human disturbances rather than natural disturbances. In fact, various human activities, such as exploitation, deforestation, encroachment, litter collection and cultivation, are observed frequently in this region (Salam et al. 1999).

The global warming may not change their distribution and area greatly, except for the worst scenario for the long term. Of the two climatic variables, precipitation, and temperature, the precipitation was the prime determinant for the distribution of *S. robusta* forests. The structures, such as forest height and canopy area of tropical rainforests are primarily determined by the amount of precipitation (Powers et al. 2009). Since *S. robusta* becomes more than 30 m tall, high precipitation is required to develop the forests. In addition, rainfall and humidity determine the species richness, diversity and floristic composition in *S. robusta* forests (Kushwaha and Nandy 2012). In contrast, the temperature weakly affected the distribution, because of the narrow range.

Of the soil chemistry, N was the most important factor that determined the distribution of *S. robusta*. Large tree species, including *S. robusta*, require the high amount of N in the soil (Hasan and Mamun 2015). Since N is often supplied by precipitation in tropical regions (Cape et al. 2001), N in soil acted as the determinant of distribution as well as precipitation. N distribution was likely to be matched with

the precipitation distribution, although N in the soil is transferred by rain and the resultant movement by erosion (Cregger et al. 2014). Therefore, the N was not autocorrelative to the precipitation at the scale of present study and affected the distribution, independent of the precipitation patterns. Ca and OC in the soil affected the distribution, although these two chemicals contributed to the distribution lower than N. OC improves soil structure, water-nutrient relationships, and supplies carbon in the soil, and Ca increase the ability of soil to support regeneration of *S. robusta* (Ankanna and Savithramma 2012). Geomorphology contributed slightly to the *S. robusta* distribution. *S. robusta* forests prefer to grow in the ground level from 2.5 m to 7.5 m above the normal flood level and at the moderate elevation of 500 m - 900 m, because this species does not tolerate waterlogging in the lowlands (Rai and Rai 1994). The *S. robusta* is intolerant to low temperature, low fertility, and low water availability to the hilltops even in the study site (Ulvdal 2016). Soil pH contributed least to the forest distribution because of homogeneity.

2.4.2. Impact of RCP scenarios

When the annual temperature was over 34°C, *S. robusta* colonization became difficult. The RCP4.5 predicted an increased area of *S. robusta* habitat for both 2046-2065 and 2081-2100. The rises of mean temperature caused positive influence on habitat regeneration of *S. robusta*, while this species colonizes well up to 34°C (Rahman et al. 2007). Therefore, the impacts of climate change predicted by RCP4.5 were not strong on the distribution of *S. robusta*. A few small patches of *S. robusta* forests will disappear in the southern part, even though the RCP4.5 scenario is conservative.

The most serious scenario, RCP8.5, predicted that *S. robusta* forests decrease greatly, owing to the extremely high temperature, while the optimal annual mean temperature for the growth of *S. robusta* is around 28°C (Das and Alam 2001; Gautam and Devoe 2006). RCP 8.5 scenario predict the reduction of precipitation while temperature

increases by the end of the 21st Century (Seneviratne et al. 2012). The amount of rainfall is decreasing in the central and northern parts of Bangladesh over the time and will decrease up to 5 mm in the future (Shahid and Khairulmaini 2009; Endo et al. 2015). Even in the present, rainfall in Bangladesh tends to decrease (2 mm/100 years) (Rouf et al. 2011). Increase in temperature and decrease in rainfall resulted in unsuitable climate for *S. robusta*.

2.4.3. Conservation planning implication

Maxent generated exquisite information for conservation and management of *S. robusta* by predicting the potential distributions with detecting the important environmental variables, precipitation and N. Of these, precipitation is often determinant on ecosystem distribution at small scale (Lewis et al. 2017). However, N has not been focused well, probably because the distribution of soil types is tightly related to the precipitation at small scale (Cregger et al. 2012). Here, I investigated at relatively large scale. At the large scale, soil factors are often more important with climatic factors (Rennenberg 2002). Therefore, I have to consider the scale-dependent environmental factors when I handle the models for the prediction of species distribution that can predict the potential distribution precisely (Sandman et al. 2013). By using Maxent, I construct valid plans on conservation and restoration of vulnerable forests. A precise inventory of the encroached *S. robusta* forest is essential to develop a feasible land reclamation plan.

2.4.4. Limitation and uncertainty of model prediction

Although Maxent detected the localities and environmental factors of *S. robusta*, the interpretation should consider a few limitations. The limitation and uncertainty in interpretation are mostly derived from the prediction of climate change induced by

greenhouse gases and aerosols (Seneviratne et al. 2012). In this study, the scenario is decrease in rainfall. However, the prediction of temperature and rainfall has been controversial (Schneider 1989). As Maxent model indicated, the distribution of *S. robusta* was sensitive to precipitation even at a narrow range. Therefore, the model prediction had a cascade structure from climate change model to species distribution model. This means the precise model is required to predict species distribution.

2.5. Conclusion

Precipitation was found as a key driver to the distribution of *S. robusta* for 2020 under HadClim Emission scenario SRES-A1B (Chitale and Behera 2012). Increased temperature and decreased precipitation causes unsuitable climate conditions for *S. robusta* forests, which lead to local extinctions of this species (Shahid 2010). Maxent results suggested that not only climatic factors but also edaphic factors are important for the potential distribution of *S. robusta*, which was not stated by previous researches. Maxent in South and Southeast Asia suggests that the *S. robusta* distribution will decline in Bangladesh by 2070 under RCP4.5 and RCP8.5 (Deb et al. 2017). Our results derived from Maxent model predicted that the suitable habitats for *S. robusta* were likely to be affected most by the climate change and will decline under the scenario of RCP8.5 by 2100. These differences are related to the observed scales and should be considered for the conservation of threatened tropical and sub-tropical forests.

Chapter 3

Leaf reflectance spectra and species traits towards plant functional groups

3.1. Introduction

Plant functional group (PFG) is developed by grouping species attributes, such as morphology, physiology and life-history, to investigate the structure and function of ecosystems (Boutin and Keddy 1993). PFG is likely to be characterized by spectral reflectance patterns because of photosynthesis abilities, represented by vegetation index (VI) (Ustin 2004). Most VIs use two or three wavelength bands, e.g., red and near-infrared (NIR) bands used by normalized difference vegetation index (NDVI) and green and NIR by green-red vegetation index (GRVI). These suggest that the reflectance patterns are tightly related to the photosynthetic strategies of plants (Evans 2013). Each plant species has each specific spectral reflectance patterns, depending on the leaf and stem structure and morphology, such as growth form, leaf trait and phenology to adapt the environments (Kooyman and Rossetto 2008; Tsuyuzaki and del Moral 1995). The other traits related to photosynthesis should also be investigated, e.g., phenology, morphology, structure, branch, flower, fruit, propagation, seed, soil pH and elevation (Cortois et al. 2016; Baxendale et al. 2014), because these traits specifies the structure and functions of the species resulting varied leaf spectral reflectance (Klančnik et al. 2015; Noda et al. 2016). However, few researches have been conducted to clarify the relationships between PFG and spectral reflectance (Asner et al. 2008).

There are two approaches to develop PFGs, inductive and deductive methods (Duckworth et al. 2000). Here, the deductive method was applied to develop PFGs to examine PFGs that are classified by numerical similarities between the species.

I hypothesized that PFGs were related to the spectral reflectance patterns. To examine this, PFGs were constructed only by spectral reflectance patterns of 112 species of which taxonomical and ecological traits were diverse. Then, PFGs were investigated by 48 traits, including growth form, morphology, phenology and others described above. The growth form trait is the structural pattern of individual plant species consisting of the similar common habit of growth. Finally, the leaf spectrum variabilities was discussed with the PFGs.

3.2. Materials and methods

3.2.1. Study area

Purbachal is located in eastern-central Bangladesh (2,489 ha , 23°49'45" - 23°52'30"N and 90°28'20" - 90°32'43"E) (Figure 3-1). The area includes floodplains and terrace developed in Pleistocene Era. The study area is surrounded by two rivers on the west and east sides. The monthly temperature varies from 15° - 24°C in January (winter) and 26° - 33°C in May (summer). The annual precipitation is approximately 2400 mm (Shapla et al. 2015). The dry season is usually from December to February and the wet season is from June to September (Rahman et al. 2016b). The soil type is an acidic red-brown terrace soil (pH = 4.5 - 6.5) with low organic matter content (0.8 - 1.8%) (Begum et al. 2009; Khan et al. 1997). The area is consisted of old alluvium and elevated plateau covered by jungles with hillocks (9 -19 m) (Harun-Er-Rashid 2012).

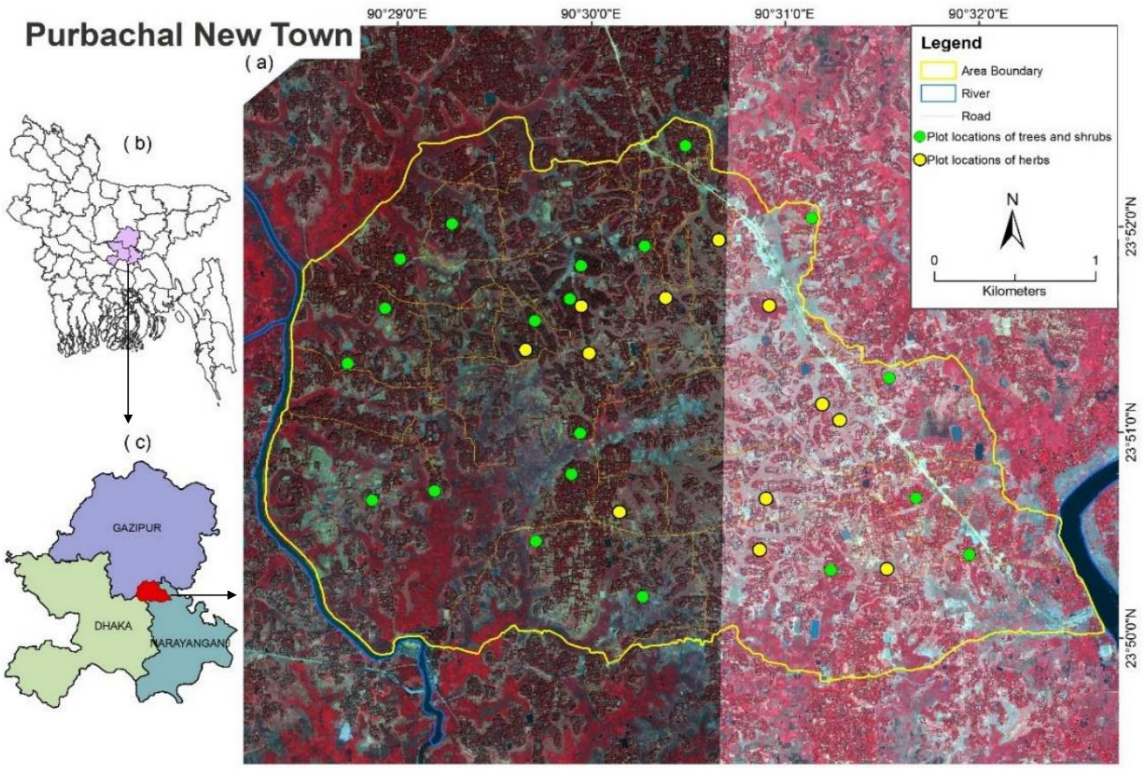

Figure 3-1. Plot locations for spectral measurements of trees and shrubs shown by green dots and herbs shown by yellow dots in Purbachal enclosed by yellow line, (b) location of Purbachal in Bangladesh, and (c) location of Purbachal in Gazipur and Narayanganj District adjacent to Capital Dhaka.

Most plants are deciduous in the study area. The potential climax forest is dominated by tall trees, such as *Mangifera indica* L., *Shorea robusta* C. F. Gaertn, *Artocarpus heterophyllus* Lam., *Albizia lebbeck* (L.) Benth. The coordinate shrubs are *Clerodendrum infortunatum* L., *Grewia serrulata* DC., *Melastoma malabathricum* L. Herbs are *Axonopus compressus* (Sw.) P. Beauv., *Agrostis canina* L., etc. (Basak and Alam 2016).

3.2.2. Acquisition and processing of spectral data

The spectral reflectance data were collected from three or more leaf samples on each of 112 species in the summer of 2017 in 32 randomly-selected sites based on WorldView-2

satellite image (Figure 3-1). The spectral signatures were obtained by a portable spectroradiometer (PSR-1100F, Spectral Evolution Inc., Lawrence, USA) with an optical fiber. This spectroradiometer measures the reflectance between 320 nm and 1100 nm at 1.5 nm intervals. The reflectance was calibrated for radiance and/or irradiance by the standard using NIST (National Institute of Standards and Technology) traceable sources (Marshall 1998).

Single reference was scanned and the dark current of instrument was measured before scanning each target under the equivalent illumination for the same sample under the darkness. The measurement was undertaken during 10 AM and 3 PM under sunny skies at 5- minute intervals. The measurements were acquired directly with no fore-optics mounted and held at 2.5 cm above the adaxial leaf surface. The spectral data were analyzed using DARWin Sp software (version 1.4.6247, Spectral Evolution, Inc., Lawrence, USA). The radiometric calibration coefficients of fiber optic field of view 8° lens with enabling reflectance spectroscopy were used to record the adaxial reflectance spectra of the leaves. The spectral reflections were measured from 320 nm to 1100 nm with 3.2 nm resolution, 1.5 nm sampling band width by a fiber optic cable with right angle diffuser (6-12V power, 5.5"× 2.5" × 6.5" dimensions and 7.5-1000 ms integration time).

3.2.3. Analysis of spectral data and species traits to PFGs

Species traits were vegetative, growth form, phenology, morphology and seed biology (Leishman and Westoby 1992). The species traits were collected from the references (Ahmed et al. 2009a; Ahmed et al. 2009b; Ahmed et al. 2009c; Ahmed et al. 2008a; Ahmed et al. 2008b; Ahmed et al. 2008c; and Siddiqui et al. 2007). The cluster groups of 112 examined species were developed by Ward's cluster method using Euclidean distance

of reflectance patterns. The size of the trees in four groups were calculated by shape index (SI).

$$SI = \text{Tree height}/DBH$$

Where, DBH is the diameter at breast height. When one-way ANOVA showed significant differences among the groups, Steel-Dwass multiple comparisons were used to characterize each cluster group based on the 48 species traits at $p < 0.05$ (Table A-1) (Zar 1999).

3.3. Results

3.3.1. Species groups using leaf reflectance spectra

There were 68 trees, 17 shrubs, 12 herbs, 10 grasses and 5 climbers of the 112 examined species. The 112 species were classified into four groups A - D (Figure 3-2). Groups A to D included 17, 11, 34 and 50 species.

There were three peaks of reflectance as a whole (Figure 3-3), one peak was at and around 550 nm (hereafter, i.e., GREEN), the other two peaks were in NIR wavelength between 700 nm and 900 nm and between 1000 nm and 1100 nm. The division of groups was derived mostly from these two wavelength ranges. Groups A and B, separated firstly from groups C and D, showed higher reflectance at GREEN, and NIR than Groups C and D. Group B was separated from Group A by the highest reflectance at all of the bands. Group D was separated from Group C by the lowest reflectance throughout the examined range of wavelengths. In particular, Group D did not form clear peaks of reflectance at GREEN.

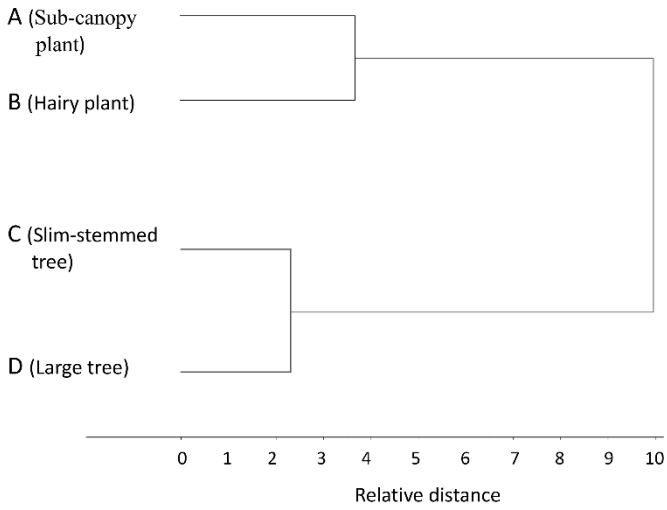

Figure 3-2. Four PFGs grouped by Ward clustering method with the Euclidean distance of spectral reflectance patterns of 112 species.

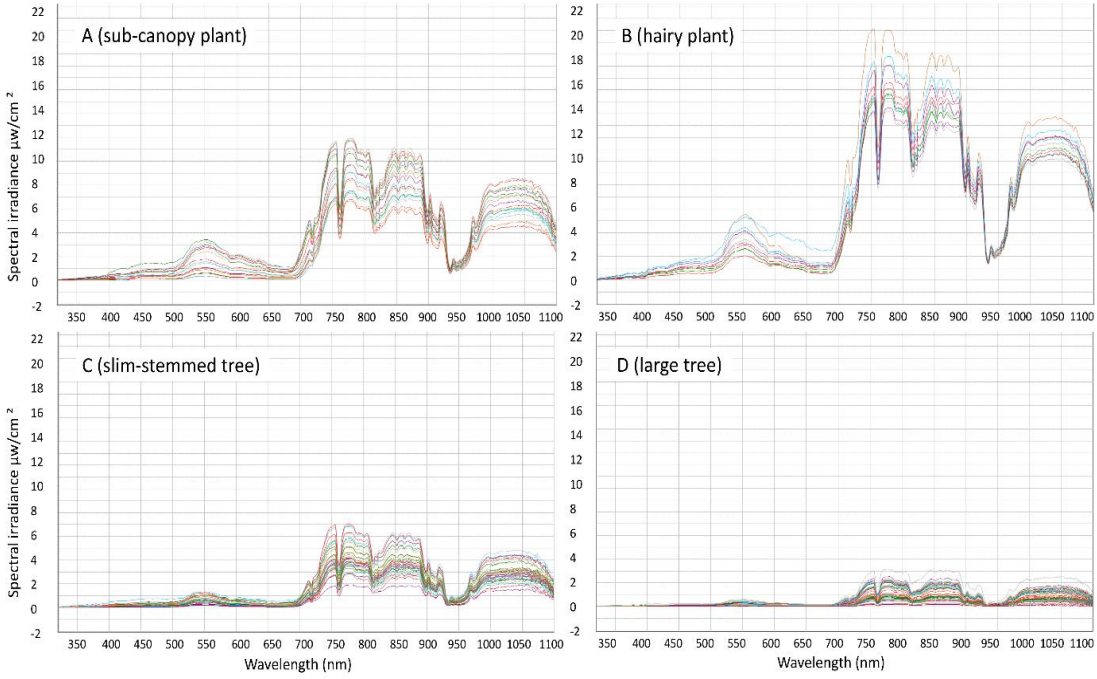

Figure 3-3. The spectral irradiance of the four PFGs. The left vertical axis is scaled for calibrated irradiance data in units of simple number labels (e.g. 100 nW/m²/nm instead of 1.0×10-7 W/m²/nm). The unit area can be used by meter squared or centimetre squared. The wavelength of UV, visible and NIR spectrum is plotted on the horizontal axis of the plot.

3.3.2. The characteristics of four PFGs

The reflectance of leaves was different with the functions and structures examined by growth form, plant size, leaf phenology and leaf morphology (Table 3-1). Ten of the 48 traits were significantly different among the four PFGs. These were growth form (tree, herb and grass), wood, height, DBH, branching pattern, leaf hair and leaf glabrousness. Two environmental factors, soil pH and elevation, did not differ among the cluster groups.

The dominance of herbs and grasses was common characteristics in groups A and B, while tree and shrub were dominant in groups C and D. Group A (sub-canopy plant and shrub) was composed of seven trees, five shrubs, two herbs and three graminoids (two perennials and one annual). The mean plant height was 9.3 m and was intermediate between group A and groups B and C. These implied that most species in this group occupied sub-canopy.

Group B (hairy plant) included five herbs, one tree, two shrubs and two climbers. This group included only one tree species (9.1%) while the other groups showed that more than 40% of species were tree. Of these 11 species, 10 species developed hairy leaf.

Table 3-1. The number of species in each group obtained by cluster analysis based on 48 traits. The differences between the four PFGs are examined by ANOVA. Bold letters indicate the results of ANOVA are significant at $p < 0.05$. The integer indicates number of species and decimal shows mean ± standard error. The same letters indicate that the PFGs are not significantly different between the groups (Steel-Dwass test, $p > 0.05$).

Species traits		A (sub-canopy plant)	B (hairy plant)	C (slim-stemmed tree)	D (large tree)	ANOVA (*P* value)
Number of species		17	11	34	50	
Growth form	Tree	7 ab	1 a	19 b	41 c	**0.000**
	Shrub	4	4	7	4	0.160
	Herb	2 abc	5 ab	6 bc	3 c	**0.007**
	Grass	4 a	1 ab	2 abc	2 bc	**0.012**
	Wood	2 a	1 ab	11 ac	27c	**0.001**
	Height (m)	9.3 ± 3.1 ab	6.0 ± 3.8 b	16.1 ± 2.2 abc	19.0 ± 1.8 c	**0.004**
	DBH (m)	0.46 ± 0.2 a	0.06 ± 0.3 ab	0.49 ± 0.2 abc	0.82 ± 0.1 c	**0.046**
	SI	140.26 ± 39.9	174.62 ± 49.6	96.99 ± 28.2	86.30 ± 23.2	0.329
Branching pattern	Erect	8 abc	4 bcd	12 cd	8 d	**0.049**
	Spreading	6 ab	7 bcd	16 ac	39 d	**0.002**
	Drooping	3	0	6	3	0.181
	Thorny/spiny	2	2	2	8	0.530
Leaf hair	Hairy	7 acd	10 ab	10 cd	18 d	**0.003**
	Glabrous	10 acd	1 ab	24 c	32 cd	**0.001**
Leaf phenology	Deciduous	13	7	22	26	0.598
	Evergreen	4	4	12	24	0.311
Leaf shape	Petiolate	9	8	17	33	0.285
	Elliptical	4	3	10	18	0.776
	Oblong	4	2	12	11	0.512
	Ovate	8	4	11	11	0.251
	Lanceolate	5	5	11	10	0.340
	Alternate	2	0	3	6	0.673
	Base rounded	3	4	6	9	0.548
	Cordate	3	0	7	2	0.470
	Acute	3	6	12	19	0.242
	Acuminate	6	4	10	11	0.632
	Coriaceous	4	2	5	16	0.320
Flower	Axillary inflorescence	7	2	9	21	0.287
	Bisexual	2	0	6	13	0.207
	Panicle	5	1	9	12	0.641
	White-cream or white colored	3	4	17	29	0.059
	Pedicellate	7	1	10	19	0.254
Fruit	Drupe	3	0	7	22	0.007
	Berry	3	2	3	6	0.768
Fruit shape	Oblong	4	3	5	4	0.234
	Globose	7	1	8	13	0.293
Fruit color	Green	4	1	7	17	0.477
	Yellowish	3	0	5	10	0.489
	Reddish	2	0	5	6	0.353
	Blackish	4	2	7	17	0.484
Reproduc-tion	Seed	15	10	28	45	0.797
	Sprout	2	1	6	5	0.535

Seed	Single	9	4	15	27	0.226
	Plural	8	7	19	23	0.440
Flowering and fruiting period	Jan-Jun	9	5	20	29	0.081
	July-December	8	6	14	21	0.495
Soil pH		6.06 ± 0.20	6.03±0.3	6.15 ± 0.2	6.29 ± 0.1	0.711
Elevation	High > 7 m	5	1	16	23	0.085
	Medium 4 -7 m	12	10	23	37	0.508
	Low < 4 m	6	5	5	9	0.081

- Leaf shape included multiple characteristics of leaf, i.e., petiole, shape of leaf, the type of leaf base and apex, and the structure of lamina.

Group C, consisted of slim-stemmed trees with mean SI 97. This group included 71% glabrous leaves that was highest of the four groups. This group included twenty trees, six shrubs, four herbs, two perennial grasses and two climbers.

Group D (large tree) had three herbs two grasses, two shrubs and trees. The 78% of species were explained by large trees with spreading branches. This group showed the largest DBH and height of the four groups, indicating that this group was occupied by large trees. The most of these trees were used for wood.

3.4. Discussion

The growth forms were tightly related to the reflectance patterns of PFGs. The leaf reflectance was determined by leaf phenology, morphology and physiology (Barret and Curtis 1992). Although soil, light and climate influence leaf reflectance (Baret et al. 2007), soil pH and elevation were not related to the PFGs. These results suggested that the innate species characteristics represented by growth form determine the spectral reflectance patterns more than the environments where they grow. An increase in solar radiation causes decreases in chlorophyll content and consequently the reflection changes (Zhang et al. 2009). The stem height was also different among the PFGs. Stem height is

related to the acquisition of solar energy (Shen et al. 2018). Therefore, the PFGs showed differences in GREEN and NIR.

Most species in Group B developed hairy leaves and showed the highest reflectance shown by the three peaks. When leaf is hairy, the reflectance becomes high at the wavelengths between 700 nm and 900 nm (Holmes and Keiller 2002). Leaf hair increases the leaf reflectance at NIR wavelengths by reducing evapotranspiration resulting high photosynthetic water use efficiency (Hamaoka et al. 2017). All of these suggested that the leaf hairiness greatly increases spectral reflectance. Therefore, group B was clearly separated from the other groups by leaf hairiness.

The reflectance of in groups C and D respectively were low. Leaf reflectance depends on the amount of obtained light energy and the exposure of the leaf surface (Lin et al. 2013). Plant species growing under fluctuated solar energy vary chlorophyll concentrations (Cao 2000). The high contents of chlorophyll and accessory pigments can absorb more light energy and therefore show low reflectance (Bündchen et al. 2016).

The acquisition of sun light is quite different between erect and spreading branching patterns. Plants with the spreading branches allows sun light to penetrate correspondingly to the leaves and thus, the leaves absorbed sufficient sunlight (Lee et al. 1990). The spreading branches influenced lower reflection in group D. On the contrary, the light penetration into the leaves under erect branches was complex and impeded the direct light acquisition. Therefore, light acquisition capacity determined by the branching patterns were important for photosynthetic activity of plants and spectral reflectance pattern (Gitelson et al. 2003).

The examined species were grouped into herbs and grasses (groups A and B) and trees (C and D). The penetration of solar radiation into leaves is determined by the structures of leaf foliage (Badarnah and Knaack 2008). Since the structures differ between

trees and herbs, the reflectance patterns should differ between the trees and herbs. The leaves of large trees (group D) had the lowest reflection throughout the entire spectral range.

The leaf reflectance spectra varied among the PFGs that were developed by species characteristics. Therefore, the PFGs were classified basically by the growth forms. The branching patterns categorized the PFGs, because the light absorption capacity of leaf depended on the patterns of branch and influenced the chlorophyll content and photosynthetic activity. The leaf hair also determined the PFGs due to the high reflectivity in NIR wavelengths, because leaf hair enhance photosynthetic activity by conserving water.

General discussion

Fundamental information on the impacts of urban growth on landscapes and ecosystems were provided by exploiting fine-scale land use classification (Chapter 1), predicting the potential distribution of *S. robusta* forests (Chapter 2), and detecting the relationships between plant functional groups and spectral reflectance patterns (Chapter 3). The present locations of *S. robusta* ecosystems were detected by hierarchical land use classification. Maxent model predicted the potential locations of *S. robusta* and suggested that the precipitation was the prime importance for the conservation. The structures and functions of plant species were examined by the PFGs clustered by the spectral reflectance.

Land use change and forest cover damage by urban growth

The fine scale analysis succeeded in the detection of land use types well. The urban growth was conducted based on road networks, small patches of land use types were not detected at coarse scale (O'Connell et al. 2013). Although VIs were used in land use classification, no single VI was efficient to separate the land use types. A hierarchical classification of the four VIs with DT improved the classification and was able to distinguish them.

S. robusta *forests distribution, global warming impact and conservation*

S. robusta in tropical rainforests is endangered not only due to anthropogenic disturbances but also natural disturbances, including global warming. Maxent predicted that the RCP8.5 scenario showed a shrinkage in *S. robusta* forest patches to the 21st century, due mostly to tolerance to temperature and reduced precipitation. In addition, N concentration in soil and precipitation were determinants on *S. robusta* forest distribution. The suitable

distributions of *S. robusta* forest was controlled by edaphic factors more than the climatic factors at local scale.

Role of species traits on leaf reflection spectra

The species traits depended on the corresponding environments, while the leaf reflectance spectra depended on the growth form, branching pattern, phenological and morphological characteristics of species. Photosynthesis was the most important factors to control the process of light absorption for photosynthesis (Baret et al. 2007). The light absorption of leaf depended on the branching pattern that should be related to the photosynthetic activity of leaf. In the NIR spectrum, the reflectance was high due to the scattering solar energy and leaf cell structure (Artigas and Yang 2005). Hairy plants showed the highest reflectance because of the presence of less absorption pigments and hair on leaf. The variability of light penetration and light absorption caused the low reflectance in the trees. Because the growth form determined the capability of leaf to absorb sunlight and consequently the leaf reflectance varied.

This study clearly confirmed the land use types and the potential distribution of endangered forest by using newly-proposed hierarchical land use classification with decision tree and Maxent model with global warming scenarios. In addition, the relationships between growth form and spectral reflectance are detected by using plant functional groups classified by spectral reflectance patterns. PFGs characterized the structure and function of *S. robusta* ecosystem. The results can be applied to the other regions of tropical forest to predict and conserve the key tropical tree species. It is worthwhile for planners and decision makers to evaluate the promises and limitations of further urban development to reduce the detrimental land exploitation and urban expansion.

Acknowledgments

I enthusiastically thank and deeply grateful to my esteemed supervisor Dr. Shiro Tsuyuzaki for his invaluable advice, suggestions, comments, guidance, and encouragements. I sincerely thank and appreciate the constructive suggestions and comments from Drs. Takashi S. Kohyama, Gaku Kudo, Takuya Kubo, Teiji Watanabe, Keiji Kushida, Tomonori Sato, Junjiro Negishi, Prof. Takada and Ram Avtar which improve this dissertation. I would like to acknowledge the Sasakawa Scientific Research Grant from The Japan Science Society (research number: 29-508) for providing the fund to this research. I am also grateful to Springer Nature Author Services for English language editing.

I extend my sincere thanks to Engr. M J Kabir, Mr. Ujjwal Mallick, Md. Mustafizur Rahman and RAJUK (Rajdhani Unnayan Kartripakkha) the capital development authority of Bangladesh for providing valuable data and information about Purbachal.

I thank Lea Vegh for her help during the satellite data acquisition, Dr. TaeOh Kwon, Hayato Kato and Saurabh Tripathi. I thank all of my lab members (Plant Ecology laboratory) for their kind help and support.

I devotedly thank Dr. Shahedur Rashid, Dr. Tanjinul Haque Mollah and Alamgir Hossen Bhuiyan for detailed advices and valuable suggestions in regarding field survey. I thank Sayem Akand, Shamoal Akand and a group of student from Jahangirnagar University for fieldwork assistance.

I eagerly thank my father (Maksudur Rahman Akand) who is my legend, mother (Rubi Akter), brothers (Himel and Nishad), sister (Shaneen), uncles/aunty (kajol and others), friends (Nupur, Anannya and Samia), and Ariful Haque kallol for their supports and encouragements throughout.

References

Aguilar, M. A., Saldaña, M. M., & Aguilar, F. J. (2013). GeoEye-1 and WorldView-2 pan-sharpened imagery for object-based classification in urban environments. *International Journal of Remote Sensing*, 34, 2583–2606. https://doi.org/10.1080/01431161.2012.747018.

Ahmed, Z. U., Begum, Z. N. T., Hassan, M. A., Khondker, M., Kabir, S. M. H., Ahmad, M., Ahmed, A.T.A., Rahman, A.K.A., & Haque, E.U. (Eds.). (2008b). *Encyclopedia of flora and fauna of Bangladesh*, vol. 6. *Angiosperms: Dicotyledons (Acanthaceae-Asteraceae)*. Asiatic society of Bangladesh, Dhaka. 408 pp.

Ahmed, Z. U., Hassan, M. A., Begum, Z. N. T., Khondker, M., Kabir, S. M. H., Ahmad, M., Ahmed, A.T.A., Rahman, A.K.A., & Haque, E.U. (Eds.). (2008a). *Encyclopedia of flora and fauna of Bangladesh*, vol. 7. *Angiosperms: Dicotyledons (Balsaminaceae-Euphorbiaceae)*. Asiatic society of Bangladesh, Dhaka. 546 pp.

Ahmed, Z. U., Hassan, M. A., Begum, Z. N. T., Khondker, M., Kabir, S. M. H., Ahmad, M., Ahmed, A.T.A., Rahman, A.K.A., & Haque, E.U. (Eds.). (2009a). *Encyclopedia of flora and fauna of Bangladesh*, vol. 8. *Angiosperms: Dicotyledons (Fabaceae-Lythraceae)*. Asiatic society of Bangladesh, Dhaka. 478 pp.

Ahmed, Z. U., Hassan, M. A., Begum, Z. N. T., Khondker, M., Kabir, S. M. H., Ahmad, M., & Ahmed, A.T.A. (Eds.). (2009b). *Encyclopedia of flora and fauna of Bangladesh*, vol. 10. *Angiosperms: Dicotyledons (Ranunculaceae-Zygophyllaceae)*. Asiatic society of Bangladesh, Dhaka. 580 pp.

Ahmed, Z. U., Hassan, M. A., Begum, Z. N. T., Khondker, M., Kabir, S. M. H., Ahmad, M., Ahmed, A.T.A., Rahman, A.K.A., & Haque, E.U. (Eds.). (2008c). *Encyclopedia of flora and fauna of Bangladesh*, vol. 12. *Angiosperms: Monocotyledons (Orchidaceae-Zingiberaceae)*. Asiatic society of Bangladesh, Dhaka. 505 pp.

Ahmed, Z. U., Hassan, M. A., Begum, Z. N. T., Khondker, M., Kabir, S. M. H., Ahmad, M., & Ahmed, A.T.A. (Eds.). (2009c). *Encyclopedia of flora and fauna of Bangladesh*, vol. 9. *Angiosperms: Dicotyledons (Magnoliaceae-punicaceae)*. Asiatic society of Bangladesh, Dhaka. 488 pp.

Akay, S. S., & Sertel, E. (2016). Urban land cover/use change detection using high resolution spot 5 and spot 6 images and urban atlas nomenclature. *The International Archives of*

the Photogrammetry, Remote Sensing and Spatial Information Sciences, XLI-B8, 789–796. XXIII ISPRS Congress, Prague, Czech Republic. https://doi.org/10.5194/isprs-archives-XLI-B8-789-2016.

Alam, M., Furukawa, Y., Sarker, S. K., & Ahmed, R. (2008). Sustainability of Sal (Shorea robusta) Forest in Bangladesh: Past, Present and Future Actions. *International Forestry Review*, 10(1), 29–37. DOI: 10.1505/ifor.10.1.29.

Alberti, M. (2005). The effects of urban patterns on ecosystem function. *International Regional Science Review*, 28 (2), 168–192.

Alekseev, V. A., & Belov, S.V. (1960). *Spectral reflectance of trees and other objects in an aerial photographic survey of West Ukraine*. Aeromethods, Trudy Lab. Aerometodov Akad. Nauk. SSSR, X, 105.

Ankanna, S., & Savithramma, N. (2012). Studies on habitat survey and seed germination of *Shorea tumbuggaia* ROXB. A globally threatened medicinal tree taxon of seshachalam biosphere reserve of India. *International Journal of Research in BioSciences*, 1, 63–70. http://www.ijrbs.in.

Anonymous, (2013). *Environmental Impact Assessment (EIA) of Purbachal New Town Project*. Rajdhani Unnayan Kartripakkha (RAJUK), Ministry of Housing and Public Works, Government of the People's Republic of Bangladesh.

Arnfield, A. J. (2003). Two decades of urban climate research: A review of turbulence, exchanges of energy and water, and the urban heat island. *International Journal of Climatology*, 23 (1), 1–26.

Asner, G. P., Jones, M. O., Martin, R. E., Knapp, D. E., & Hughes, R. F. (2008). Remote sensing of native and invasive species in Hawaiian rainforests. *Remote Sensing of Environment*, 112, 1912–1926.

Badarnah, L., & Knaack, U. (2008). Organizational features in leaves for application in shading systems for building envelopes. *WIT Transactions on Ecology and the Environment*, 114, 87–96. DOI: 10.2495/DN080101.

Banglapedia, (2008). *National encyclopedia of Bangladesh*, Sal *forest*, Banglapedia. http://banglapedia.search.com.bd/HT/S_0035.htm.

Baret, F., Houlès, V., & Guérif, M. (2007). Quantification of plant stress using remote sensing observations and crop models: the case of nitrogen management. *Journal of Experimental Botany*, 58, 869–880.

Barros, C., Thuiller, W., Georges, D., Boulangeat, I., & Münkemüller, T. (2016). N-dimensional hypervolumes to study stability of complex ecosystems. *Ecology Letters*, 19(7), 729–742. DOI: 10.1111/ele.12617.

Barzegar, M., Ebadi, H., & Kiani, A. (2015). Comparison of different vegetation indices for very high-resolution images, specific case UltraCam-D imagery. *Remote Sensing and Spatial Information Sciences*, XL-1/W5. https://doi.org/10.5194/isprsarchives-XL-1-W5-97-2015.

Baxendale, C., Orwin, K. H., Poly, F., Pommier, T., & Bardgett, R. D. (2014) Are plant–soil feedback responses explained by plant traits? *New Phytologist*, 204, 408–423.

BBS (Bangladesh Bureau of Statistics), (2013). *District statistics 2011 Gazipur*. Statistics and Informatics Division (SID), Ministry of planning, government of the people's republic of Bangladesh. Parishankhan Bhaban. E-27/A, Agargaon, Dhaka-1207. www.bbs.gov.bd.

BCA (Bangladesh Country Almanac), (2006). *Bangladesh Country Almanac*, Ministry of Agriculture, Bangladesh. http://www.cimmyt.org/bangladesh-country-almanac.

Begum, K., Jahan, I., Rahman, M. H., Chowdhury, M. S., & Elahi, S. F. (2009). Status of some micronutrients in different soils of Gazipur district as related to soil properties and land type. *Bangladesh Journal of Scientific and Industrial Research*, 44(4), 425–430.

BMD (Bangladesh Meteorological Department), (2017). *Bangladesh Meteorological Department*, Ministry of Defense of the Government of Bangladesh. www.bmd.gov.bd.

Booth, D. B., Karr, J. R., Schauman, S., Konrad, C. P., Morley, S. A., Larson, M. G., & Burges, S. J. (2004). Reviving urban streams: Land use, hydrology, biology, and human behavior. *Journal of the American Water Resources Association*, 40 (5), 1351–1364.

Boutin, C., & Keddy, P. A. (1993). A functional classification of wetland plants. *Journal of Vegetation Science*, 4, 591–600.

Boyle, S. A., Kennedy, C. M., Torres, J., Colman, K., Pérez-Estigarribia, P. E., & de la Sancha, N. U. (2014). High-Resolution Satellite Imagery Is an Important yet Underutilized Resource in Conservation Biology. *PLoS ONE*, 9, 1–11. http://doi.org/10.1371/journal.pone.0086908.

Brammer, H. T. (2012). *The Physical Geography of Bangladesh*. Dhaka, Bangladesh: University Press. ISBN 978-984-506-049-3.

Brown De Colstoun, E. C. B., Story, M. H., Thompson, C., Commisso, K., Smith, T. G., & Irons, J. R. (2003). National Park vegetation mapping using multi-temporal Landsat 7 data and a decision tree classifier. *Remote Sensing of Environment*, 85, 316−327.

Bündchen, M., Boeger, M. R. T., Reissmann, C. B., & Geronazzo, K. M. (2016). Interspecific variation in leaf pigments and nutrients of five tree species from a subtropical forest in southern Brazil. *Annals of the Brazilian Academy of Sciences*, 88(1), 467–477. http://dx.doi.org/10.1590/0001-3765201620140605.

Cao, K. F. (2000). Leaf anatomy and chlorophyll content of 12 woody species in contrasting light conditions in a Bornean heath forest. C*anadian Journal of Botany*, 78, 1245–1253.

Cape, J. N., Kirika, A., Rowland, A. P., Wilson, D. R., Jickells, T. D., & Cornell, S. (2001). Organic nitrogen in precipitation: real problem or sampling artefact? *Scientific World Journal*, 1, 230–237. DOI:10.1100/tsw.2001.278.

Chitale, V., & Behera, M. (2012). Can the distribution of *sal* (*Shorea robusta* Gaertn. f.) shift in the northeastern direction in India due to changing climate? *Current Science*, 102, 1126–1135.

Cortois, R., Schröder‐Georgi, T., Weigelt, A., Putten, W. H. van der, & Deyn, G. B. De. (2016). Plant–soil feedbacks: role of plant functional group and plant traits. *Journal of Ecology*, 104(6), 1608–1617. https://doi.org/10.1111/1365-2745.12643.

Cotter, A. S., Chaubey, I., Costello, T. A., Soerens, T. S., & Nelson, M. A. (2004). Water quality model output uncertainty as affected by spatial resolution of input data. *Journal of the American Water Resources Association*, 72701, 977–986.

Cregger, M. A., Schadt, C. W., McDowell, N. G., Pockman, W. T., & Classen, A. T. (2012). Response of the soil microbial community to changes in precipitation in a semiarid ecosystem. *Applied and Environmental Microbiology*, 78, 8587–8594. http://doi.org/10.1128/AEM.02050-12.

Cristiano, P. M., Madanes, N., Campanello, P. I., di Francescantonio, D., Rodríguez, S. A., Zhang, Y-J., Carrasco, L. O., & Goldstein, G. (2014). High NDVI and potential canopy photosynthesis of South American subtropical forests despite seasonal changes in leaf area index and air temperature. *Forests*, 5, 287–308. doi:10.3390/f5020287.

Das, D., & Alam, M. (2001). *Trees of Bangladesh*. Chittagong, Bangladesh: Bangladesh Forest Research Institute.

Deb, J. C., Salman, M. H. R., Halim, M. A., Chowdhury, M. Q., & Roy, A. (2014). Characterising the diameter distribution of *Sal* plantations by comparing normal, lognormal and Weibull distributions at Tilagarh Eco-park, Bangladesh. *Southern Forests: A Journal of Forest Science*, 76, 201–208.

Dewan, A. M., & Yamaguchi, Y. (2009). Using remote sensing and GIS to detect and monitor land use and land cover change in Dhaka Metropolitan of Bangladesh during 1960–2005. *Environmental Monitoring and Assessment*, 150, 237–249. DOI: 10.1007/s10661-008-0226-5.

Dhar, P. P., & Mridha, M. A. U. (2006). Biodiversity of arbuscular mycorrhizal fungi in different trees of Madhupur forest, Bangladesh. *Journal of Forestry Research*, 17, 201–205.

Dibs, H., Idrees, M. O., & Alsalhin, G. B. A. (2017). Hierarchical classification approach for mapping rubber tree growth using per-pixel and object-oriented classifiers with SPOT-5 imagery. *The Egyptian Journal of Remote Sensing and Space Sciences*, 20, 21–30. http://dx.doi.org/10.1016/j.ejrs.2017.01.004.

Duckworth, J. C., Kent, M., & Ramsay, P. M. (2000). Plant functional types: an alternative to taxonomic plant community description in biogeography? *Progress in Physical* Geography, 24 (4), 515–542. DOI: 10.1177/030913330002400403.

EIA, (2013). *Environmental Impact Assessment (EIA) of Purbachal New Town Project*. Rajdhani Unnayan Kartripakkha (RAJUK), Ministry of Housing and Public Works, Government of the People's Republic of Bangladesh.

Elith, J., & Leathwick, J. R. (2006). *Conservation prioritisation using species distribution modelling*. In: Moilanen A, Wilson KA, Possingham HP, editors. Spatial conservation prioritization: quantitative methods and computational tools. Oxford, UK: Oxford University Press.

Elith, J., Graham, C. H., Anderson, R. P., Dudı´k, M., Ferrier, S., et al. (2006). Novel methods improve prediction of species' distributions from occurrence data. *Ecography*, 29, 129–151.

Elith, J., Phillips, S. J., Hastie, T., Dudík, M., Chee, Y. E. et al. (2011). A statistical explanation of MaxEnt for ecologists. *Diversity and Distributions*, 17, 43–47.

Endo, N., Matsumoto, J., Hayashi T., Terao, T., Murata, F., Kiguchi, M., Yamane, Y., & Alam, M. S. (2015). Trends in precipitation characteristics in Bangladesh from 1950 to 2008. *Scientific Online Letters on the Atmosphere*, 11, 113−117. DOI:10.2151/sola.2015-027.

Erener, A., Düzgün, S., & Yalciner, A. C. (2012). Evaluating land use/cover change with temporal satellite data and information systems. *Procedia Technology*, 1, 385–389. https://doi.org/10.1016/j.protcy.2012.02.079.

Evans, J. R. (2013). Improving photosynthesis. *Plant Physiology*, 162, 1780–1793. www.plantphysiol.org.

Evrendilek, F., & Gulbeyaz, O. (2008). Deriving Vegetation Dynamics of Natural Terrestrial Ecosystems from MODIS NDVI/EVI Data over Turkey. *Sensors* (Basel, Switzerland), 8(9), 5270–5302. http://doi.org/10.3390/s8095270.

Ferrier, S. (1984). *The status of the Rufous Scrub-bird Atrichornis rufescens: habitat, geographical variation and abundance*. PhD thesis. Armidale, Australia: University of New England.

Fielding, A. H., & Bell, J. F. (1997). A review of methods for the measurement of prediction errors in conservation presence/absence models. *Environmental Conservation*, 24, 38–49.

Fisher, B., Nakicenovic, N., Alfsen, K., Corfee, Morlot, J., De la Chesnaye, F., et al. (2007). Chapter 3: *Issues related to mitigation in the long-term context*. In: Climate change 2007: Mitigation. Contribution of Working Group III to the Fourth Assessment Report of the Intergovernmental Panel on Climate Change. Cambridge University Press, Cambridge, United Kingdom and New York, NY, USA.

Fisher, J. R. B., Acosta, E. A., Dennedy-Frank, P. J., Kroeger, T., & Boucher, T. M. (2017). Impact of satellite imagery spatial resolution on land use classification accuracy and modeled water quality. *Remote Sensing in Ecology and Conservation*, 1–13. https://doi.org/10.1002/rse2.61.

Fonji, S. F., & Taff, G. N. (2014). Using satellite data to monitor land-use land-cover change in North-eastern Latvia. *Springer Plus*, 3(61). https://doi.org/10.1186/2193-1801-3-61.

Foody, G. M. (2002). Status of land cover classification accuracy assessment. *Remote Sensing of Environment*, 80, 185–201. https://doi.org/10.1016/S0034-4257(01)00295-4.

Gautam, K. H., & Devoe, N. N. (2006). Ecological and anthropogenic niches of sal (*Shorea robusta* Gaertn. f.) forest and prospects for multiple-product forest management – a review. *Forestry (Lond),* 79, 81–101. https://doi.org/10.1093/forestry/cpi063.

Gautam, M. K., Manhas, R. K., & Tripathi, A. K. (2014). Plant species diversity in unmanaged moist deciduous forest of Northern India. *Current Scinece*, 106, 277–287.

Gitelson, A. A., Gritz, Y., & Merzlyak, M. N. (2003). Relationships between leaf chlorophyll content and spectral reflectance and algorithms for non-destructive chlorophyll assessment in higher plant leaves. *Journal of Plant Physiology*, 160, 271 –282. http://www.urbanfischer.de/journals/jpp.

Green, K. M. (1981). Preliminary observations on the ecology and behavior of the Capped Langur, Presbytis pileatus, in the Madhupur forest of Bangladesh. *International Journal of Primatology*, 2, 131–151.

Hamaoka, N., Yasui, H., Yamagata, Y., Inoue, Y., Furuya, N., Araki, T., & Yoshimura, A. (2017). A hairy-leaf gene, blanket leaf, of wild Oryza nivara increases photosynthetic water use efficiency in rice. *Rice*, 10, 20. http://doi.org/10.1186/s12284-017-0158-1.

Harun-Er-Rashid (2012). *Madhupur Tract*. In Islam, S. & Jamal, A. A. Banglapedia: National Encyclopedia of Bangladesh (Second ed.). Asiatic Society of Bangladesh.

Hasan, M. K., & Mamun, M. B. (2015). Influence of different stands of *Sal* (*Shorea robusta* C. F. Gaertn.) forest of Bangladesh on soil health. *Research in Agriculture Livestock and Fisheries*, 2, 17–25. http://dx.doi.org/10.3329/ralf.v2i1.23025.

Hasnat, M. M., & Hoque, M. S. (2016). Developing Satellite Towns: A Solution to Housing Problem or Creation of New Problems. *IACSIT International Journal of Engineering and Technology*, 8, 50–56.

Hassan, M. M. (2004). *A study on flora species diversity and their relations with farmers' socio-agro-economic condition in Madhupur Sal forest*. Dissertation, Department of Agroforestry, Bangladesh Agricultural University, Mymensingh, Bangladesh.

Holben, B. N., & Justice, C. O. (1981). An examination of spectral band ratioing to reduce the topographic effect on remotely sensed data. *International Journal of Remote Sensing*, 2, 115–133. http://dx.doi.org/10.1080/01431168108948349.

Holmes, M. G. & Keiller, D. R. (2002). Effects of pubescence and waxes on the reflectance of leaves in the ultraviolet and photosynthetic wavebands: a comparison of a range of species. *Plant, Cell & Environment*, 25, 85–93. doi:10.1046/j.1365-.

Hossain, S. (2013). Migration, urbanization and poverty in Dhaka, Bangladesh. *Journal of the Asiatic Society of Bangladesh (Hum.)*, 58, 369–382. https://doi.org/10.1080/01431161.2012.682660.

Huete, A. (1988). A soil-adjusted vegetation index (SAVI). *Remote Sensing of Environment*, 25, 295–309.

Huete, A. R., Justice, C., & van Leeuwen, W. (1999). *MODIS Vegetation Index (MOD13) Algorithm Theoretical Basis Document.* Version 3.1. Vegetation Index and Phenology Lab, The University of Arizona.

Huete, A. R., Liu, H. Q., Batchily, K., & van Leeuwen, W. (1997). A Comparison of Vegetation Indices over a Global set of TM Images for EOS-MODIS. *Remote Sensing of Environment*, 59, 440–451. DOI: 10.1016/S0034-4257(96)00112-5.

Huete, A., Didan, K., Miura, T., Rodriguez, E. P., Gao, X., & Ferreira, L. G. (2002). Overview of the Radiometric and Biophysical Performance of the MODIS Vegetation Indices. *Remote Sensing of Environment*, 83, 195–213. DOI: 10.1016/S0034-4257(02)00096-2.

Huete, A., Justice, C., & Liu, H. (1994). Development of vegetation and soil indices for MODIS-EOS. *Remote Sensing of Environment*, 49, 224–234.

IPCC AR5 WG1, (2013). *Climate Change 2013: The Physical Science Basis. Working Group 1 (WG1) Contribution to the Intergovernmental Panel on Climate Change (IPCC) 5th Assessment Report (AR5)*, Cambridge University Press.

IPCC, (2008). *Towards new scenarios for analysis of emissions, climate change, impacts, and response strategies*. IPCC Expert Meeting Report on New Scenarios, Intergovernmental Panel on Climate Change.

IUCN Species Survival Commission, (2015). *The IUCN red list of threatened species*. http://www.iucnredlist.org/.

Jiang, Z., Huete, A. R., Kim, Y., & Didan, K. (2007). 2-band enhanced vegetation index without a blue band and its application to AVHRR data. *Remote Sensing and Modeling of Ecosystems for Sustainability*, 6679 667905, 1–9. http://dx.doi.org/10.1117/12.734933.

Jiang, Z., Huete, A. R., Didan, K., & Miura, T. (2008). Development of a two-band enhanced vegetation index without a blue band. *Remote Sensing of Environment*, 112, 3833–3845.

Joshi, & Chandra, P. (2011). Performance evaluation of vegetation indices using remotely sensed data. *International journal of geomatics and geosciences*, 2, 231–240. ISSN 0976 – 4380.

Joshi, N., Baumann, M., Ehammer, A., Fensholt, R., Grogan, K., Hostert, P., Jepsen, M. R. et al. (2016). A Review of the Application of Optical and Radar Remote Sensing Data Fusion to Land Use Mapping and Monitoring. *Remote Sensing*, 8(1), 70. https://doi.org/10.3390/rs8010070.

Julien, Y., Sobrino, J. A., Mattar, C., Ruescas, A. B., Jime´nez-Munoz, J. C., So`ria, G., Hidalgo, V., Atitar, M., Franch, B., & Cuenca, J. (2011). Temporal analysis of normalized difference vegetation index (NDVI) and land surface temperature (LST) parameters to detect changes in the Iberian land cover between 1981 and 2001. *International Journal of Remote Sensing*, 32, 2057–2068. https://doi.org/10.1080/01431161003762363.

Kabir, D. S. & Ahmed, A. Z. (2005). Wildlife biodiversity in Bhawal National Park: management techniques and drawbacks of wildlife management and, nature conservation. *Our Nature*, 3, 83-90.

Kalyani, P., & Govindarajulu, P. (2015). Multi-Scale Urban Analysis Using Remote Sensing and GIS. *Geoinformatica: An International Journal (GIIJ)*, 5, 1–11.

Karnieli, A., Bayarjargal, Y., Bayasgalan, M., Mandakh, B., Dugarjav, C., Burgheimer, J., Khudulmur, S., Bazha, S. N., & Gunin, P. D. (2013). Do vegetation indices provide a reliable indication of vegetation degradation? A case study in the Mongolian pastures. *International Journal of Remote Sensing*, 34, 6243–6262. https://doi.org/10.1080/01431161.2013.793865.

Khan, Z. H., Mazumder, A. R., Moduddin, A. S. M., Hussain, M. S., & Saheed, S. M. (1997). Physical properties of some Benchmark soil from the floodplains of Bangladesh. *Journal of Indian Society of Soil Science*, 46, 442–446.

Khatun, H., Falgunee, N., & Kutub, M. J. R. (2015). Analyzing urban population density gradient of Dhaka Metropolitan Area using Geographic Information Systems (GIS) and Census Data. *Malaysian Journal of Society and Space*, 13, 1–13. ISSN 2180-2491.

Kinthada N. R., Gurram, M. K., Eadara, A., & Velagala, V. R. (2014). Land Use/Land Cover and NDVI Analysis for Monitoring the Health of Micro-watersheds of Sarada River Basin, Visakhapatnam District, India. *Journal of Geology & Geophysics*, 3, 146. doi:10.4172/2329-6755.1000146.

Klančnik, K., Zelnik, I., Gnezda, P. et al. (2015). *Do reflectance spectra of different plant stands in wetland indicate species properties?* In Vymazal J (Ed.). The Role of Natural and Constructed Wetlands in Nutrient Cycling and Retention on the Landscape. Heidelberg: Springer, 73–86.

Kooyman, R., & Rossetto, M. (2008). Definition of plant functional groups for informing implementation scenarios in resource-limited multi-species recovery planning. *Biodiversity and Conservation*, 17, 2917–2937. DOI 10.1007/s10531-008-9405-5.

Kumar, S., & Stohlgren, T. J. (2009). Maxent modeling for predicting suitable habitat for threatened and endangered tree *Canacomyrica monticola* in New Caledonia. *Journal of Ecology and Natural Environment*, 1, 94–98. http://www.academicjournals.org/JENE.

Kushida, K., Hobara, S., Tsuyuzaki, S., Kim, Y., Watanabe, M., Setiawan, Y., Harada, K., Shaver, G. R., & Fukuda, M. (2015). Spectral indices for remote sensing of phytomass, deciduous shrubs, and productivity in Alaskan Arctic tundra. *International Journal of Remote Sensing*, 36, 4344–4362. https://doi.org/10.1080/01431161.2015.1080878.

Kushwaha, S. P. S., & Nandy, S. (2012). Species diversity and community structure in *sal* (*Shorea robusta*) forests of two different rainfall regimes in West Bengal, India. *Biodiversity and Conservation*, 21, 1215–1228.

Laliberte, A. S., Fredrickson, E. L., & Rango, A. (2007). Combining decision trees with hierarchical object-oriented image analysis for mapping arid rangelands. *Journal of Photogrammetric Engineering and Remote Sensing*, 73, 197−207.

Lee, D. W., Bone, R. A. Tarsis, S. L., & Storch, D. (1990). Correlates of leaf optical properties in tropical forest sun and extreme-shade plants. *American Journal of Botany*, 77, 370–380.

Leishman, M. R., & Westoby, M. (1992). Classifying plants into groups on the basis of associations of individual traits evidence from Australian semi-arid woodlands. *Journal of Ecology*, 80, 417-424.

Lewis, J. S., Farnsworth, M. L., Burdett, C. L., Theobald, D. M., Gray, M., & Miller, R. S. (2017). Biotic and abiotic factors predicting the global distribution and population density of an invasive large mammal. *Scientific Reports*, 7, 44152. http://doi.org/10.1038/srep44152.

Lin, Y., Puttonen, E., & Hyyppä, J. (2013). Investigation of Tree Spectral Reflectance Characteristics Using a Mobile Terrestrial Line Spectrometer and Laser Scanner. *Sensors* (Basel, Switzerland), 13(7), 9305–9320. http://doi.org/10.3390/s130709305.

Lu, D. & Weng, Q. (2009). Extraction of urban impervious surface from an IKONOS image. *International Journal of Remote Sensing*, 30(5), 1297–1311.

Lunetta, R. S., Knight, J. F., Ediriwickrema, J., Lyon, J. G., & Worthy, L. D. (2006). Land-cover change detection using multi-temporal MODIS NDVI data. *Remote Sensing of Environment, 105, 142–154.*

Malinverni, E. S. & Tassetti A. N., & Bernardini, A. (2010). *Automatic Land Use/Land Cover Classification System with Rules Based both on Objects Attributes and Landscape Indicators*. In GEOgraphic Object-Based Image Analysis GEOBIA 2010, Ghent, Belgium, 29 June – 2 July 2010, geobia.ugent.be/proceedings/html/papers.html.

Mamun, A. (2007). *Traditional ecological knowledge and its importance for conservation and management of fresh water fish habitats of Bangladesh*. A thesis of Master of Natural Resources Management. Natural Resources Institute, University of Manitoba, Canada R3T 2N2.

Mandal, R. A., Yadav, B. K. V., Yadav, K. K., Dutta, I. C., & Haque, S. M. (2013). Biodiversity comparison of natural *Shorea robusta* mixed forest with *Eucalyptus Camaldulensis* plantation in Nepal. *Scholars Academic Journal of Biosciences (SAJB),* 1, 144–149. www.saspublisher.com.

Marcer, A., Sáez, L., Molowny-Horas, R., Pons, X., & Pino, J. (2013). Using species distribution modelling to disentangle realised versus potential distributions for rare species conservation. *Biological Conservation*, 166, 221–230.

Markogianni, V., Dimitriou, E., & Kalivas, D. P. (2013). Land-use and vegetation change detection in Plastira artificial lake catchment (Greece) by using remote sensing and GIS techniques. *International Journal of Remote Sensing*, 34, 1265-1281. https://doi.org/10.1080/01431161.2012.718454.

Marshall, J. L. (1998). *NIST Calibration Services Users Guide 1998*. National Institute of Standards and Technology. U.S. Government Printing Office, Washington, DC 20402.

Marzluff, J. M. (2001). *Worldwide urbanization and its effects on birds*. In Marzluff, J. M., Bowman, R., Donnelly, R. eds. Avian Ecology in an Urbanizing World. Norwell (MA): Kluwer. Pages. 19-47.

Matsushita, B., Yang, W., Chen, J., Onda, Y., & Qiu, G. (2007). Sensitivity of the Enhanced Vegetation Index (EVI) and Normalized Difference Vegetation Index (NDVI) to Topographic Effects: A Case Study in High-Density Cypress Forest. *Sensors*, 7, 2636–2651.

McDonald, R. I., Kareiva, P., & Forman, R. (2008). The implications of urban growth for global protected areas and biodiversity conservation. *Biological Conservation*, 141, 1695–1703.

Merlotto, A., Piccolo, M. C., & Bertola, G. R. (2012). Urban growth and land use/cover change at Necochea and Quequen cities, Buenos Aires province, Argentina. *Revista de Geografia Norte Grande*, 53, 159–176.

Merow, C., Smith, M. J., & Silander, J. A. (2013). A practical guide to MaxEnt for modeling species' distributions: what it does, and why inputs and settings matter. *Ecography*, 36, 1058–1069.

Miura, T., Huete, A. R., Yoshioka, H., & Holben, B. N. (2001). An error and sensitivity analysis of atmospheric resistant vegetation indices de-rived from dark target-based atmospheric correction. *Remote Sensing of Environment*, 78, 284–298.

Motohka, T., Nasahara, K. N., Oguma, H., & Tsuchida, S. (2010). Applicability of green-red Vegetation Index for remote sensing of vegetation phenology. *Remote Sens*ing, 2, 2369–2387. 10.3390/rs2102369.

Mountrakis, G., Im, J., & Ogole, C. (2011). Support vector machines in remote sensing: a review. *ISPRS Journal of Photogrammetry and Remote Sensing*, 66 (3), 247–259.

Mustapha, M. R., Lim, H. S., & Mat Jafri, M. Z. (2010). Comparison of Neural Network and Maximum Likelihood Approaches in Image Classification. *Journal of Applied Sciences*, 10, 2847–2854.

Myers, N., Mittermeier, R. A., Mittermeier, C. G., Da Fonseca, G. A., & Kent, J. (2000). Biodiversity hotspots for conservation priorities. *Nature*, 403, 853–858.

Myneni, R. B., Keeling, C. D., Tucker, C. J., Asrar, G., & Nemani, R. R. (1997). Increased plant growth in the northern high latitudes from 1981 to 1991. *Nature*, 386, 698–702. DOI: 10.1038/386698a0.

Nagai, S., Saitoh, T. M., Kobayashi, H., Ishihara, M., Suzuki, R., Motohka, T., Nasahara, K. N., & Muraoka, H. (2012). In *situ* examination of the relationship between various Vegetation Indices and canopy phenology in an evergreen coniferous forest, Japan. *International Journal of Remote Sensing*, 33, 6202–6214.

Nigam, R. K. (2000). Application of Remote Sensing and Geographical Information System for Land Use / Land Cover Mapping and Change Detection in the Rural Urban Fringe Area of Enschede City, The Netherlands. *International Archives of Photogrammetry and Remote Sensing*, 33, 993–998.

Noda, H. M., Nasahara, K. N., & Muraoka, H. (2016). *Biophysical relationship between leaf level optical properties and phenology of canopy spectral reflectance in a cool temperate deciduous broadleaf forest at Takayama, central Japan*. American Geophysical Union, Fall General Assembly 2016, abstract id. B42C-07.2016AGUFM.B42C.07N.

Noss, R. F., & Csuti, B. (1994). *Habitat fragmentation*. In: Meffe, G. K., Carroll, C. R., Eds. Principles of conservation biology. Sunderland, MA: Sinauer Associates, Inc.: 237–264.

Nouri, H., Beecham, S., Anderson, S., & Nagler, P. (2014). High Spatial Resolution WorldView-2 Imagery for Mapping NDVI and Its Relationship to Temporal Urban Landscape Evapotranspiration Factors. *Remote Sensing*, 6, 580–602. 10.3390/rs6010580.

O'Connell, J., Connolly, J., Vermote, E. F., & Holden, N. M. (2013). Radiometric normalization for change detection in peatlands: a modified temporal invariant cluster approach. *International Journal of Remote Sensing*, 34, 2905–2924. https://doi.org/10.1080/01431161.2012.752886.

Pacifici, M., Foden, W. B., Visconti, P., Watson, J. E., Butchart, S. H., Kovacs, K. M., & Akçakaya, H. R. (2015). Assessing species vulnerability to climate change. *Nature Climate Change*, *5*, 215–224.

Pearson, R. G., Stanton, J. C., Shoemaker, K. T., Aiello-Lammens, M. E., Ersts, P. J., Horning, N., & McNees, J. (2014). Life history and spatial traits predict extinction risk due to climate change. *Nature Climate Change*, *4*, 217–221.

Peterson, A. T., & Shaw, J. (2003). *Lutzomyia* vectors for cutaneous leishmaniasis in southern Brazil: ecological niche models, predicted geographic distribution, and climate change effects. *International Journal for Parasitology*, 33, 919–931.

Phillips, S. J. (2008). Transferability, sample selection bias and background data in presence-only modeling: a response to Peterson et al. and (2007). *Ecography*, 31, 272–278.

Phillips, S. J., Andersonb, R. P., & Schapire, R. E. (2006). Maximum entropy modeling of species geographic distributions. *Ecological Modelling*, 190, 231–259. DOI:10.1016/j.ecolmodel.2005.03.026.

Phillips, S. J., Dudík, M., & Schapire, R. E. (2018). *Maxent software for modeling species niches and distributions*, 3.4.1. Available from URL: http://biodiversityinformatics.amnh.org/open_source/maxent/.

Phillips, S. J., Dudík, M., & Schapire, R. E. (2004). *A maximum entropy approach to species distribution modeling.* Proceedings of the twenty-first international conference on Machine learning, Page 83, Banff, Alberta, Canada. ACM New York, NY, USA. 10.1145/1015330.1015412.

Phompila, C., Lewis, M., Ostendorf, B., & Clarke, K. (2015). MODIS EVI and LST Temporal Response for Discrimination of Tropical Land Covers. *Remote Sensing*, 7, 6026–6040. 10.3390/rs70506026.

Pigeon, G., Lemonsu, A., Long, N., Barrié, J., Masson, V., & Durand, P. (2006). Urban thermodynamic island in a coastal city analysed from an optimized surface network. *Boundary-Layer Meteorology*, 120, 315–351.

Pijanowski, B. C., Brown, D. G., Shellito, B., & Manik, G. (2002). Using neural networks and GIS to forecast land use changes: a land transformation model. *Computers, Environment and Urban Systems*, 26, 553–575. https://doi.org/10.1016/S0198-9715(01)00015-1.

Popradit, A., Srisatit, T., Kiratiprayoon, S., Yoshimura, J., Ishida, A., Shiyomi, M., Murayama, T., Chantaranothai, P., Outtaranakorn, S., & Phromma, I. (2015). Anthropogenic effects on a tropical forest according to the distance from human settlements. *Scientific Reports*, 5, 14689. DOI: 10.1038/srep14689. www.nature.com/scientificreports/.

Powers, J. S., Montgomery, R. A., Adair, E. C., Brearley, F. Q., & DeWalt, S. J. (2009). Decomposition in tropical forests: a pan-tropical study of the effects of litter type, litter placement and mesofaunal exclusion across a precipitation gradient. *Journal of Ecology*, 97, 801–811. DOI: 10.1111/j.1365-2745.2009.01515.x.

Purvis, A., Gittleman, J. L., Cowlishaw, G., & Mace, G. M. (2000). Predicting extinction risk in declining species. *Proceedings Biological Sciences*, 267, 1947–1952.

Qin, A., Liu, B., Guo, Q., Bussmann, R. W., Ma, F., Jian, Z., Xu, G., & Pei, S. (2017). Maxent modeling for predicting impacts of climate change on the potential distribution of *Thuja sutchuenensis* Franch., an extremely endangered conifer from southwestern China. *Global Ecology and Conservation*, 10, 139–146. http://dx.doi.org/10.1016/j.gecco.2017.02.004.

Rafiuddin, M., Uyedaa, H., & Islam, M. N. (2010). Characteristics of monsoon precipitation systems in and around Bangladesh. *International Journal of Climatology*, 30, 1042–1055. https://doi.org/10.1002/joc.1949.

Rahman, M. A., Mostafa Kamal, S. M., & Maruf Billah, M. (2016b). Rainfall Variability and Linear Trend Models on North-West Part of Bangladesh for the Last 40 Years. *American Journal of Applied Mathematics*, 4, 158–162. DOI: 10.11648/j.ajam.20160403.16.

Rahman, M. A., Woobaidullah, A. S. M., Quamruzzaman, C., Rahman, M. M., Khan, A. U., & Mustahid, F. (2016a). Probable Liquefaction Map for Purbachal New Town, Dhaka, Bangladesh. *International Journal of Emerging Technology and Advanced Engineering*, 6, 345–356.

Rahman, M. M., Motiur, M. R., Guogang, Z., & Islam, K.S. (2010). A review of the present threats to tropical moist deciduous Sal (Shorea robusta) forest ecosystem of central Bangladesh. *Tropical Conservation Science*, 3(1), 90–102. www.tropicalconservationscience.org.

Rahman, M. M., Vacik, H., Begum, F., Nishad, A., & Islam, K. K. (2007). Comparison of structural diversity of tree-crop associations in peripheral and buffer zones of Gachabari *Sal* forest area, Bangladesh. *Journal of Forestry Research*, 18, 23−26. http://dxdoi.org/10.1007/s11676-007-0004-1.

Rai, T., & Rai, L. (1994). *Trees of the Sikkim Himalaya*. Indus publishing. Pp. 98. ISBN 8173870012, 9788173870019.

RAJUK (Rajdhani Unnayan Kartripakkha), (2016). *Rajdhani Unnayan Kartripakkha*, Capital City Development Authority, Ministry of Housing and Public Works (MoHPW), Government of Bangladesh. http://www.rajukdhaka.gov.bd.

Rashid, H. E. (1991). *Geography of Bangladesh*. Dhaka, Bangladesh: University Press. ISBN 984-05-1159-9.

Rashid, T., Monsur, Md. H., & Suzuki, S. (2006). A review on the quaternary characteristics of Pleistocene tracts of Bangladesh. *Earth Science Reports*, 13, 1–13.

Rennenberg, N. (2002). Assessment of land use changes in Mukdaham and Nakhon Phanom provinces (NE Thailand) by means of remote sensing. *diplom.de*, 49–51. ISBN3832461353, 9783832461355.

Rocha, A. V., & Shaver, G. R. (2009). Advantages of a two band EVI calculated from solar and photosynthetically active radiation fluxes. *Agricultural and Forest Meteorology*, 149, 1560–1563.

Rouf, M. A., Uddin, M. K., Debsarma, S. K., & Rahman, M. M. (2011). Climate of Bangladesh: an analysis of northwestern and southwestern part using high resolution atmosphere-ocean general circulation model (AOGCM). *The Agriculturists*, 9(1&2), 143-154.

Rouse, J. W., Haas, R. H., Deering, D. W., Schell, J. A., & Harlan, J. C. (1974). *Monitoring the vernal advancement and retrogradation (green wave effect) of natural vegetation*. Technical Report, No E74-10676, NASA-CR-139243, PR-7. ID: 19740022555. Texas A&M Univ.; Remote Sensing Center. College Station, TX, United States.

Sahebjalal, E., & Dashtekian, K. (2013). Analysis of land use-land covers changes using normalized difference vegetation index (NDVI) differencing and classification methods. *African Journal of Agricultural Research*, 8, 4614–4622. doi:10.5897/AJAR11.1825.

Salam, M. A., Noguchi, T., & Koike, M. (1999). The causes of forest cover loss in the hill forests in Bangladesh. *GeoJournal*, 47, 539–549.

Saleska, S. R., Didan, K., Huete, A. R., & da Rocha, H. R. (2007). Amazon forests green-up during 2005 drought. *Science*, 318, 612.

Sandman, A. N., Wikström, S. A., Blomqvist, M., Kautsky, H., & Isaeus, M. (2013). Scale-dependent influence of environmental variables on species distribution: a case study on five coastal benthic species in the Baltic Sea. *Ecography*, 36, 354–363. DOI:10.1111/j.1600-0587.2012.07053.x

Sarma, S. K., & Das, R. K. R. (2009). Soil nutrient status in the *Sal* (*Shorea robusta*) forests of Goalpara district, Assam. *Journal of Advanced Plant Sciences*, 4, 14–17.

Schneider, S. H. (1989). The greenhouse effect: Science and policy. *Science*, 243, 771–81.

Seneviratne, S. I., Nicholls, N., Easterling, D., Goodess, C., Kanae, S., Kossin, J., Luo, Y., Marengo, J., McInnes, K., Rahimi, M., Reichstein, M., Sorteberg, A., Vera, C., & Zhang, X. (2012). *Changes in climate extremes and their impacts on the natural physical environment, in: Managing the Risks of Extreme Events and Disasters to*

Advance Climate Change Adaptation. A Special Report of Working Groups I and II of the Intergovernmental Panel on Climate Change (IPCC), edited by: Field, C. B., Barros, V., Stocker, T., Qin, D., Dokken, D., Ebi, K., Mastrandrea, M., Mach, K., Plattner, G.-K., Allen, S., Tignor, M., & Midgley, P., 109–230, Cambridge University Press, Cambridge, UK, and New York, NY, USA.

Sesnie, S. E., Gessler, P. E., Finegan, B., & Thessler, S. (2008). Integrating Landsat TM and SRTM-DEM derived variables with decision trees for habitat classification and change detection in complex neotropical environments. *Remote Sensing of Environment,* 112(5), 2145−2159.

Seto, K. C., Güneralp, B., & Hutyra, L. R. (2012). Global forecasts of urban expansion to 2030 and direct impacts on biodiversity and carbon pools. *Proceedings of the National Academi of Sciences*, USA, 109, 16083–88. https://doi.org/10.1073/pnas.1211658109.

Shahid, S., & Khairulmaini, O. S. (2009). Spatio-temporal variability of rainfall over Bangladesh during the time period 1969-2003. *Asia-Pacific journal of atmospheric sciences*, 45 (3), p.375−389.

Shapla, T., Park, J. Hongo, C., & Kuze, H. (2015). Agricultural land cover change in Gazipur, Bangladesh, in relation to local economy studied using Landsat images. *Advances in Remote Sensing*, 4, 214–223. DOI:10.4236/ars.2015.43017.

Shen, Y., Xiang,Y., Xu, E., Ge, X., & Li, Z. (2018). Major Co-localized QTL for plant height, branch initiation height, stem diameter, and flowering Time in an alien introgression derived Brassica napus DH population. *Frontiers in Plant Science*, 9, 390. https://www.frontiersin.org/article/10.3389/fpls.2018.00390.

Shivashankar, S., & Hiremath, P. S. (2011). PCA Plus LDA on Wavelet Co-occurrence Histogram Features for Texture Classification. *International Journal of Remote Sensing*, 3(4), 302−306.

Siddiqui, K.U., Islam, M.A., Ahmed, Z. U., Begum, Z. N. T., Hassan, M. A., Khondker, M., Rahman, M.M., Kabir, S. M. H., Ahmad, M., Ahmed, A.T.A., Rahman, A.K.A., & Haque, E.U. (Eds.). (2007). *Encyclopedia of flora and fauna of Bangladesh*, 11. *Angiosperms: Monocotyledons (Agavaceae-Najadaceae)*. Asiatic society of Bangladesh, Dhaka. 399 pp.

Singh, R. P., Singh, N., Singh, S., & Mukherjee, S. (2016). Normalized Difference Vegetation Index (NDVI) Based Classification to Assess the Change in Land Use/Land Cover (LULC) in Lower Assam, India. *International Journal of Advanced*

Remote Sensing and GIS, 5, 1963−1970. DOI: https://doi.org/10.23953/cloud.ijarsg.74.

SRDI (Soil Resources Development Institute), (2015). *Soil Resources Development Institute*, Ministry of Agriculture, Bangladesh. http://www.srdi.gov.bd/.

Stockwell, D. R. B., & Peters, D. G. (1999). The GARP modelling system: problems and solutions to automated spatial prediction. *International Journal of Geographic Information Systems*, 13, 143–158.

Tittensor, D. P., Walpole, M., Hill, S. L., Boyce, D. G., Britten, G. L., Burgess, N. D., et al. (2014). A mid-term analysis of progress toward international biodiversity targets. *Science*, 346, 241–244.

Tsumura, Y., Kado, T., Yoshida, K., Abe, H., Ohtani, M., Taguchi, Y., & Lee, S. L. (2011). Molecular database for classifying Shorea species (Dipterocarpaceae) and techniques for checking the legitimacy of timber and wood products. *Journal of Plant Research*, 124, 35–48. http://doi.org/10.1007/s10265-010-0348-z.

Tsuyuzaki, S., & del Moral, R. (1995). Species attributes in early primary succession on volcanoes. *Journal of Vegetation Science*, 6, 517–522. DOI: 10.2307/3236350.

Tucker, C. J. (1979). Red and photographic infrared linear combinations for monitoring vegetation. *Remote Sensing of Environment*, 8, 127–150. https://doi.org/10.1016/0034-4257(79)90013-0.

Ulvdal, P. (2016). *Stand dynamics and carbon stock in a* Sal *(*Shorea robusta *C.F. Gaertn) dominated forest in Southern Nepal*. Master Thesis no. 264. Swedish University of Agricultural Sciences, Southern Swedish Forest Research Centre, Alnarp.

Ustin, S., Zarco Tejada, P., Jacquemoud, S., & Asner, G. (2004). *Remote sensing of environment: State of the science and new directions.* In Remote Sensing for Natural Resources Management and Environmental Monitoring. Manual of Remote Sensing, (3rd. Ed.). Ustin, S.L., Ed., John Wiley and Sons, Inc.: Hoboken, NJ, USA, 4, 679–729.

Van Leeuwen, W. J. D., & Huete, A. R. (1996). Effects of standing litter on the biophysical interpretation of plant canopies with spectral indices. *Remote Sensing of Environment*, 55, 123–138. https://doi.org/10.1016/0034-4257(95)00198-0.

Wardlow, B. D., Egbert, S. L., & Kastens, J. H. (2007). Analysis of time-series MODIS 250 m vegetation index data for crop classification in the U.S. Central Great Plains. *Remote Sensing of Environment*, 108, 290–310.

Wilby, R. L., & Perry, G. L. W. (2006). Climate change, biodiversity and the urban environment: A critical review based on London, UK. *Progress in Physical Geography*, 30 (1), 73–98.

Xie, Y., Sha, Z., & Yu, M. (2008). Remote sensing imagery in vegetation mapping: a review. *Journal of Plant Ecology*, 1, 9–23. https://doi.org/10.1093/jpe/rtm005.

Xue, J., & Su, B. (2017). Significant remote sensing vegetation indices: a review of developments and applications. *Journal of Sensors*, ID 1353691, 17 pages. https://doi.org/10.1155/2017/1353691.

Yang, X. Q., Kushwaha, S. P. S., Saran, S., Xu, J., & Roy, P.S. (2013). Maxent modelling for predicting the potential distribution of medicinal plant, *Justicia adhatoda* L. in Lesser Himalayan foothills. *Ecological Engineering*, 51, 83–87. DOI: 10.1016/j.ecoleng.2012.12.004.

Zaman, A. K. M. A. (2016). *Precarious Periphery: Satellite township development causing socio-political economic and environmental threats at the fringe areas of Dhaka*. Unpublished Paper. Department of Architecture, KU Leuven. https://doi.org/10.13140/rg.2.2.30067.32807.

Zar, J. H. (1999). *Biostatistical Analysis*. Department of Biological Sciences, Northern Illinois University. 4th Ed. New Jersey 07458, USA. Prentice Hall, Inc. Simon & Schuster. ISBN 0-13-082390-2.

Zhang, L., Wen, D. Z., & Fu, S. L. (2009). Responses of photosynthetic parameters of Mikania micrantha and Chromolaena odorata to contrasting irradiance and soil moisture. *Biologia Plantarum*, 53(3), 517–522.

Zhou, N. Q., & Zhao, S. (2013). Urbanization process and induced environmental geological hazards in China. *Natural Hazards*, 67, 797–810. DOI: 10.1007/s11069-013-0606-1.

Zipperer, W. C. (1993). Deforestation patterns and their effects on forest patches. *Landscape Ecology*. 8(3), 177–184.

Appendices

Seven figures: Figure A-1 to A-7

One table: Table A-1

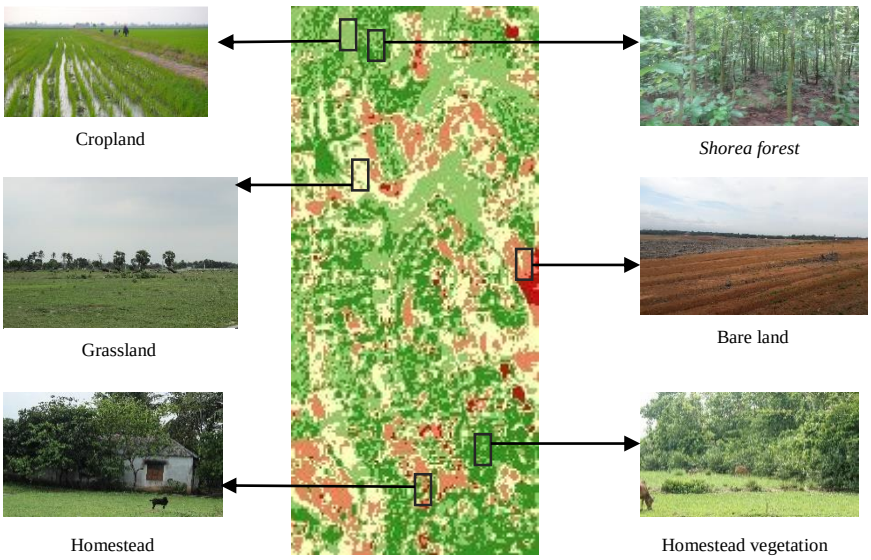

Figure A-1: A visual representation of original land use types reflected by the spectral bands of satellite data in Purbachal.

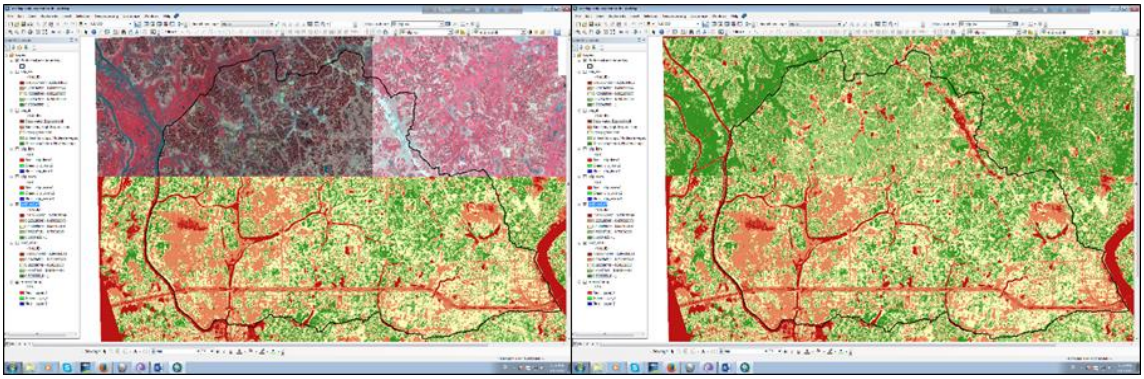

Figure A-2: Detection of land use change using swipe tool in Arc-GIS by overlapping two satellite data, IKONOS in 2001 at previous phase and WV2 in 2015 at recent phase. This technique has generated from EVI2 measurements.

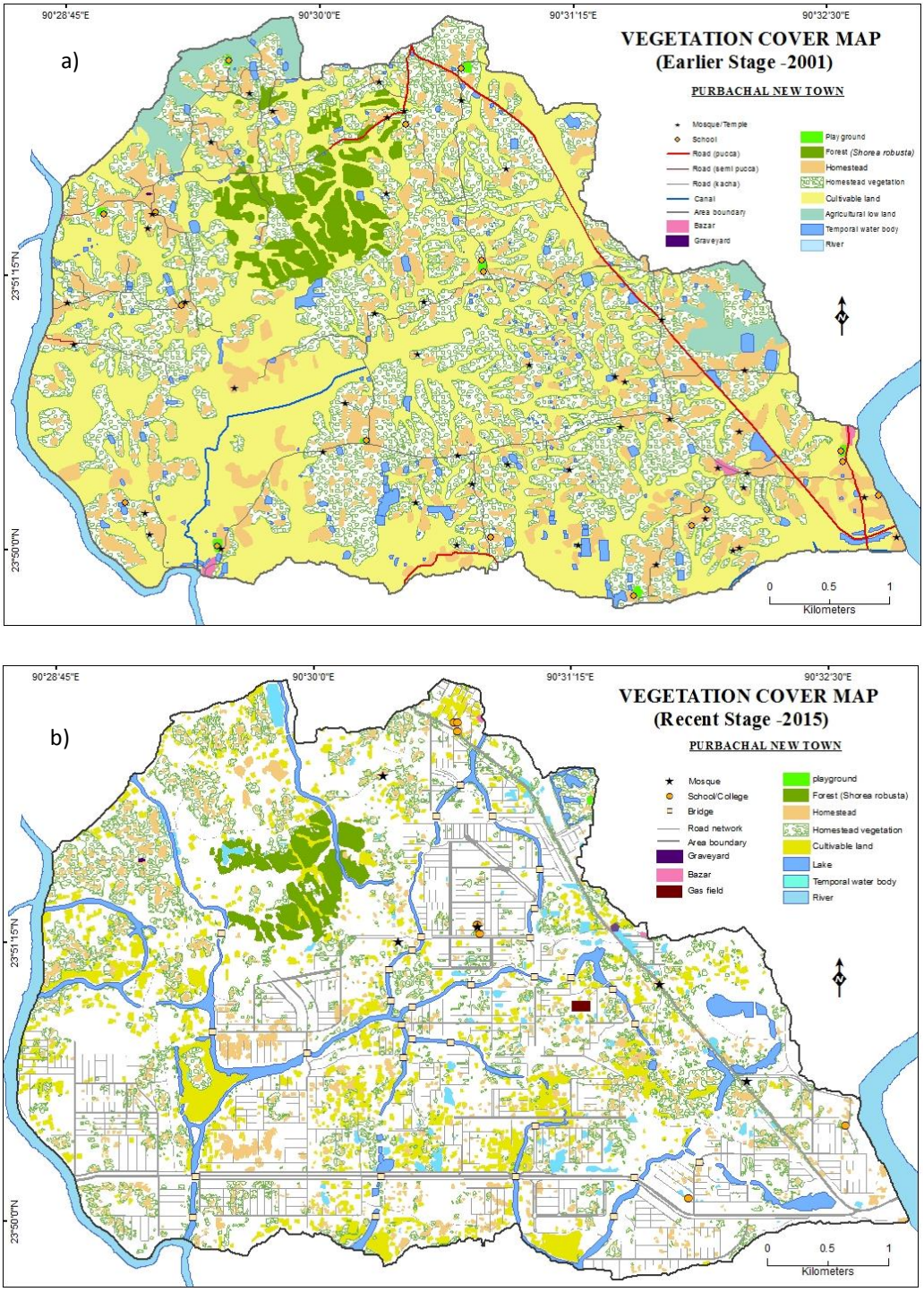

Figure A-3: Map of general LULC (Land Use Land Cover) of Purbachal with vegetation types. a) illustrates the potentiality of IKONOS (0.8 m) data for detecting LULC patterns in Purbachal. These data were modified and recorded from both of existing pre-project land use map of Purbachal (Anonymous 2013) and satellite data of IKONOS as well. b) Similar LULC patterns of current stage 2015 were detected in figure 4.b, derived from WV2 (0.5 m) multi-spectral imagery. General land cover types (e.g., vegetation and cropland), specific vegetation types (e.g., homestead vegetation, shorea forest), and water body with agricultural low land were visually demonstrated here.

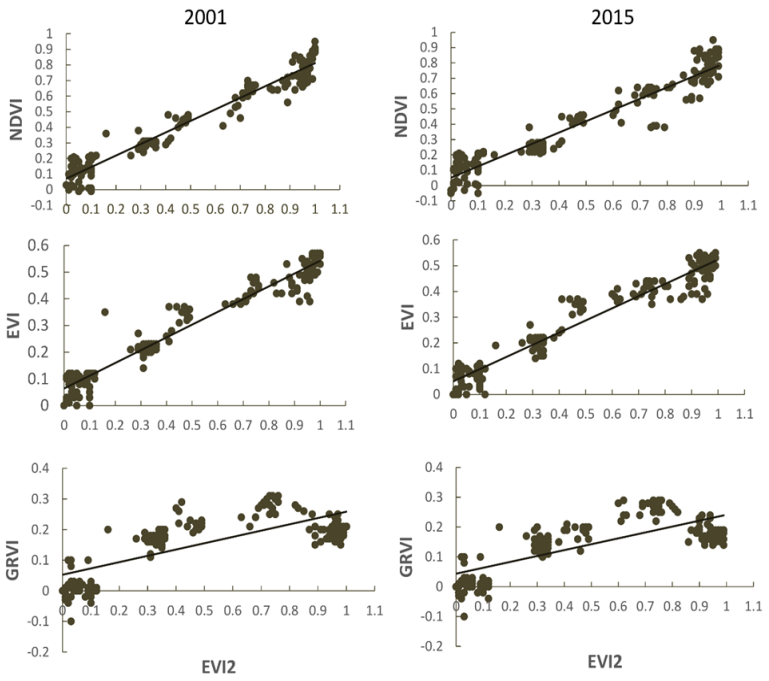

Figure A-4: Relationships between EVI2, EVI, NDVI and GRVI in 2001 and 2015 examined on the 182 ground truth points. All the linear regressions are significant at $P < 0.001$.

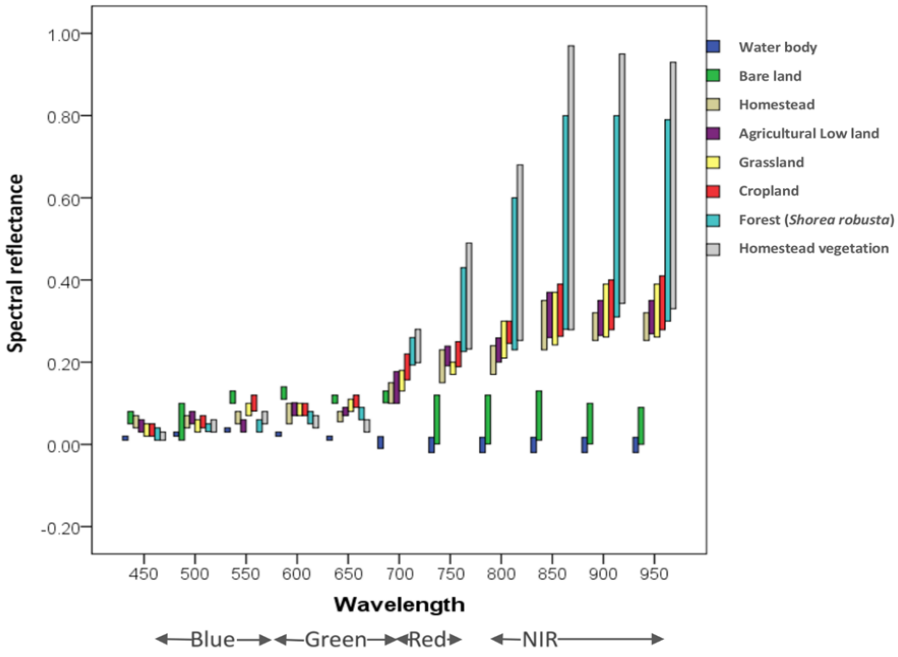

Figure A-5: The dynamic responses of the VIs for the representative conditions of the sites based on the wavelength of IKONOS and WV2 data. The range of minimum and maximum reflectance on each land use type was plotted based on each wavelength of the satellite data.

Table A-1: The plant species list of the four PFGs

Group	Species	Family name	Growth form								Branching pattern				Leaf hair		Leaf phenology		Leaf shape																Flower					Fruit	Fruit shape			Fruit color				Repro-duction		Seed		Flowering and fruiting period		Soil pH	Elevation		
			T	S	H	G	W	H (m)	SD (m)	SI	E	Sp	Dr	Ts	Ha	G	D	E	P	El	O	Ov	L	A	R	C	Ac	Acu	Co	Ax	Pa	B	Wc/w	Pe	Dr	Be	Ob	Gl	Gr	Y	R	B	Se	Sp	Si	Pl	Jan-Jun	Jul-Dec	pH	Hi	Me	Lo
A	*Ficus religiosa* L.	Moraceae	1	0	0	0	0	30.00	3.00	10.00	0	1	0	0	0	1	1	0	1	0	0	0	0	1	0	0	0	1	0	1	0	0	0	1	0	0	0	1	0	0	0	1	1	0	0	0	1	0	7	1	1	0
	Murdannia keisak (Hassk.) Hand.-Maz.	Commelinaceae	0	0	0	1	0	0.76	0.00	190.50	0	1	0	0	1	0	1	0	0	0	0	0	0	0	0	0	0	0	0	0	0	0	0	0	0	0	0	0	0	0	0	0	1	0	0	0	0	0	6	0	1	0
	Aegle marmelos (L.) Corr.	Rutaceae	1	0	0	0	0	15.00	0.20	75.00	0	0	1	1	0	1	1	0	1	1	0	1	0	0	0	0	0	0	0	1	0	0	0	0	0	1	1	1	0	1	0	0	1	0	0	1	0	1	7	0	1	1
	Flacourtia indica (Burm. f.) Merr.	Salicaceae	0	1	0	0	0	3.00	0.03	100.00	0	1	0	1	0	1	1	0	0	0	1	0	1	0	0	1	0	1	0	1	0	0	0	1	0	0	0	1	1		1	1	1	0	0	0	1	0	5.5	1	1	0
	Grewia serrulata DC.	Malvaceae	1	0	0	0	0	15.00	0.03	500.00	0	0	1	0	1	0	0	1	1	0	1	1	1	0	0	0	1	1	0	1	0	0	0	1	1	0	1	1	1	0	0	1	1	0	1	0	1	0	6.5	0	1	0
	Chrysopogon aciculatus (Retz.) Trin.	Poaceae	0	0	0	1	0	0.60	0.01	66.67	1	0	0	0	0	1	0	0	0	0	0	0	1	1	0	0	0	0	0	0	1	1	0	1	0	0	1	0	0	0	0	0	1	0	0	0	0	0	5.5	0	1	0
	Cynodon dactylon Pers.	Poaceae	0	0	0	1	0	0.15	0.00	150.00	1	0	0	0	1	0	0	0	0	0	0	0	0	1	0	0	0	0	1	0	0	0	0	0	0	0	0	0	0	0	0	0	1	0	0	0	0	1	5	0	0	1
	Shorea robusta Gaertn.f.	Dipterocarpaceae	1	0	0	0	1	35.00	3.50	10.00	0	1	0	0	0	1	1	0	1	0	1	1	0	0	1	1	0	1	1	1	1		0	1	0	0	1	0	0	0	0	0	1	1	0	0	0	1	6	1	0	0
	Lipocarpha squarrosa (L.) Goetgh.	Cyperaceae	0	0	1	0	0	0.32	0.00	160.00	1	0	0	0	0	1	0	0	0	0	0	0	0	0	0	0	0	0	0	0	0	0	0	0	0	0	0	0	0	0	0	0	1	0	0	0	0	0	6.5	0	0	1
	Colocasia esculanta (L) Schott.	Araceae	0	0	1	0	0	1.00	0.00	500.00	1	0	0	0	0	1	1	0	0	0	0	0	0	0	0	0	0	0	0	0	0	0	0	0	0	0	0	0	0	0	0	0	0	0	0	0	0	0	5.7	0	0	1
	Glycosmis pentaphylla (Retz.) DC.	Rutaceae	0	1	0	0	0	4.00	0.09	44.44	0	1	0	0	0	1	0	1	1	1	1	1	0	1	0	0	1	0	1	1	1	0	1	0	0	1	0	1	0	0	1	0	1	1	1	0	0	0	5	0	1	1
	Abroma augusta L.	Sterculiaceae	0	1	0	0	0	2.00	0.02	100.00	0	1	0	0	1	0	1	0	0	0	0	0	0	0	0	0	0	0	0	0	0	0	0	0	0	0	0	0	0	0	0	0	1	0	0	0	0	0	5	0	1	0
	Carica papaya L.	Caricaceae	1	0	0	0	0	5.00	0.30	16.67	1	0	0	0	0	1	1	0	1	0	1	0	0	0	0	0	1	0	0	1	1	0	1	1	0	1	0	0	1	1	0	0	1	0	0	1	0	0	6.5	0	1	0
	Oryza sativa L.	Poaceae	0	0	0	1	0	0.62	0.00	206.67	1	0	0	0	1	0	1	0	0	0	0	0	0	0	0	0	0	0	0	0	0	0	0	0	0	0	0	0	0	0	0	0	1	0	0	0	0	0	6.1	0	0	1
	Clerodendrum infortunatum L.	Lamiaceae	0	1	0	0	0	4.00	0.15	26.67	1	0	0	0	1	0	1	0	0	1	0	0	1	0	0	1	1	0	0	0	0	0	1	0	1	1	0	0	0	1	1	0	0	1	1	0	0	0	7	0	1	0
	Streblus asper Lour.	Moraceae	1	0	0	0	0	14.00	0.18	77.78	0	0	1	0	1	0	0	1	1	1	0	1	1	0	0	1	0	1	1	0	0	0	1	0	0	1	0	0	1	0	1	0	0	1	0	0	0	0	6	1	1	0
	Borassus flabellifer L.	Arecaceae	1	0	0	0	1	30.00	0.20	150.00	1	0	0	0	0	1	0	1	1	0	0	0	1	0	0	0	0	0	1	0	0	0	0	0	1	0	0	0	0	0	0	0	1	0	0	0	0	0	6.7	1	1	0
B	*Desmodium triflorum* (L.) DC.	Fabaceae	0	0	1	0	0	0.20	0.01	14.29	0	1	0	0	1	0	1	0	1	0	0	0	1	0	0	0	0	0	0	0	0	0	0	0	0	0	0	0	0	0	0	0	1	0	0	0	0	0	5	0	1	1
	Schizostachyum dullooa (Gamble) R.	Poaceae	0	0	1	0	1	40.00	0.25	160.00	1	0	0	0	1	0	0	1	1	0	0	0	1	0	1	0	0	1	0	0	0	0	0	0	0	0	0	0	0	0	0	0	0	1	0	0	1	1	7	0	1	1
	Justicia adhatoda L.	Acanthaceae	0	1	0	0	0	3.00	0.02	150.00	0	1	0	0	1	0	0	1	0	0	0	0	0	0	0	0	0	0	0	0	0	0	0	0	0	0	0	0	0	0	0	0	1	0	0	0	0	0	7	0	1	0
	Melastoma malabathricum L.	Melastomataceae	0	1	0	0	0	3.00	0.00	750.00	0	1	0	0	1	0	0	1	1	1	0	0	1	0	1	0	1	1	0	0	0	0	0	0	0	0	0	0	0	0	0	0	1	1	0	0	1	0	0	4.5	0	1	0
	Ampelocissus latifolia (Roxb.) Planch.	Vitaceae	0	1	0	0	0	6.00	0.01	545.45	0	1	0	0	1	0	1	0	1	0	0	1	0	0	0	0	1	0	0	0	0	1	0	1	0	0	1	1	0	0	0	1	1	0	1	0	1	0	5.5	1	0	0
	Holarrhena antidysenterica (L.) Wall. ex Decne.	Apocynaceae	1	0	0	0	0	2.40	0.08	30.00	0	1	0	0	0	1	0	1	1	1	1	1	0	0	1	0	1	1	1	0	0	0	1	1	0	0	1	0	0	0	0	0	1	0	0	1	1	0	6.5	0	1	0
	Mimosa pudica L.	Fabaceae	0	0	1	0	0	1.00	0.03	40.00	1	0	0	1	1	0	0	0	0	0	0	0	1	0	0	0	1	0	1	1	0	0	0	0	0	1	0	0	0	0	0	0	1	0	1	0	0	1	6.5	0	1	1
	Canavalia virosa (Roxb.) Wight & Arn.	Fabaceae	0	1	0	0	0	6.00	0.08	78.95	0	1	0	0	1	0	1	0	1	1	1	1	0	0	1	0	1	0	0	0	0	0	0	0	0	0	0	0	1	0	0	0	1	0	0	1	0	0	5.3	0	1	0
	Chromolaena odorata (L.)	Asteraceae	0	0	1	0	0	2.10	0.20	10.50	1	0	0	0	1	0	1	0	0	1	0	0	1	1	0	0	0	1	1	0	0	0	0	1	0	0	0	0	0	0	0	0	1	0	0	0	0	0	7	0	1	1
	Axonopus compressus (Sw.) P. Beauv.	Poaceae	0	0	0	1	0	0.20	0.00	66.67	0	1	0	0	1	0	0	0	0	0	0	0	0	0	0	0	0	0	0	0	0	0	0	0	0	0	0	0	0	0	0	0	1	0	0	0	0	0	7	0	1	0
	Solanum sisymbriifolium Lam.	Solanceae	0	0	1	0	0	1.20	0.02	75.00	1	1	0	1	1	0	1	0	1	0	0	0	0	0	0	0	0	0	1	0	0	1	0	0	1	0	1	0	1	0	0	0	1	0	0	1	0	1	5	0	1	1

	Phyllanthus emblica L.	Phyllanthaceae	1	0	0	0	0	20.00	0.03	666.67	0	0	1	0	0	1	1	0	1	0	1	0	0	0	0	0	0	0	0	0	0	0	1	1	0	0	0	1	0	1	0	0	1	0	0	0	1	0	7	1	0	0
	Terminalia arjuna (Roxb.) Wight & Arn.	Combretaceae	1	0	0	0	1	25.00	2.00	12.50	0	0	1	0	0	1	1	0	1	0	1	1	0	0	1	1	1	1	1	1	1		1	0	0	0	0	0	0	0	0	0	1	0	0	0	0	1	6.5	1	0	0
	Senna occidentalis (L.)	Fabaceae	0	1	0	0	0	2.00	0.03	66.67	1	0	0	0	0	1	1	0	0	0	0	0	0	0	0	0	0	0	0	0	0	0	0	0	0	0	0	0	0	0	0	0	1	0	0	0	0	0	6	0	1	0
	Musa × paradisiaca L.	Musaceae	0	0	1	0	0	9.00	0.61	14.75	1	0	0	0	0	1	1	0	0	0	0	0	0	0	0	0	0	0	0	0	0	0	0	0	0	0	0	0	0	0	0	0	0	0	0	0	0	0	7	0	1	0
	Xanthozylum budrunga DC.	Rutaceae	1	0	0	0	0	35.00	0.75	46.67	1	0	0	1	0	1	1	1	0	0	0	0	0	0	0	0	0	1	0	0	1	0	0	0	1	0	0	0	0	0	0	1	1	0	1	0	1	0	7	1	1	0
	Uraria lagopus DC.	Aceraceae	0	0	1	0	0	0.61	0.01	61.00	1	0	0	0	1	0	1	0	1	0	1	0	0	0	1	0	0	0	0	1	0	0	1	1	0	0	0	0	0	0	0	0	1	0	1	0	0	1	6	1	0	0
	Ricinus communis L.	Euphorbiaceae	0	0	1	0	0	12.00	0.06	200.00	1	0	0	0	1	0	1	0	1	0	0	1	1	0	0	0	1	1	0	0	0	0	1	1	0	0	0	0	0	0	0	0	1	0	0	0	0	0	6.5	0	1	0
	Mucuna pruriens (L.) DC.	Fabaceae	0	0	0	0	0	0.00	0.01	0.00	0	1	0	0	1	0	1	0	0	0	0	0	1	0	0	1	0	1	0	0	0	0	0	0	0	1	0	0	0	0	1	0	1	0	0	1	1	0	6.3	1	0	0
	Ficus benghalensis L.	Moraceae	1	0	0	0	0	25.00	0.15	166.67	0	1	0	0	0	1	1	1	1	1	0	1	0	0	1	0	0	0	1	1	0	0	0	0	0	0	0	1	0	0	1	0	1	0	0	0	0	1	6.7	1	1	0
	Polyalthia longifolia Sonn.	Annonaceae	1	0	0	0	0	4.00	0.10	40.00	0	0	1	0	1	0	1	0	0	0	0	0	1	0	0	0	0	1	0	0	0	0	1	0	0	0	1	0	1	0	0	0	1	0	1	0	1	0	6.5	0	1	0
	Luffa aegyptiaca Mill.	Cucurbitaceae	0	0	1	0	0	15.00	0.03	500.00	0	1	0	0	1	0	1	0	0	0	0	0	0	0	0	0	1	0	0	0	0	1	0	0	0	0	1	0	1	0	0	0	1	0	0	1	1	0	6.5	0	1	0
	Ficus hispida L.f.	Moraceae	1	1	0	0	0	15.00	0.25	60.00	1	0	0	0	1	0	0	1	1	1	1	0	0	0	0	1	0	1	0	0	0	0	1	1	0	0	0	1	0	1		0	1	0	0	0	1	0	6.8	0	1	0
	Shorea robusta Roth.	Dipterocarpaceae	1	0	0	0	1	30.00	2.50	12.00	0	1	0	0	0	1	1	0	0	0	0	1	0	0	0	0	1	0	0	0	1	1	1	0	1	0	0	0	1	0	0	0	1	0	0	0	1	0	6.5	1	0	0
	Cyperus rotundus L.	Cyperaceae	0	0	0	1	0	0.30	0.00	100.00	1	0	0	0	0	1	1	0	0	0	1	0	0	0	0	0	1	0	0	0	1	1	0	0	0	0	0	0	0	0	0	0	1	0	0	1	0	1	6	0	0	1
	Trema orientalis (L.) Blume	Cannabaceae	1	0	0	0	1	15.24	1.02	14.94	0	0	1	0	1	0	0	1	1	1	0	1	1	0	0	1	1	0	0	1	0	0	0	0	1	0	0	1	0	0	0	1	1	1	0	0	1	0	6.1	0	1	0
	Acacia nilotica (L.)	Mimosaceae	1	0	0	0	0	12.00	0.20	60.00	0	1	0	0	0	1	1	0	0	0	0	0	0	0	0	0	0	0	0	0	1	0	0	0	0	0	1	0	1	0	0	0	0	1	0	1	0	1	7	1	0	0
	Coix lacryma-jobi L.	Poaceae	0	0	0	1	0	1.20	0.00	400.00	1	0	0	0	1	0	1	0	0	0	0	0	1	0	0	1	0	0	0	0	0	0	1	0	0	0	0	1	0	0	0	1	1	0	1	0	0	1	5.5	0	0	1
C	*Artocarpus heterophyllus* Lam.	Moraceae	1	0	0	0	1	25.00	0.80	31.25	0	1	0	0	0	1	0	1	1	1	0	1	0	1	0	0	1	0	0	1	0	0	0	0	0	0	0	1	1	0	0	0	1	0	0	1	1	0	6.5	1	1	0
	Eichhornia crassipes (Mart.) Solms-Laub.	Pontederiaceae	0	0	1	0	0	0.65	0.40	1.63	1	0	0	0	0	1	0	0	0	0	0	1	0	0	1	1	0	0	0	0	0	0	0	0	0	0	0	0	0	0	0	0	0	0	0	0	0	1	5.9	0	0	0
	Lpomoea fistulosa Mart. ex Choisy	Convolvulaceae	0	1	0	0	0	2.50	0.09	27.78	1	0	0	0	1	0	1	0	1	0	1	1	0	0	0	1	0	0	0	1	0	0	0	0	0	0	0	0	1	0	0	0	1	1	0	0	0	1	6.6	0	0	1
	Mangifera indica L.	Anacardiaceae	1	0	0	0	1	40.00	24.38	1.64	0	1	0	0	0	1	0	1	1	1	1	0	1	0	0	0	0	0	0	1	1	1	1	0	1	0	0	0	0	1	0	1	1	0	1	0	1	0	6.5	1	1	0
	Mangifera longipes Griff.	Anacardiaceae	1	0	0	0	0	40.00	0.50	80.00	0	1	0	0	0	1	0	1	1	1	1	0	1	0	0	0	0	1	0	0	0	0	0	1	1	0	0	0	0	0	0	0	1	0	0	0	0	1	6.5	1	1	0
	Thevetia peruviana (Pers.) K. Schum.	Apocynaceae	0	1	0	0	0	4.00	0.06	66.67	0	1	0	0	0	1	0	1	0	0	0	0	1	1	0	0	0	0	1	0	0	0	1	1	0	0	0	0	0	0	0	1	1	0	0	0	1	0	6	1	1	0
	Cocos nucifera L.	Arecaceae	1	0	0	0	1	30.00	0.50	60.00	1	0	0	0	0	1	0	1	1	0	0	0	0	0	0	0	0	0	0	0	0	0	0	0	0	0	0	0	0	1	0	0	1	0	1	0	1	0	6	0	1	1
	Melia sempervirens (L.) All.	Meliaceae	1	0	0	0	0	45.00	2.10	21.43	0	1	0	0	0	1	1	0	0	0	0	0	1	0	0	0	0	1	0	0	1	0	1	0	1	0	0	0	1	0	0	0	0	1	1	0	1	0	6.7	0	1	0
	Aphanamixis polystachya (wall.)	Meliaceae	1	0	0	0	1	20.00	1.18	16.95	0	1	0	0	0	1	0	1	1	1	1	0	0	0	1	0	0	0	1	1	0	0	1	1	0	0	0	0	0	1	1	0	1	0	1	0	1	0	5.5	1	1	0
	Moringa oleifera Lam.	Moringaceae	1	0	0	0	0	10.00	0.08	125.00	0	1	0	0	0	1	1	0	0	1	1	1	0	1	0	0	1	0	0	0	1	1	1	1	0	0	1	0	0	0	0	0	1	1	0	1	1	0	7	0	1	0
	Bombax ceiba L.	Bombacaceae	1	0	0	0	1	30.00	2.30	13.04	0	1	0	1	0	1	1	0	1	1	0	0	0	0	0	0	1	1	0	0	0	1	0	0	0	0	0	0	0	0	0	1	1	1	0	1	1	0	4	1	1	0
	Phyllanthus reticulatus Poir.	Phyllanthaceae	0	1	0	0	0	3.00	0.03	120.00	0	0	1	0	0	1	0	1	0	0	0	0	0	0	0	0	1	0	0	0	0	0	0	0	1	0	0	0	0	0	1	0	1	0	1	0	1	0	0	0	0	1
	Coccinia grandis (L.) Voigt	Cucurbitaceae	0	0	1	0	0	0.30	0.06	5.00	0	1	0	0	0	1	1	0	1	0	0	0	0	0	0	0	0	0	0	0	0	0	1	0	0	0	0	0	0	0	1	0	1	1	0	0	1	0	7	0	1	0
	Tamarindus indica L.	Fabaceae	1	0	0	0	1	24.00	2.00	12.00	0	1	0	0	0	1	1	0	1	0	1	0	0	0	1	0	0	0	0	0	0	0	0	1	0	0	1	0	0	0	0	0	1	0	0	1	1	0	7	1	1	0
	Syzygium fruticosum DC.	Myrtaceae	0	1	0	0	1	3.00	0.09	33.33	0	1	0	0	0	1	0	1	1	1	1	0	1	0	0	0	1	0	1	0	1	0	1	0	0	1	0	1	0	0	0	0	1	0	0	0	0	1	6	0	1	0
	Ocimum basilicum L.	Lamiaceae	0	1	0	0	0	1.10	0.01	110.00	1	0	0	0	1	0	1	0	0	0	0	1	0	0	0	0	1	0	0	0	0	0	1	0	0	0	0	0	0	0	0	0	1	0	0	1	1	0	7	0	1	0
	Flacourtia jangomas (Lour.) raeusch.	Salicaceae	1	0	0	0	1	15.00	0.10	150.00	0	0	1	1	0	1	0	1	0	0	0	1	1	0	0	0	0	1	0	1	0	0	1	1	0	1	0	1	0	0	0	1	1	0	0	1	0	1	5	1	1	0

	Alangium salvifolium (L. f.) Wang.	Alangiaceae	1	0	0	0	0	30.00	1.60	18.75	0	0	1	1	0	1	1	0	1	0	1	0	1	0	0	0	0	0	1	1	0	1	1	1	1	0	0	0	0	0	0	1	1	0	1	0	1	0	6.8	0	1	0
	Acacia auriculiformis A. Cunn. ex Benth.	Fabaceae	1	0	0	0	1	28.00	0.80	35.00	0	0	1	0	0	1	0	1	1	0	0	0	0	1	0	0	1	0	1	1	0	0	0	0	0	0	0	0	0	0	0	1	0	0	0	1	0	6	0	1	1
	Lepisanthes rubiginosa (Roxb.) Leenh.	Sapindaceae	1	0	0	0	1	16.00	0.41	39.02	0	1	0	0	1	0	1	0	1	1	0	0	1	0	1	0	1	0	0	0	1	0	1	0	0	0	1	0	1	0	0	1	1	0	1	0	1	0	6	0	1	0
	Senna obtusifolia (L.)	Fabaceae	0	0	1	0	0	2.00	0.00	571.43	1	0	0	0	1	1	1	0	0	0	0	1	0	0	0	0	1	0	0	1	0	0	0	1	0	0	0	0	0	0	0	0	1	0	0	1	0	1	7	0	1	0
	Calamus tenuis Roxb.	Arecaceae	0	0	0	0	0	20.00	0.03	800.00	0	1	0	1	1	0	0	1	1	0	0	0	0	1	0	0	0	0	0	0	0	0	1	0	1	0	0	0	0	0	0	1	1	0	1	0	1	0	5.8	0	1	0
	Diospyros blancoi A. DC.	Ebenaceae	1	0	0	0	1	19.00	2.01	9.45	1	0	0	0	0	1	0	1	0	0	1	0	0	1	1	1	0	0	1	1	0	0	1	1	0	1	0	1	0	0	1	1	1	0	0	1	0	1	6.1	0	1	0
	Agrostis canina L.	Poaceae	0	0	0	1	0	0.60	0.00	200.00	1	0	0	0	1	0	1	0	0	0	0	0	0	0	0	0	0	0	0	0	1	0	1	0	0	0	0	0	0	0	0	0	1	0	0	0	1	0	7	0	0	1
	Terminalia bellirica (Gaertn.) Roxb.	Combretaceae	1	0	0	0	1	40.00	1.50	26.67	0	1	0	0	0	1	1	0	1	1	1	0	0	0	1	0	0	1	1	1	0	0	0	0	1	0	0	1	0	0	0	0	1	0	0	0	0	1	6.5	0	1	0
	Mimusops elengi L.	Sapotaceae	1	0	0	0	0	34.00	1.00	34.00	0	1	0	0	0	1	0	1	1	0	1	0	0	0	0	0	0	1	0	0	0	1	1	1	0	1	0	0	0	0	0	0	1	0	1	0	1	0	6.5	1	1	0
	Ziziphus mauritiana Lam.	Rhamnaceae	1	0	0	0	1	15.00	0.40	37.50	0	1		1	0	1	1	0	1	1	0	0	0	0	0	0	0	0	0	1	0	1	0	1	1	0	0	0	1	1	0	0	1	0	1	0	0	1	7	1	1	0
	Antidesma montanum Blume var.	Euphorbiaceae	1	0	0	0	1	18.00	0.03	600.00	0	1	0	0	0	1	0	1	1	1	0	0	0	0	0	0	0	0	0	1	0	0	0	1	0	1	0	0	1	0	0	1	1	0	0	0	0	1	5.6	0	1	0
	Dillenia indica L.	Dilleniaceae	1	0	0	0	1	40.00	1.20	33.33	0	1	0	0	1	0	0	1	1	0	1	0	0	1	0	0	0	0	1	0	0	0	1	0	0	0	0	1	1	0	0	0	1	1	0	0	1	0	6	1	0	0
	Artocarpus lacucha Buch.-Ham.	Moraceae	1	0	0	0	1	20.00	0.13	153.85	0	1	0	0	0	1	1	0	1	1	0	0	0	0	0	0	1	0	1	0	0	0	0	0	0	0	0	1	0	1	0	0	1	0	0	1	1	0	7	1	1	0
	Diospyros malabarica (Desr.) Kostel	Ebenaceae	1	0	0	0	1	37.00	2.00	18.50	0	0	1	0	0	1	0	1	1	0	1	0	0	0	0	0	1	0	0	1	0	0	1	0	0	0	0	1	0	1	0	0	1	0	0	1	1	0	7	0	1	1
	Dipterocarpus turbinatus Gaertn. f.	Dipterocarpaceae	1	0	0	0	1	45.00	4.50	10.00	0	1	0	0	0	1	1	0	1	1	0	0	0	0	0	0	1	0	1	1	0	0	1	0	1	0	0	0	0	0	0	1	1	0	1	0	1	0	5.5	1	0	0
	Croton caudatus Geiseler	Euphorbiaceae	0	1	0	0	0	13.00	0.05	260.00	0	1	0	0	1	0	1	0	0	0	0	1	0	0	0	0	0	0	0	0	0	0	1	0	1	0	0	0	1	0	0	0	1	0	0	1	0	0	5.5	0	1	0
	Cleistanthus collinus (ROXB.) BENTH. & HOOK.	Phyllanthaceae	1	0	0	0	0	15.00	0.50	30.00	0	1	0	0	0	1	1	0	0	0	0	0	0	0	0	0	0	0	0	0	0	0	0	0	1	0	0	0	0	0	0	1	1	0	0	0	0	0	7	1	0	0
	Dipterocarpus alatus Roxb.	Dipterocarpaceae	1	0	0	0	1	40.00	3.50	11.43	0	1	0	0	1	0	0	1	0	1	0	0	0	0	0	0	0	0	0	0	0	1	0	0	1	0	0	0	0	0	0	1	1	0	1	0	0	0	6	1	0	0
	Syzygium jambos (L.) Alston.	Myrtaceae	1	0	0	0	1	10.00	0.50	20.00	0	1	0	0	0	1	0	1	1	1	0	0	0	0	0	0	0	0	1	0	0	0	1	1	0	0	0	1	0	1	0	0	1	0	1	0	1	0	6.5	1	1	0
	Barringtonia acutangula (L.) Gaertn.	Lecythidaceae	1	0	0	0	0	13.00	0.90	14.44	0	1	0	0	1	1	0	1	1	0	0	0	0	1	0	0	1	0	0	0	0	1	0	1	0	1	0	0	1	0	0	0	1	0	0	0	0	1	7	0	1	1
	Terminalia chebula Retz.	Combretaceae	1	0	0	0	1	20.00	0.60	33.33	0	1	0	0	0	1	1	0	1	0	0	1	0	0	1	0	1	0	1	1	1	0	1	0	1	0	0	0	0	1	0	1	1	0	1	0	1	0	6.5	1	0	0
	Syzygium cumini (L.)	Myrtaceae	1	0	0	0	1	35.00	4.00	8.75	0	1	0	0	0	1	0	1	1	0	0	0	1	0	0	0	0	1	1	0	0	0	1	0	0	1	0	0	0	0	0	1	1	0	1	0	1	0	6.6	1	1	0
	Citrus maxima (Burm.) Merr.	Rutaceae	1	0	0	0	1	9.00	0.20	45.00	0	1	0	1	0	1	0	1	1	0	0	1	0	0	1	0	1	0	1	1	0	1	1	1	0	0	0	1	1	1	0	0	1	0	0	1	0	1	7	0	1	0
D	*Syzygium samarangense* Merr. & Perry	Myrtaceae	1	0	0	0	1	20.00	4.00	5.00	0	1	0	0	0	1	0	1	1	1	0	0	0	0	0	0	0	1	1	0	0	0	1	1	0	0	1	0	0	0	0	0	1	0	1	0	0	1	6.6	1	1	0
	Lagerstroemia speciosa (L.) Pers.	Lythraceae	1	0	0	0	1	18.00	1.50	12.00	0	1	0	0	0	1	1	0	1	0	1	0	0	0	1	0	1	0	0	0	1	0	0	1	0	0	0	1	0	0	0	0	1	0	0	0	1	0	7	0	1	0

	Alangium salvifolium (L. f.) Wang.	Alangiaceae	1	0	0	0	0	30.00	1.60	18.75	0	0	1	1	0	1	1	0	1	0	1	0	1	0	0	0	0	0	1	1	0	1	1	1	1	0	0	0	0	0	0	1	1	0	1	0	1	0	6.8	0	1	0
	Acacia auriculiformis A. Cunn. ex Benth.	Fabaceae	1	0	0	0	1	28.00	0.80	35.00	0	0	1	0	0	1	0	1	1	0	0	0	0	1	0	0	1	0	1	1	0	0	0	0	0	0	0	0	0	0	0	0	1	0	0	0	1	0	6	0	1	1
	Lepisanthes rubiginosa (Roxb.) Leenh.	Sapindaceae	1	0	0	0	1	16.00	0.41	39.02	0	1	0	0	1	0	1	0	1	1	0	0	1	0	1	0	1	0	0	0	1	0	1	0	0	0	1	0	1	0	0	1	1	0	1	0	1	0	6	0	1	0
	Senna obtusifolia (L.)	Fabaceae	0	0	1	0	0	2.00	0.00	571.43	1	0	0	0	1	1	1	0	0	0	0	1	0	0	0	0	1	0	0	1	0	0	0	1	0	0	0	0	0	0	0	0	1	0	0	1	0	1	7	0	1	0
	Calamus tenuis Roxb.	Arecaceae	0	0	0	0	0	20.00	0.03	800.00	0	1	0	1	1	0	0	1	1	0	0	0	0	1	0	0	0	0	0	0	0	0	1	0	1	0	0	0	0	0	0	1	1	0	1	0	1	0	5.8	0	1	0
	Diospyros blancoi A. DC.	Ebenaceae	1	0	0	0	1	19.00	2.01	9.45	1	0	0	0	0	1	0	1	0	0	1	0	0	1	1	1	0	0	1	1	0	0	1	1	0	1	0	1	0	0	1	1	1	0	0	1	0	1	6.1	0	1	0
	Agrostis canina L.	Poaceae	0	0	0	1	0	0.60	0.00	200.00	1	0	0	0	1	0	1	0	0	0	0	0	0	0	0	0	0	0	0	0	1	0	1	0	0	0	0	0	0	0	0	0	1	0	0	0	1	0	7	0	0	1
	Terminalia bellirica (Gaertn.) Roxb.	Combretaceae	1	0	0	0	1	40.00	1.50	26.67	0	1	0	0	0	1	1	0	1	1	1	0	0	0	1	0	0	1	1	1	0	0	0	0	1	0	0	1	0	0	0	0	1	0	0	0	0	1	6.5	0	1	0
	Mimusops elengi L.	Sapotaceae	1	0	0	0	0	34.00	1.00	34.00	0	1	0	0	0	1	0	1	1	0	1	0	0	0	0	0	0	1	0	0	0	1	1	1	0	1	0	0	0	0	0	0	1	0	1	0	1	0	6.5	1	1	0
	Ziziphus mauritiana Lam.	Rhamnaceae	1	0	0	0	1	15.00	0.40	37.50	0	1		1	0	1	1	0	1	1	0	0	0	0	0	0	0	0	0	1	0	1	0	1	1	0	0	0	1	1	0	0	1	0	1	0	0	1	7	1	1	0
	Antidesma montanum Blume var.	Euphorbiaceae	1	0	0	0	1	18.00	0.03	600.00	0	1	0	0	0	1	0	1	1	1	0	0	0	0	0	0	0	0	0	1	0	0	0	1	0	1	0	0	1	0	0	1	1	0	0	0	0	1	5.6	0	1	0
	Dillenia indica L.	Dilleniaceae	1	0	0	0	1	40.00	1.20	33.33	0	1	0	0	1	0	0	1	1	0	1	0	0	1	0	0	0	0	1	0	0	0	1	0	0	0	0	1	1	0	0	0	1	1	0	0	1	0	6	1	0	0
	Artocarpus lacucha Buch.-Ham.	Moraceae	1	0	0	0	1	20.00	0.13	153.85	0	1	0	0	0	1	1	0	1	1	0	0	0	0	0	0	1	0	1	0	0	0	0	0	0	0	0	1	0	1	0	0	1	0	0	1	1	0	7	1	1	0
	Diospyros malabarica (Desr.) Kostel	Ebenaceae	1	0	0	0	1	37.00	2.00	18.50	0	0	1	0	0	1	0	1	1	0	1	0	0	0	0	0	1	0	0	1	0	0	1	0	0	0	0	1	0	1	0	0	1	0	0	1	1	0	7	0	1	1
	Dipterocarpus turbinatus Gaertn. f.	Dipterocarpaceae	1	0	0	0	1	45.00	4.50	10.00	0	1	0	0	0	1	1	0	1	1	0	0	0	0	0	0	1	0	1	1	0	0	1	0	1	0	0	0	0	0	0	1	1	0	1	0	1	0	5.5	1	0	0
	Croton caudatus Geiseler	Euphorbiaceae	0	1	0	0	0	13.00	0.05	260.00	0	1	0	0	1	0	1	0	0	0	0	1	0	0	0	0	0	0	0	0	0	0	1	0	1	0	0	0	1	0	0	0	1	0	0	1	0	0	5.5	0	1	0
	Cleistanthus collinus (ROXB.) BENTH. & HOOK.	Phyllanthaceae	1	0	0	0	0	15.00	0.50	30.00	0	1	0	0	0	1	1	0	0	0	0	0	0	0	0	0	0	0	0	0	0	0	0	0	1	0	0	0	0	0	0	1	1	0	0	0	0	0	7	1	0	0
	Dipterocarpus alatus Roxb.	Dipterocarpaceae	1	0	0	0	1	40.00	3.50	11.43	0	1	0	0	1	0	0	1	0	1	0	0	0	0	0	0	0	0	0	0	0	1	0	0	1	0	0	0	0	0	0	1	1	0	1	0	0	0	6	1	0	0
	Syzygium jambos (L.) Alston.	Myrtaceae	1	0	0	0	1	10.00	0.50	20.00	0	1	0	0	0	1	0	1	1	1	0	0	0	0	0	0	0	0	1	0	0	0	1	1	0	0	0	1	0	1	0	0	1	0	1	0	1	0	6.5	1	1	0
	Barringtonia acutangula (L.) Gaertn.	Lecythidaceae	1	0	0	0	0	13.00	0.90	14.44	0	1	0	0	1	1	0	1	1	0	0	0	0	1	0	0	1	0	0	0	0	1	0	1	0	1	0	0	1	0	0	0	1	0	0	0	0	1	7	0	1	1
	Terminalia chebula Retz.	Combretaceae	1	0	0	0	1	20.00	0.60	33.33	0	1	0	0	0	1	1	0	1	0	0	1	0	0	1	0	1	0	1	1	1	0	1	0	1	0	0	0	0	1	0	1	1	0	1	0	1	0	6.5	1	0	0
	Syzygium cumini (L.)	Myrtaceae	1	0	0	0	1	35.00	4.00	8.75	0	1	0	0	0	1	0	1	1	0	0	0	1	0	0	0	0	1	1	0	0	0	1	0	0	1	0	0	0	0	0	1	1	0	1	0	1	0	6.6	1	1	0
	Citrus maxima (Burm.) Merr.	Rutaceae	1	0	0	0	1	9.00	0.20	45.00	0	1	0	1	0	1	0	1	1	0	0	1	0	0	1	0	1	0	1	1	0	1	1	1	0	0	0	1	1	1	0	0	1	0	0	1	0	1	7	0	1	0
D	*Syzygium samarangense* Merr. & Perry	Myrtaceae	1	0	0	0	1	20.00	4.00	5.00	0	1	0	0	0	1	0	1	1	1	0	0	0	0	0	0	0	1	1	0	0	0	1	1	0	0	1	0	0	0	0	0	1	0	1	0	0	1	6.6	1	1	0
	Lagerstroemia speciosa (L.) Pers.	Lythraceae	1	0	0	0	1	18.00	1.50	12.00	0	1	0	0	0	1	1	0	1	0	1	0	0	0	1	0	1	0	0	0	1	0	0	1	0	0	0	1	0	0	0	0	1	0	0	0	1	0	7	0	1	0

T=Tree, S=Shrub, H=Herb, G=Grass, W=Wood, H (m)=Height, DBH (m)=Diameter at breast height, SI=Shape Index, Er=Erect, Sp=Spreading, Dr=Drooping, Ts=Thorny/spiny, Ha=Hairy, G=Glabrous, D=Deciduous, E=Evergreen, P=Petiolate, El=Elliptical, O=Oblong, Ov=Ovate, L=Lanceolate, A=Alternate, R=Rounded, C=Cordate, Ac= Acute, Acu=Acuminate, Co=Coriaceous, Ax=Axillary inflorescence, Pa=panicle, B=Bisexual, Wc/W=White-cream or white, Pe=Pedicellate, Dr=Drupe, Be=Berry, Ob=Oblong fruit, Gl=Globose, Gr=Green, Y=Yellowish, R=Reddish, B=Blackish, Se=Seeder, Sp=Sprouter, Si=Single, Pl=Plural, Jan-Jun=January-June, Jul-Dec=July-December, pH=Soil pH, Hi=High >7 m, Me=Medium 4-7 m, Lo=low < 4 m.

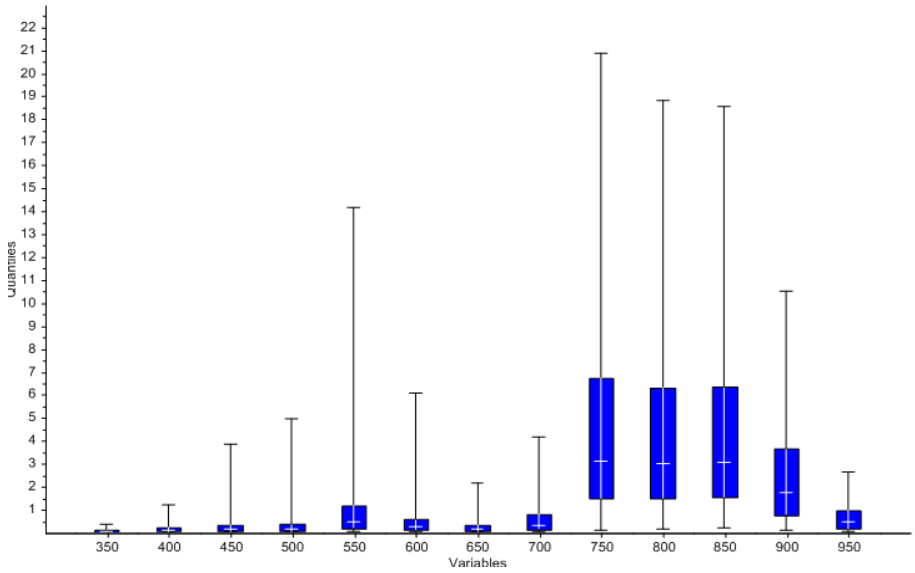

Figure A-6: Descriptive statistics of species spectral responses. Horizontal axis represents the wavelength range and vertical axis represents the mean and standard deviation of spectra reflectance of the 112 plant species.

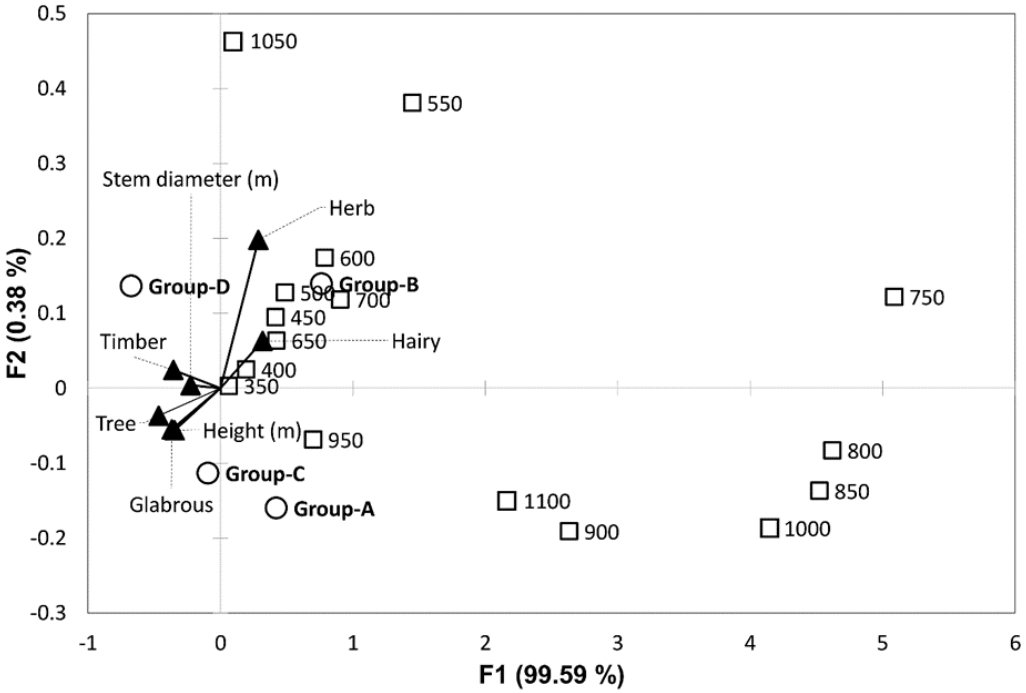

Figure A-7: RDA biplots show the relationships between the species biological and morphological traits (filled triangles) and the wavelength of leaf reflectance spectra (open squares) within the four PFGs (open circles) of 112 species. The significant variables ($P < 0.05$) are represented by the arrows. Distances between samples in the plots reflect differences among them regarding to explanatory variables that significantly correlated with spectral bands.